BONE TISSUE ENGINEERING WITH MESENCHYMAL STEM CELL SEEDED SCAFFOLD ASSISTED PERFUSION BIOREACTORS

MEZENKİMAL KÖK HÜCRE EKİLMİŞ DOKU İSKELESİ DESTEKLİ PERFÜZYON BİYOREAKTÖRLERLE KEMİK DOKU MÜHENDİSLİĞİ
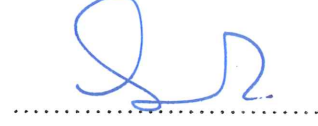
ALPER CENGİZ

PROF. DR. MENEMŞE GÜMÜŞDERELİOĞLU
Supervisor

Submitted to Graduate School of Science and Engineering
of Hacettepe University as a Partial Fulfillment
to the Requirements for the Award of
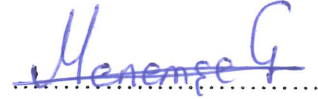the Degree of Master of Science in Bioengineering.

2017

This work named "**Bone Tissue Engineering With Mesenchymal Stem Cell Seeded Scaffold Assisted Perfusion Bioreactors**" by ALPER CENGİZ has been approved as a thesis fort he Degree of **MASTER OF SCIENCE IN BIOENGINEERING** by the below mentioned Examining Committee Members.
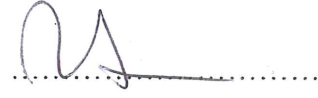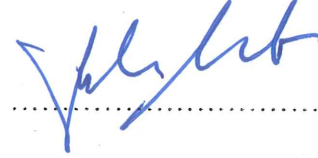
Prof. Dr. Serpil TAKAÇ
Head

Prof. Dr. Menemşe GÜMÜŞDERELİOĞLU
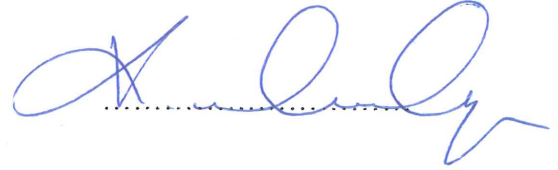Supervisor

Prof. Dr. Zümriye AKSU
Member

Prof. Dr. Selma MUTLU
Member

Prof. Dr. Kezban ULUBAYRAM
Member

This thesis has been approved as a thesis for the Degree of MASTER OF SCIENCE IN BIOENGINEERING by Board of Directions of the institute for Graduate School of Science and Engineering.

Prof. Dr. Menemşe GÜMÜŞDERELİOĞLU
Director of the Institute of
Graduate Schol of Science and Engineering

YAYINLAMA VE FİKRİ MÜLKİYET HAKLARI BEYANI

Enstitü tarafından onaylanan lisansüstü tezimin/raporumun tamamını veya herhangi bir kısmını, basılı (kağıt) ve elektronik formatta arşivleme ve aşağıda verilen koşullarla kullanıma açma iznini Hacettepe üniversitesine verdiğimi bildiririm. Bu izinle Üniversiteye verilen kullanım hakları dışındaki tüm fikri mülkiyet haklarım bende kalacak, tezimin tamamının ya da bir bölümünün gelecekteki çalışmalarda (makale, kitap, lisans ve patent vb.) kullanım hakları bana ait olacaktır.

Tezin kendi orijinal çalışmam olduğunu, başkalarının haklarını ihlal etmediğimi ve tezimin tek yetkili sahibi olduğumu beyan ve taahhüt ederim. Tezimde yer alan telif hakkı bulunan ve sahiplerinden yazılı izin alınarak kullanması zorunlu metinlerin yazılı izin alarak kullandığımı ve istenildiğinde suretlerini Üniversiteye teslim etmeyi taahhüt ederim.

☑ **Tezimin/Raporumun tamamı dünya çapında erişime açılabilir ve bir kısmı veya tamamının fotokopisi alınabilir.**
(Bu seçenekle teziniz arama motorlarında indekslenebilecek, daha sonra tezinizin erişim statüsünün değiştirilmesini talep etseniz ve kütüphane bu talebinizi yerine getirse bile, tezinin arama motorlarının önbelleklerinde kalmaya devam edebilecektir.)

☐ **Tezimin/Raporumun .... tarihine kadar erişime açılmasını ve fotokopi alınmasını (İç Kapak, Özet, İçindekiler ve Kaynakça hariç) istemiyorum.**
(Bu sürenin sonunda uzatma için başvuruda bulunmadığım taktirde, tezimin/raporumun tamamı her yerden erişime açılabilir, kaynak gösterilmek şartıyla bir kısmı ve ya tamamının fotokopisi alınabilir)

☐ **Tezimin/Raporumun .... tarihine kadar erişime açılmasını istemiyorum, ancak kaynak gösterilmek şartıyla bir kısmı veya tamamının fotokopisinin alınmasını onaylıyorum.**

☐ **Serbest Seçenek/Yazarın Seçimi**

11 / 07 / 2017

(İmza)

Öğrencinin Adı Soyadı
Alper Cengiz

ETHICS

In this thesis study, prepared in accordance with the spelling rule of Institute of Graduate Studies in Science of Hacettepe University.

I declare that

- All the information and documents have been obtained in the base of the academic rules
- All audio-visual and written information and results have been presented according to the rules of scientific ethics
- In case of using other Works, related studies have been cited in accordance with the scientific standards
- All cited studies have been fully referenced
- I did not do any distortion in the data set
- and any part of this thesis has not been presented as another thesis study at this or any other university.

04/07/2017

Alper CENGİZ

ABSTRACT

BONE TISSUE ENGINEERING WITH MESENCHYMAL STEM CELL SEEDED SCAFFOLD ASSISTED PERFUSION BIOREACTORS

Alper CENGİZ

Master of Science, Department of Bioengineering

Supervisor: Prof. Dr. Menemşe GÜMÜŞDERELİOĞLU

July 2017, 97 Pages

This study was financially supported by Turkish Scientific and Research Council (Tübitak) Project no: 214M100. In the present thesis study, it was aimed to investigate the potential of proliferation and osteogenic differentiation of human mesenchymal stem cells (hMSCs) in perfusion bioreactors.

In the first step of this study, chitosan-hydroxyapatite superporous hydrogel (chitosan-HA SPHC) scaffolds were prepared by using sodium bicarbonate ($NaHCO_3$) as a foaming agent and glyoxal as a cross-linking agent. The microwave assisted gas foaming technique has produced tissue scaffolds that are faster to obtain, in high yield and higher reproducibility in vitro studies.

In the second step of the experimental study, the installation of the perfusion bioreactor system, in which leakage and diffusion problems can be solved and which provides sustainable sterility through long-term dynamic culture studies has been completed. At the next stage of the study, dynamic cell culture studies were carried out for 21 days using hMSCs

at different flow velocities and tissue scaffolds of different sizes (P3D-6: 0.1 mL/min, P3D-6: 0.2 mL/min; P3D-10: 0.27 mL/min) and media changes were made on certain days (days 3, 6, 9, 12, 15 and 18) of the culture. MTT (3-[4,5-dimethylthiazol-2-yl]-2,5 diphenyltetrazolium bromide) analysis was performed to observe viability and proliferation of cells on certain days of cell culture studies. SEM (Scanning Electron Microscopy) analysis was performed to observe cell morphologies and penetrations. At the end of the cell culture studies, RT-PCR (Real Time Polymerase Chain Reaction) analyzes were performed to determine the expression levels of Collagen1 (Col1), Runt Associated Transcription Factor 2 (RUNX2), Osteocalcin (OCN) and Osteopontin (OPN) genes in hMSCs.

In the last part of the thesis study, flow and mass transfer simulation studies were carried out in the perfusion bioreactor using COMSOL software. The accuracy of the model was tested with models developed for low and high flow rates in a bioreactor without a tissue scaffold and in the presence of a non-porous tissue scaffold. Afterwards the flow model and mass transfer model in perfusion bioreactor in the presence of a permeable tissue scaffold took place. The results obtained from the Computational Fluid Dynamics (CFD) modeling studies conducted within the scope of the thesis seem to support the experimental findings.

In the light of all these analyzes and findings, it has been shown that the dynamic culture approach performed with P3D-6 scaffolds at 0.1 mL/min and 0.2 mL/min flow rates support the osteogenic differentiation of hMSCs in the perfusion bioreactor. In addition, it can be seen that the CFD approach is the decisive factor in achieving successful results in vitro production of engineered bone grafts when different operating parameters are considered.

Key Words: bone tissue engineering, human mesenchymal stem cells, dynamic cell culture, chitosan-hydroxyapatite superporous hydrogels, P3D-6 and P3D-10 scaffolds, perfusion bioreactor, computational fluid dynamics.

ÖZET

MEZENKİMAL KÖK HÜCRE EKİLMİŞ DOKU İSKELESİ DESTEKLİ PERFÜZYON BİYOREAKTÖRLERLE KEMİK DOKU MÜHENDİSLİĞİ

Alper CENGİZ

Yüksek Lisans, Biyomühendislik Anabilim Dalı

Tez Danışmanı: Prof. Dr. Menemşe GÜMÜŞDERELİOĞLU

Temmuz 2017, 97 Sayfa

Bu çalışma, Türkiye Bilimsel ve Teknolojik Araştırma Kurumu (Tübitak) Projesi No: 214M100 tarafından maddi olarak desteklenmiştir. Bu tez çalışmasında, durağan hücre kültürü ve dinamik yaklaşım olan perfüzyon biyoreaktörlerinde farklı ebat ve farklı boyuttaki doku iskelelerine dayanan hücre kültürü çalışmalarının insan mezenkimal kök hücreleri (hMSC) üzerindeki üreme ve osteojenik farklılaşmanın potansiyelinin araştırılması amaçlanmıştır.

Deneysel çalışmaların ilk aşamasında, kitosan-hidroksiapatit süpergözenekli hidrojel (kitosan-HA SGPH) doku iskeleleri, köpükleşme ajanı olarak sodyum bikarbonat ($NaHCO_3$) ve çapraz bağlayıcı olarak glioksal kullanılarak hazırlanmıştır. Mikrodalga destekli gaz köpükleşme tekniği, in vitro çalışmalarda yüksek verim ve daha yüksek tekrarlanabilirlik elde etmenin yanında doku iskelelerinin üretiminin hızlandırılmasını desteklediğinden tercih edilmiştir.

Deneysel çalışmanın ikinci aşamasında, olası bir sızıntının önlendiği ve besin maddeleri / atık madde difüzyon sorunlarının çözülebildiği, uzun vadeli dinamik kültür çalışmaları ile sürdürülebilir sterilite sağlayan perfüzyon biyoreaktör sisteminin kurulumu gerçekleştirilmiştir. Çalışmanın bir sonraki safhasında, hMSC'ler kullanılarak farklı akış hızlarında ve farklı boyutlarda doku iskeleleriyle (P3D-6: 0.1 mL/dk, P3D-6: 0.2 mL/dk; P3D-

10: 0.27 mL/dk) 21 gün süreyle dinamik hücre kültürü çalışmaları gerçekleştirilmiş ve kültürün 3, 6, 9, 12, 15 ve 18. günlerinde ortam değişiklikleri yapılmıştır. Hücre kültürü çalışmalarının 7, 14 ve 21. günlerinde hücre canlılığı ve çoğalmasını gözlemlemek için MTT (3-[4,5-Dimethylthiazol-2-yl]-2,5-Diphenyltetrazolium Bromide) analizi gerçekleştirilmiş ve SEM (Taramalı Elektron Mikroskopisi) analizi ile hücre morfolojileri ve penetrasyonları gözlemlenmiştir. Hücre kültürü çalışmalarının sonunda insan mezenkimal kök hücrelerinin Kolajen1 (COL1), Runt İlişkili Transkripsiyon Faktörü 2 (RUNX2), Osteokalsin (OCN) ve Osteopontin (OPN) ekspresyon düzeylerini belirlemek için RT-PCR (Gerçek Zamanlı Polimeraz Zincir Reaksiyonu) analizi yapılmıştır.

Tez çalışmasının son bölümünde, perfüzyon biyoreaktörde akış ve kütle transferi simülasyon çalışmaları COMSOL yazılımı kullanılarak gerçekleştirilmiştir. Modelin doğruluğu, doku iskelesi olmayan bir biyoreaktörde düşük ve yüksek akış hızı uygulamaları için geliştirilen modellerle test edilmiştir. Ardından, farklı akış hızlarında ve farklı boyutlarda üretilmiş olan geçirgen doku iskeleleri varlığında perfüzyon biyoreaktörün akış modeli ve kütle transferi modeli ortaya konulmuştur. Tez kapsamında yapılan hesaplamalı akışkanlar dinamiği (CFD) modelleme çalışmalarından elde edilen sonuçların deneysel bulguları desteklediği görülmüştür.

Tüm analizler ve bulgular ışığında perfüzyon biyoreaktöründe 0.1 ve 0.2 mL/dk akış hızı ve 3mm çapında ve 6mm yüksekliğindeki doku iskeleleri ile yapılan dinamik kültür yaklaşımının insan mezenkimal kök hücrelerinin osteojenik farklılaşmasını desteklediği gösterilmiştir. Buna ek olarak, CFD yaklaşımının, farklı çalışma parametreleri göz önüne alındığında, mühendislik ürünü kemik yamalarının in vitro üretiminde başarılı sonuçlar elde edilmesinde belirleyici faktör olduğu sonucuna varılmıştır.

Anahtar kelimeler : kemik doku mühendisliği, insan mezenkimal kök hücreleri, dinamik hücre kültürü, kitosan-hidroksiapatit süpergözenekli hidrojeller, P3D-6 ve P3D-10 doku iskeleleri, perfüzyon biyoreaktör, hesaplamalı akışkanlar dinamiği.

ACKNOWLEDGEMENT

TABLE OF CONTENTS

LIST OF TABLES

LIST OF FIGURES

SYMBOLS AND ABBREVIATIONS

Symbols

c	Concentration
D	Diameter
V	Volume
μm	Micrometer
μL	Microliter
nm	Nanometer
W	Watt
$D_{A,B}$	Diffusion Coefficient of A in B
K_m	Michaelis-Menten Coefficient
N_A	Flux
p	Pressure
Q	Volumetric Flow Rate
r_A	Net Reaction Rate
$R_{A,B}$	Cellular Consumption Rate
u	Linear Velocity
ε_p	Porosity
Δt	Time Step
κ	Porous Media Permeability
η	Dynamic Viscosity (Pa.s)
ρ	Density
τ	Shear Stress

Abbreviations

hMSC	Human Mesenchymal Stem Cell
MSC	Mezenchymal Stem Cell
Col1	Collagen Type I
DPBS	Dulbecco's Phosphate Buffered Saline
dNTP	Deoxynucleotide triphosphate
ECM	Extracellular Matrix
FBS	Fetal Bovine Serum
FDA	Food and Drug Administration
HA	Hydroxyapatite
HMDS	Hexamethyldisilazane
MTT	(3-(4,5-Dimethylthiazol-2-yl)-2,5-Diphenyltetrazolium Bromide)
$NaHCO_3$	Sodium Bicarbonate
OPN	Osteopontin
OCN	Osteocalcin
PBS	Phosphate Buffered Saline
RNA	Reoxiribonucleic asit
RT-PCR	Real Time Polymerise Chain Reaction

RUNX2	Runt Related Transcription Factor 2
SEM	Scanning Electron Microscopy
SPHC	Superporous Hydrogel Composite
TCPS	Tissue Culture Polystyrene
α-MEM	Minimum Essential Medium Alpha Modification
μCT	Micro Computed Tomography
ALP	Alkaline Phosphatase
TGF-β1	Transforming Growth Factor Beta 1
VEGF	Vascular Endothelial Growth Factor
BMP-2	Bone Morphogenetic Protein 2
FGF-2	Fibroblast Growth Factor 2
μPIV	Micro Particle Image Velocimetry

1. INTRODUCTION

Bones are the essential components of the skeletal system in terms of acting as a framework that supports and protects internal organs and enabling the ability to move. Furthermore, bones participate in adjusting mineral homeostasis, and endocrine regulation of energy metabolism [1]. Bone tissue, unlike most other tissues, possesses the ability of self-renewal and even displays spontaneous healing capacity when damaged [2]. Numerous bone deformations, like craniofacial deformity, due to congenital anomalies, tumor resections or hurtful injuries, may be treated through reconstruction of the bone [3].

The bone grafts consist of autografts, allografts, xenografts, synthetic materials or demineralized bone matrix, and have been widely used for the treatment of large bone defects [5]. Among them, autologous bone graft treatment proves to be the most successful approach for large bone defects, due to the minimal immune rejection rate when transplated to the target tissue [4]. However, this treatment is restricted due to the limited availability of bone, which is harvested from the iliac crest and medical complications following the harvesting such as infection, nerve and arterial injury and chronic pain [6-8]. Due to these complications, alternative strategies for bone healing that would allow absolute shape reconstruction, mechanical strength and biocompatibility in both the short and long term are needed. To this end, bone tissue engineering has evolved as a practical method of regenerating large bone defects [4].

Renewal and regeneration of a defective bone without expecting one or multiple adverse side effects can be done by promoting osteogenesis with the aid of appropriate scaffolds including biocompatible carriers and specific growth factors via tissue engineering [9]. The biocompatible and biodegradable materials [10] possess osteoconductive [11] and/or osteoinductive properties [12]. In addition, tissue engineering approach contributes to the formation of autologous bone tissue grafts that can be acquired from cells cultured on scaffolds, hence proving an alternative for the shortage of donor tissue. Osteogenic cells from suitable sources, biocompatible scaffolds, bioreactor culture systems and subsequent functional integration with the host are critical components for the production of engineered functional bone grafts [13].

Present bone formation modelling in vitro assumes that cellular differentiation and functionality may be modified with the aid of signal molecules that play a significant part as embryonic development takes place [14]. To design and imitate the conditions that would enable the bone development, the combination of biosignals must be presented to the cells in a 3D setting in a way that would allow cellular interactions with the cells that surround the formation and the extracellular matrix (ECM), while considering the complexity of signaling presents significant challenges for fully applicable, functional bone [15].

The scaffold, which considerably affects the cell behaviour while granting structural and formal frame for the development of the tissue, is considered as an integral element of the in vitro bone modelling. Numerous types of scaffolds known for their porosity proved to support in vitro bone development when treated with human cells. The mentioned scaffolds are reported to be made of ceramics [16,17], polymers [18,19], and composites [20].

Properties of the scaffolds that are essential for bone development may be listed as the size, distribution and shape of the pores [21]; roughness of the surface [22]; the location of cell attachment sites [23]; and biomechanic features of both the material [24] and the scaffold. Generally, it is expected from a suitable scaffold for bone tissue to have large and interdependent pores, an inner surface based on osteoconductive materials and mechanical properties that shows resemblance to native bone in order to promote cell infiltration, cell adhesion and stimulation of osteogenesis respectively while supporting anisotropic structure, vascularization capacity and anatomically correct shaping [15]. Scaffolds may also organize and adjust the distribution of molecular signals that control cellular functions [25].

Bioreactor systems may be redesigned to regulate the transportation of nutrients and gases in appropriately evaluated structures and can provide biological stimulants in numerous parts of the construct [26]. Furthermore, bioreactor systems enhance the functional and mechanical properties of the bone graft in order to imitate the physical capacity of the desired tissue. Bioreactor designs offer to maintain and regulate the physiological properties in the cell microenvironment by perfusion flow of culture medium. Bioreactors can also be customized to recapitulate the developmentally related biophysical signals in a periodic manner. To exemplify, enhanced mass transport and fluid shear [27,28], as well as cyclic loading [30] appear to promote the osteogenesis and the homogenity of bone constructs. It is expected from

a bioreactor to coordinate biological, physiological and mechanical stimulants, as well as to apply these stimulants in a dimensionally and temporally controlled aspect in grafts of clinical accordance. The scientific utility of tissue engineering chiefly relies on one's capability to precisely redirect the cells to differentiate into the right phenotypes in a pattern that is spatially and temporally predefined [15]. Understanding and evaluation of the environmental conditioning and the scaffold properties can provide a better understanding on bioreactors that play an important role in defining the environmental parameters that affect the bone formation from numerous types of osteocompetent cells.

In order to provide a better understanding on how various flow patterns and shear stress factor affect the proliferation and differentiation of the cells; the hydrodynamic conditions of bioreactors need to be characterized numerically and must be analyzed alongside the experimental data. The ability to establish a correlation between the operational parameters of bioreactors and cell migration and differentiation using Computational Fluid Dynamics (CFD) is of great importance in terms of in vitro production of functional tissues as an engineering product [31]. Although there are alternative experimental techniques to characterize the flow in the bioreactor, CFD is considered as one of the most important techniques in terms of being able to simulate three-dimensional flow in a short time and to be expressed with visual arguments [32]. In this method, microenvironments that affect tissue scaffolds and cells can be identified by taking advantage of fundamental mass and momentum equations [31,33].

The main aim of this study is to investigate the effect of different flow rates and different sizes of tissue scaffolds on the differentiation of human mesenchymal stem cells (hMSCs) to bone tissue by static/dynamic cell seeding and dynamic cell cultures performed in a perfusion bioreactor. For this purpose, the studies are divided into two parts: In the first part, reproduction and differentiation behavior of hMSCs in chitosan-hydroxyapatite superporous hydrogels under static seeding and dynamic culture conditions were investigated at different flow rates. Cell viability, relative gene expression and cell morphology were examined and the effects of perfusion cultures and operating parameters on cell behavior were investigated. The installation of the perfusion bioreactor system was carried out in order to overcome mass transfer constraints and mechanically stimulate the cells. To this end, a multichannel syringe pump suitable for working at different flow rates, a perfusion chamber in which the tissue

scaffolds can be provided to allow operation with tissue scaffolds of different sizes, the use of suitable fittings, valves and filters were used to prevent contamination during long-term in vitro culture runs, to control flow rate and flow direction, to allow manipulation and to prevent leakage. In order to acquire an efficient cell cultivation, dynamic cell culture studies using the perfusion bioreactor have been completed comparatively with static approach. To examine the effects of dynamic conditions on the hMSCs in the perfusion bioreactor, MTT assay was used to measure cell viability and proliferation, SEM analysis for cell penetration imaging and RT-PCR analysis for the detection of osteogenic gene expression levels in cells. In the second and final part of the study, shear stress rates and nutrient concentration profiles were calculated by CFD modeling studies in order to be able to identify the microenvironment affecting the cells at different flow rates in the perfusion bioreactor. The data obtained from the simulation studies were evaluated together with the experimental results and interpretations were made on the appropriate conditions for mesenchymal stem cell proliferation and its differentiation.

2. LITERATURE REVIEW

In this section, the literature on the topics underlying the thesis work is presented under three headings. In the first section, bone tissue engineering is defined, the current state of clinical trial of engineered bone grafts are given and the limitations on their usage are discussed. In the second part, the definition, function and influential applications of tissue engineering bioreactors are presented. In the third chapter, information about the CFD approach used for the simulation of flow and mass transfer in bioreactors is presented and examples from the literature and functional applications are given.

2.1. Bone Tissue Engineering

Bone tissue is a highly uniform and programmed tissue that has the capacity to repair itself and repair damage, but the treatment of large-scale injuries in the clinic is still a major problem [34]. The first approach in treatment methods used in case of tissue loss or injury is graft applications. Among these applications, "autograft" application is preferred as the gold standard. The autograft is applied in the form of a piece of tissue taken from a healthy area of the patient, placed in the area of tissue loss or damage. However, major inadequacies, limitations, and complications have been identified in patching (graft use) procedures commonly used clinically nowadays [35, 36]. In autografting applications performed with tissues from patients themselves, surgical interventions lead to increased postoperative morbidity in patients and consequently high costs in the health care system [37]. The second option is to transplant the tissue from another source into the patient. When this resource is human, the application is called "allograft" and when it is an animal it is called "xenograft" [38]. Although autograft is considered as the gold standard in graft applications, it may cause complications such as surgical problems and tissue structure [34]. In addition, the insufficiency of adequate and suitable tissue source to be taken from the patient, treatment cost problem and infection progression in the surgical area are some of the encountered problems. In the allograft method, problems such as bacterial and viral infections, rejection by the immunological system are on the agenda [35,38]. Today, the other treatment method used in large fractures that occur in the bone tissue is the center of the metal implant, providing both mechanical and structural support. Metal implants are regarded as materials that will replace

the bone, especially in long bone injuries. However, while metal implants provide advantages in providing mechanical support, they also introduce some complications such as infection and corrosion that makes them difficult to use [34].

The emergence of bone tissue engineering as an alternative treatment for bone injuries has a history of about 30 years. Interest in bone tissue engineering methods and the studies in the mentioned field are increasing all over the world. Bone tissue engineering products have begun to be obtained and the clinical trial stages are evaluated. The aim of the studies is to obtain products that will yield positive results at low cost in clinic. The number of patients who are treated for bone damage is very high worldwide and the number of the cases are increasing exponentially. Especially in countries with aging populations, low physical activity rates and obesity problems, this problem is frequently encountered. Although many steps have been taken to date from the onset of bone tissue engineering applications, a critical set of obstacles still does not make possible clinical applications [36,39].

Thanks to the advances in materials science and processing technologies, it is possible to produce tissue scaffolds with the desired physical and chemical properties. Angiogenic growth factors may be used to provide tissue integration and vascularization. In preclinical studies, large animal models are considered to be better models for transportation, patch size, and healing properties, as opposed to generally preferred small animal studies. [32] Patient-free practices should be developed instead of patient-specific approaches in order to reduce costs and increase efficiency. However, single-component systems should be designed instead of multiple systems so that the approaches developed can more easily be approved for clinical applications. At this stage it is of utmost importance to improve the cell isolation methods and to implement pre-implantation culture with bioreactor-based approaches [36]. Table 2.1 summarizes the current limitations and challenges that bone tissue engineering has encountered with.

Table 2.1; Fundamental, evaluation and clinical challenges and knowledge limitations in bone tissue engineering [36].

Fundamental Challenges
- Selection of Optimal Cell Source, Tissue Scaffold, and Growth Factor   - Providing Homogenous Tissue Formation in Scaffolds   - Vascularization   - Providing Tissue Integration
Knowledge Limitations
- Participation of Recipient and Donor Cells in Regeneration   - Suitable Agents that Regulate the Immune System   - Complications and Side Effects of Donor Cells and Growth Factors   - The Most Suitable Animal Model
Evaluation Challenges
- Quality of the Regenerated Bone   - Functionality of the Regenerated Bone   - Long-Term Tracking of the Regenerated Bone
Clinical Challenges
- Approval of Food and Drug Administration (FDA)   - Single and Multiple Components   - High Cost   - The Necessity of Patient-specific Approach

2.2. Bioreactors in Bone Tissue Engineering

2.2.1. Definition, Structure and Function of Bioreactors

Bioreactors can basically be defined as devices that enable biochemical and biophysical microenvironment that mimics physiological environment and provide ease of use, reduce contamination risk, provide scalability, allowing control over many operating conditions such as oxygen, temperature, pH, nutrient concentration, carbon dioxide amount, flow rate, and flow direction [9]. Originally, bioreactors are used in industrial fermentation processes, waste water treatment, food and pharmaceutical industries, but they have become one of the key elements of tissue engineering studies since they perform cellular activity in the original tissue that has been shown to accelerate tissue regeneration and provide controlled, reproducible cell

proliferation [9]. Bioreactors are needed to increase numbers for transplantation of cells such as hematopoietic cells, embryonic stem cells or mature blood cells. Another important area of application is the production of 3D tissues to be used in the treatment of damages of bone, cartilage, skin and blood vessels. Tissue engineering bioreactors help to understand cell and tissue behavior by providing controlled culture conditions. In addition, organ support systems are also evaluated as bioreactors, such as the kidney and liver. [33]. Various types of bioreactors used in tissue engineering and traditional cultures are given in Figure 2.1.

Figure 2.1; Conventional culture equipments and bioreactors used in dynamic cell cultures.

There are several major problems encountered in providing controlled conditions during scaffold based culture studies in bioreactors; primarily based on the insufficiency of nutrients that the cells require, and the inability to acquire a homogenous cell distribution when seeding

takes place within the scaffold. Table 2.2 summarizes the parameters expected to allow controlled monitoring of bioreactors during cell culture and their location in cellular events.

Table 2.2 parameters to allow controlled monitoring of bioreactors during cell culture and their location in cellular events [40]

Physicochemical Parameters
- pH is a mandatory parameter to be kept within the physiological limit in terms of the continuity of the cell culture.   - The temperature must be maintained at 37°C for stem cell cultivation and plays crucial part.   - Osmolarity, being a highly efficient parameter in terms of cell functioning, plays an important part in the maintenance of cell viability and functions.   - Dissolved oxygen rate can be considered as another important parameter for the growth and the livelihood of the stem cells. Hypoxia considerably affects the preservation and differentiation of stem cells, and therefore the dissolved oxygen levels in the fluid environment is needed to be observed continuously.   - Hydrodynamic shear stress plays an important role in the physiological environment of the mechanical load bearing tissues. Considering that the stem cells can easily be affected by the culture parameters, it is important to keep the track of hydrodynamic shear stress in bioreactors
Biochemical Parameters
- Nutrients are essential for the continuation of cell metabolism and its use as an energy source in cellular processes.   - Moreover, the presens of waste products can affect the cell viability and therefore must be monitored.   - Growth factors and cytokines are signal proteins that modulate a variety of cell functions, such as self-renewal, differentiation, or survival. Therefore, they are essential to acquire.

2.2.1.1. The Role of Bioreactors in Cell Culture

In culture studies conducted with tissue scaffolds and cells, the distribution of cells within the 3D scaffold has a crucial effect on the texture, composition, and functionality of the engineered tissue. For this reason, it is possible to say that cell seeding is one of the most critical steps for the production of functional tissues [33]. In many applications, including

clinically applied autologous grafting, the cell source is often limited, so cells must be seeded both at high yield and at high viability. It is particularly difficult to realize cell cultivation in an efficient and reproducible manner for 3D scaffolds with complex pore geometry. The most commonly used seeding technique is a simple application based on the release of a concentrated cell suspension by pipetting onto the scaffold, which is referred to as "static seeding". This method, which depends on the experience of the person performing the seeding, is not sufficient in terms of control and standardization [33]. Conventional seeding methods are inadequate because of the quantitative limitations of large bone grafts used for repairing large bone injuries [41]. Dynamic seeding approaches have been developed by utilizing bioreactors to provide the high cell yield and the all he at of the cells in the scaffold. Table 2.3 compares different cell seeding approaches.

Table 2.3; List of cell seeding methods under various parameters [42]

	Static	Rotational	Centrifugal	Vacuum	Cell Sheet	Magnetic	Electrostatic	Hydrogel	Rotational Vacuum	Bioreactor
Efficiency	10%–25%	90%	38%	60%–90%	N/A	90%–99%	90%	Not shown	60%–90%	75%–94%
Quantification	Hemocytometer, DNA assay	Hemocytometer	Picogreen, MTT assay	Picogreen, SEM, histology	Histology	WST-1 assay, hemocytometer	SEM	Picogreen, histology	Hemocytometer	Hemocytometer, DNA assay, MTT assay
Cell Type	EC,SMC, BM-MNC	EC	BM-MNC	EC, MDSC	EC, SMC, fibroblast	EC, SMC	EC	SMC, fibroblast	EC, MDSC, BMPC	EC, SMC, EPC, BMSC
Ingrowth	Minimal	None	Good	Good	N/A	Good	None	Good	Good	Excellent
Phenotype	None	None	None	Not shown	Yes	Yes	Yes	None	None	Yes
Matrix	↓ Production	↓ Production	↑ Production	↓ Production	↑↑ Production	↑↑ Production	None	↑↑ Production	None	↑↑ Production
Reproducibility	Yes	Yes	Yes	Yes	Yes	Yes	No	Yes	No	Yes
Cost Effectiveness	↑	↑↑↑	↑	↑↑	↑↑	↑↑	↑↑	↑↑	↑↑	↑↑
Clinical Use	In vivo (human)	In vitro	In vitro	In vitro	In vivo (human)	In vitro	In vivo (animals)	In vitro	In vitro	In vivo (animals)
Advantages	Simple, rapid, well established	High seeding efficiency	High seeding efficiency, increased cell	High seeding efficiency, rapid, simple	High pressure systems, arteries	High seeding efficiency, simple, cell specific,	High seeding efficiency, fast	Scaffold characteristic manipulation	High seeding efficiency, reproducible	Good seeding efficiency, morphological maturation
Disadvantages	Variable, operator dependent	Slow (~24 h), risk of contamination	Adverse effects on cell morphology	Culture for days to weeks, untested in vivo	Complex, prolong culture times	Adverse effects on cell proliferation, long-term adverse	Only for endothelial cells, long-term adverse effects unknown	UV light exposure, untested in vivo	Complex, costly	Complex, high risk of contamination, prolonged culture times (weeks)

In the perfusion bioreactor system, in which the cell suspension is pumped through a 3D scaffold with the aid of a pump, it achieves a more productive and efficient cell cultivation than other methods [44]. Moreover, in dynamic cultivation with perfusion bioreactors, controlled seeding and non-uniform distribution of cells using anisotropic architectural scaffolds can be performed [43, 45].

Figure 2.2 summarizes the bone regeneration strategies followed to obtain bone-like structures. It has been found that cell cultivation by conventional seeding methods using the flasks and plates have limited proliferative activity. On the other hand, it has been observed that 3D tissue scaffolds and dynamic approach support the proliferation and differentiation potentials of the cells. The goal of dynamic cell cultivation techniques in bioreactors against conventional cultivation methods is to develop high quality, reproducible, efficient and homogeneous cell-dispersed cultivation processes, and these processes can be carried out with a wide variety of bioreactor types allowing specific applications [46].
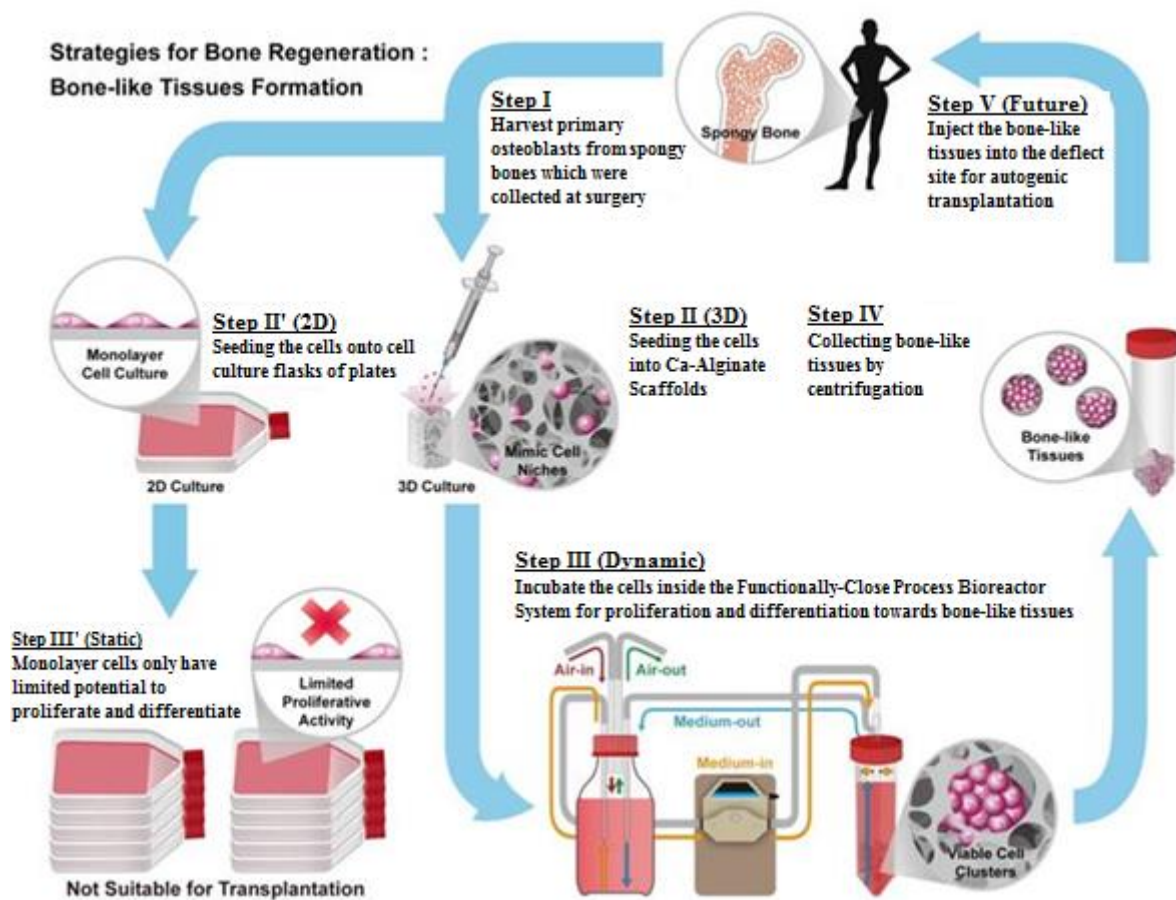
Figure 2.2; Strategies for bone regeneration and comparison of static and dynamic approaches [47]

2.2.1.2. Mechanical Stimulation in Bioreactors

Establishing the physiological microenvironment in the bioreactor according to the type of tissue targeted for repair is an important step for successful bioreactor application. It is

noteworthy that biomimetic culture conditions have an important place in mechanical stimulation as much as mass transduction criterion because bone tissue is vascular, it is exposed to mechanical stresses and is a load bearing tissue. Physical factors such as mechanical stress, shear stress, pressure and gravity are important criteria in bone remodeling and are thought to have effects on the morphology, proliferation and differentiation of the cultured cells in bone tissue studies. Since conventional culture methods are used for culturing by stationary approach, it is not possible to obtain mechanical stimulation. However, different stimuli are provided through bioreactors to obtain the targeted touch. Mechanical stirring is achieved by continuous mixing in spinner flask bioreactors, by flow induced mechanical stimulation in perfusion bioreactor. Pressure-based mechanical stimulation can be achieved in mechanical compression bioreactors [48,49].

2.2.1.3. Mass Transfer in Bioreactors

Mass transfer in cell culture is an important issue in terms of determining the behavior of cells under different culture conditions. It has been observed that the supply of nutrients supports the proliferation and differentiation of cells. For this reason, cellular mechanisms at micro level are supported by molecular factors, while at the macro level engineering approaches for cell-ECM interaction are needed [33,50]. The greatest challenge to be overcome by engineering multi-layered tissues is the ability to create large sized and fully live grafts. Depending on the cause or extent of tissue damage, the graft should be several centimeters in diameter. This size criterion, coupled with the risk of infection, makes transfer of metabolites to cells in the graft center difficult [51]. In vitro production of clinically sufficient quantitative patches is predominant in that tissue engineering bioreactors are systems that can reduce mass transfer constraints by transporting nutrients through the diffusion pathway to the cells and provide physical stimuli to the developing tissue [32,52]. In bioreactors, mass transfer of nutrients and gases occurs by convection and diffusion mechanisms. When mass transfer is evaluated in bioreactors, the two important components are oxygen and glucose. In aerobic metabolic cycles, oxygen is the most important factor for cells. However, due to its low solubility in the culture medium, oxygen is often the limiting component for tissue development in vitro [48]. After the appropriate design of the bioreactor is completed, it is required to allow 3D culture for cells growing in vitro and to form 3D tissue. In 2D culture,

culture is carried out in conventional cell culture vessels, because of mass transfer limitations the tissues in the complex structure can not be obtained. But in a bioreactor, controlled 3D culture conditions and more complex structures can be obtained [50].

2.2.2. Design Requirements in Bioreactors

Bioreactors are devices that allow controllable physiological parameters (such as temperature, pH) to remain at the same level throughout the cell culture. It is preferred that bioreactors carry out cell seeding and cultivation processes automatically because of their simple organization and user-friendliness [41]. Restrictions on 3D cultures in bioreactors are specified in Section 2.5.2. There are specific design requirements of bioreactors to enable cells to survive through long-term culture after seeding into tissue scaffolds [53]. In the body, cells are key elements in the formation of tissue and organ architecture. Under appropriate conditions, they can be modeled into functional tissue units in their microenvironment. While bioreactors are being developed, designs are carried out by considering the information on this natural-based approach [54]. Tissue engineering bioreactors must meet the following criteria [45,55]:

- Cells must be able to provide true physiological environmental conditions *in vivo*.
- Homogeneous cell distribution must be accomplished on the tissue scaffolds.
- Tissue-specific physical or mechanical stimuli must be provided.
- The mass transfer problem must be overcome.
- Nutrients, oxygen and carbon dioxide concentrations must be controlled.
- Monitoring of environmental parameters applied to cells must take place continuously.

2.2.3. Types of Bioreactors in Tissue Engineering

Different types of bioreactors are used in studies to provide different working conditions in consideration of design requirements. It is also observed that the combinations of different types of bioreactors have a higher ability to mimic bone physiology [55]. Despite the presence of bioreactors in a wide variety of designs, the following information has been given on the most widely used bioreactor types for tissue engineering studies. These include spinner flask bioreactors, rotating wall bioreactors and perfusion bioreactors used in the thesis study.

2.2.3.1. Spinner Flask Bioreactors

In stirred container bioreactors, tissue scaffolds are held suspended in the culture medium by being fixed to the needles hanging from the shaft. It has the simplest bioreactor design and is a widely used bioreactor type in tissue engineering studies [56]. In a glass or plastic container, with two arms, with a magnetic stirrer at the center, the culture medium is continuously stirred. Gas exchange is carried out in the arms on both sides. Mixing improves cell cultivation efficiency when compared to static culture [33,54,55]. This also allows both the composition of the culture medium to be homogeneous and also improves mass transfer within the scaffold by reducing the thickness of the stationary boundary layer on the scaffold surface. However, the cells that are continuously mixed with the magnetic stirrer are exposed to the turbulent flow and due to the mass transfer, the cells move towards the center of the tissue scaffold [55]. The mixing speed and mixer type in the bioreactor are important because the vortices formed during mixing can damage the developing tissue [48]. In Figure 2.3, a stirred vessel bioreactor is presented schematically.
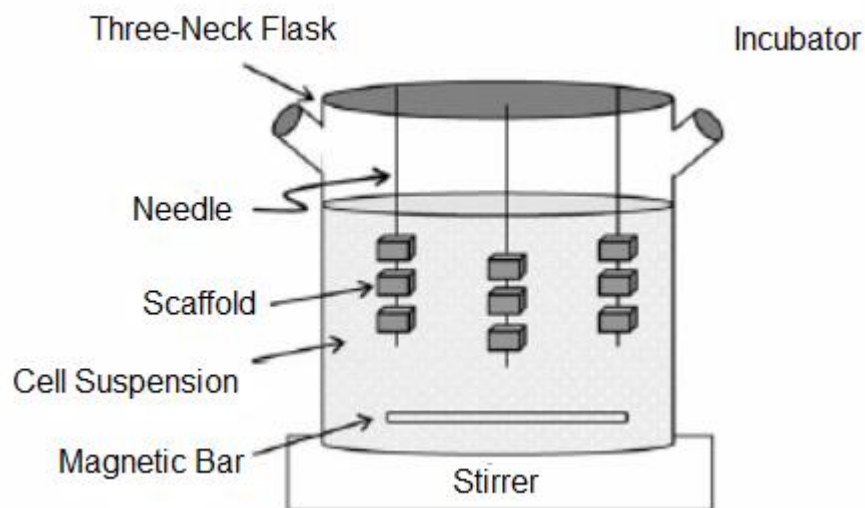
Figure 2.3; A spinner flask bioreactor. Scaffolds are secured in medium and the medium is stirred using a magnetic stirrer to improve nutrient delivery to the scaffold [57].

2.2.3.2. Rotating Wall Bioreactors

Rotating-wall bioreactors were first used in tissue engineering studies after being designed by NASA to be used in simulation applications of microgravity conditions. The culture medium

is continuously mixing by two horizontally positioned concentric cylinders at the same angular velocity [33,55]. When the velocity of the culture medium being rotated equals to the sedimentation rate, the cells are subjected to continuous free fall and low shear stress [33,48]. This free motion of the tissue scaffolds provides a microgravity environment, while the fluid flow created by the centrifugal force of the cylinder is counterbalanced by the gravitational force [58,59]. In Figure 2.4, a rotating wall bioreactor is presented schematically.
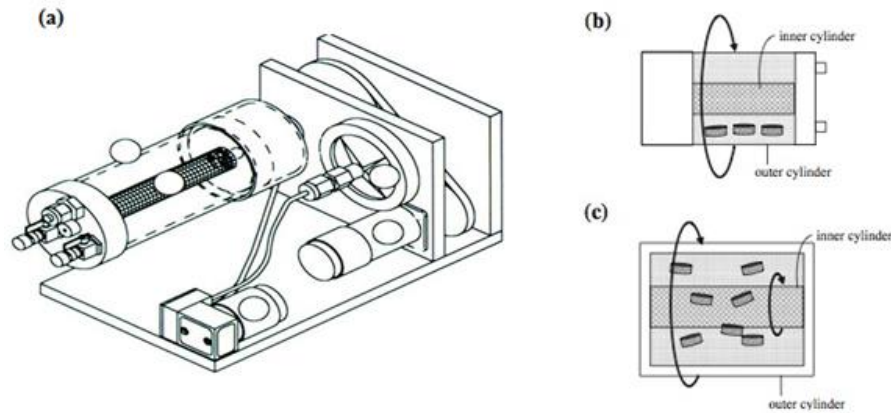
Figure 2.4; A schematic representation of a rotating wall bioreactor (a). Scaffolds are mobile in medium (b) and the rotation within the bioreactor improves the nutrient delivery rate to the scaffolds (c). [60]

2.2.3.3. Perfusion Bioreactors

Perfusion bioreactors provide a wide range of uses in tissue engineering. They supply flow through the pores in porous tissue scaffolds, and realize the necessary mechanical stimuli in this way [54]. It is a system that is able to provide flow-based bone regeneration that can overcome the mass transfer problems encountered in 3D cultures. Perfusion bioreactors are devices that can control physical operating parameters such as flow rate, flow direction and flow rate and provide physical stimulation that is more effective when compared to other designed bioreactors providing homogeneous cell distribution when the culture medium is merged with the continuous flow [56]. Perfusion bioreactor types are available in various designs. Some fundamental parts are commonly used throughout these designs that can be enlisted as the reservoir, the perfusion ring, the pump and the tubes that provide the connection. The most important part of the perfusion bioreactor assembly is the perfusion chamber where tissue scaffolds are maintained throughout the culture. The culture medium

flows through the pores of the scaffold past the connection points of this chamber and the sterility of the scaffolds along the flow is preserved [32]. Another important part is the multi-channel syringe pump, which allows operation at different flow rates and directions. With the aid of this pump, the flow rate and flow direction are automated, allowing the continuous monitoring of the flow rate from the front panel [61]. In Figure 2.5-A, a gap between the tissue scaffold and the circular walls can be observed, so the flow is seen to occur both inside and around the tissue scaffold. Thus, the physiological vasculature can be mimicked by the pore flow. In Figure 2.5 B, there is no gap between the tissue scaffold and the chamber walls, so the flow occurs only within the scaffold and does not provide natural physiological application [62]. The flow rate is the most important parameter in dynamic cell culture / culture studies to be performed with a perfusion bioreactor. Studies conducted at high flow rates do not allow to the cells enough time to adhere, which makes it difficult for the cells to attach to the surface and the seeding efficiency is reduced [54]. In bone tissue engineering studies conducted with stem cells, perfusion reactors are widely used and successful results are obtained [52, 63].
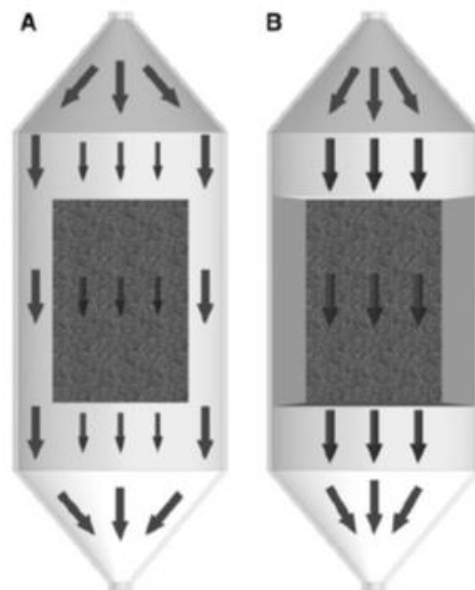
Figure 2.5 The perfusion bioreactor. Left : Schematic representation of (A) indirect perfusion, (B) direct perfusion [64].

2.2.4. Bioreactor Applications in Bone Tissue Engineering

The most comprehensive bioreactor studies in the relevant literature are, appropriately, on the comparison of the MSC's reproducibility and differentiation potentials in different reactors by using a tissue scaffold. In Table 2.4, examples of studies using bioreactors in bone tissue engineering are given.

Table 2.4 The related literature review using bioreactors in bone tissue engineering. [65]

Bioreactor Design	Results and Findings	References
Flow Perfusion Culture Bioreactor	Fluid flow was found to affect matrix deposition positively and promoted the osteoblastic differentiation of rat BMSCs.	Bancroft et al. 2002[66]
	Extracellular matrix on titanium scaffolds has promoted osteoblastic differentiation with shear stress and fluid flow.	Datta et al. 2006 [67]
	Calcium phosphate ceramics have enhanced the osteoblastic differentiation of rat BMSCs in flow perfusion bioreactor.	Holtorf et al. 2005 [68]
	Calcium deposition has been found to be promoted by the flow. Alkaline phosphatase expression and proliferation of rat BMSCs have been found to be affected by the porosity of the scaffolds.	Gomes et al. 2006/7 [69, 70]
	Flow perfusion has found to promote the osteoblastic differentiation of rat BMSCs in the absence of osteogenic supplements.	Holtorf et al. 2005 [71]
	Flow perfusion enhances the calcium production, proliferation and differentiation of rat BMSCs on nonwoven PLLA scaffolds and improves the cell distribution.	Sikavitsas et al. 2005 [72]
	Flow perfusion augments production and localization of various bone related growth factors: transforming growth factor-β1,A, fibroblast growth factor-2, vascular endothelial growth factor, and bone morphogenetic protein- 2	Gomes et al. 2006 [73]
	Flow perfusion bioreactor has contributed to the seeding potential of rat BMSCs in oscillatory flow setting.	Alvarez-Barreto et al. 2007 [74,75]
	Constant flow rate and increased shear stress has enhanced the matrix production in rat BMSCs.	Sikavitsas et al. 2003 [28]
	hMSCs have found to increase the expressions of bone morphogenetic protein 2, bone sialoprotein 2, Runt-related transcription factor-2 and alkaline phosphatase in correlation with fluid flow.	Bjerre et al. 2008 [76]
	Titanium fiber mesh scaffolds seeded with rat BMSCs and cultured in flow perfusion bioreactor has been successfully used in cranial defect model.	Sikavitsas et al. 2003 [77]
Radial Channel Perfusion System	A novel bioreactor has been used to promote the cell number and distribution and to investigate the osteogenic differentiation potentials of hMSCS on 3D scaffolds.	Grayson et al. 2008 [27]
	Radial channel has promoted the cell distribution and bone matrix formation of human adipose derived stem cells.	Frohlich et al. 2010 [13]
Complex Geometry Perfusion System	hMSCs cultured on a biomimetic scaffold-bioreactor system has enabled the production of bone grafts of non-uniform geometries.	Grayson et al. 2010 [78]
Central Tunnel Perfused Scaffold	The 3D flow perfusion system has enabled a constant and homogenous nutrient provision and proliferation for sheep MSCs seeded on β –tricalcium phosphate scaffolds of critical sizes.	Xie et al. 2006 [79]
	Shear stress has been found to promote osteoblastic differentiation of hBMSCs, mass transport has been found to promote differentiation in lower ranges.	Li et al. 2009 [80]
Indirect Perfusion Bioreactor	Dynamic approach proved to be more advantageous in terms of the proliferation compared to the static approach. Convergent flow gave better results than divergent flow, and homogenous cell distribution has been achieved.	Oliver et al. 2007 [81]
	The proliferation and osteogenic differentiation of human bone marrow-derived stromal cells (hBMSC) on membranes of mineralised collagen type I was investigated. In comparison with the cells cultured in tissue culture polystyrene, an increase in osteogenic differentiation of hBMSCs was detected, while a decrease was observed in proliferation rates. Perfusion of the 2D cell matrix constructs was found to be ineffective in terms of improving proliferation and osteogenic differentiation of the hBMSCs.	Bernhardt et al. 2008 [82]
	Osteoblastic differentiation was promoted in tubular perfusion culture in comparison with static culture due to the high alkaline phosphatase activation in 250 μm pore size group. Bone morphogenetic protein 2 was also found to be most prominent in 250 μm and 500 μm pore sized groups. Cellular response to pore size and the culture type were found to promote the effects given.	Pisanti et al. 2012 [83]
	Tubular perfusion bioreactor has enhanced bone tissue regeneration and has shown the importance of employing the appropriate bioreactor system to culture MSCS for bone tissue engineering.	Yeatts et al. 2014 [62]

(Continuation) Table 2.4 The related literature review using bioreactors in bone tissue engineering. [65]

Direct Perfusion Bioreactor	A homogenous cell growth and distribution of goat BMSCs wes successfully maintained and oxygen consumption was successfully measured during the experiment	Janssen et al. 2006 [84]
	Goat BMCSs on calcium phosphatase ceramic scaffolds cultured on a direct perfusion bioreactor has successfully produced relevant volumes of bone and has shown bone formation after its implantation into mice.	Janssen et al. 2006 [85]
	A semi-automated perfusion bioreactor system has found to be able to produce tissue engineered bone in mice after dynamic culture.	Janssen et al. 2010 [86]
Tissue Culture Under Perfusion	Tissue Culture Under Perfusion bioreactor system has enabled the formation of bone when implanted into mice.	Timmins et al. 2007 [87]
U-tube Cell Seeding Perfusion Bioreactor System	A bioreactor system that enables a continuous perfusion through the scaffold pores in oscillating directions has successfully improved cell viability, uniformity and increased the cell number.	Wendt et al. 2003 [88]
	Human BMSCs seeded directly on 3D scaffolds and expanded by perfusion culture, allowing a reproducible, uniform and efficient graft that has produced bone tissue when implanted into mice.	Braccini et al. 2005 [89]
Stainless Steel Perfusion Block	Higher proliferation was detected for lower flow rates while Runt Related Transcription Factor 2, Osteocalcin and Alkaline Phosphatase expressions relatively increased.	Cartmell et al. 2003 [90]
Axial Perfusion Bioreactor System	A micro-CT imaging based technique has been developed to measure the rate of mineralized matrix production of rat BMSCs over time.	Porter et al. 2007 [91]
Gradient Container	The viability of hMSCs lasted for 14 days in vitro and 12 weeks in vivo cultures.	Seitz et al 2007 [92]
	Perfusion system has highly prevented cell death in the central regions of 3D scaffolds due to hypoxia.	Volkmer et al. 2008 [93]
Perfusion Bioreactor System	Perfusion bioreactor system has found to promote the proliferation and differentiation of hTERT–hMSCs.	Yang et al. 2010 [94]
	Higher cell densities of hMSCs seeded in non-woven poly ethylene terephthalate fibrous matrices and cultured in 3-D perfusion bioreactor system have been reached after 40 days.	Zhao et al. 2005 [95]
	Higher metabolic rates and homogenous distributions of hMSCs in perfusion culture have been obtained and mathematical modelling has been established.	Zhao et al. 2005 [96]
	Shear stress has been shown to regulate the construction and differentiation of hMSCs.	Zhao et al. 2007 [97]
	The abundance of extracellular matrix proteins suggested that dynamic culture has promoted hMSCs to form organized matrix and their osteogenic ability.	Zhao et al. 2009 [98]
	Perfusion culture has promoted bone morphogenetic protein 2 expressions of MSCs cultured in PGA-reinforced sponge by the perfusion method due to the presence of a high amount of plasmid DNA.	Hosseinkhani et al. 2005 [99]
	The combination of plasmid DNA-impregnated PGA-reinforced collagen sponge and perfusion bioreactor has enhanced the gene expressions for rat MSCs.	Hosseinkhani et al. 2006 [100]
	The combination of MSC-seeded collagen–PGA scaffolds and perfusion bioreactor was found to promote the osteogenic differentiation in ectopic rat model.	Hosseinkhani et al. 2006 [101]
	The perfusion culture system has enabled the of bone marrow derived osteoblasts in a porous ceramic scaffolds to present a higher alkaline phosphatase and osteocalcin expressions, alongside with a significant enhancement in bone formation.	Wang et al. 2003 [102]

2.3. Computational Fluid Dynamics in Bone Tissue Engineering

2.3.1. Computational Fluid Dynamics

Partial differential equations are used to express the laws of conservation of mass, momentum and energy to solve problems related to fluids. Computational Fluid Dynamics (CFD) can be defined as an analytical approach to solving these equations only with special conditions and assumptions.

Fluid motion is encountered in almost all areas; Heat exchangers, chemical reactors, automobile engines, meteorological phenomena, and the functioning of the human body. In computational fluid dynamics studies it is possible to perform both qualitative and quantitative analysis of flow by using mathematical modeling, numerical methods and computer software [103].

It can be said that scientists and engineers can do numerical experiments through computer simulations. In order to be able to identify the flow in laboratory experiments, a limited number of measurements can be taken in small scale systems under certain operating conditions. Repeatability of the experiments is reduced due to measurement errors and changes occurring in the system when measurements are made. In simulations that are accomplished with computational fluid dynamics, it is possible to estimate the values that would be taken under different conditions for real flow problems without any size and time constraints. Simulation studies are multi-purposed as well as a much cheaper and faster application, but it is not possible for simulations to take full advantage of experimental approaches, for the reliability of CFD simulation results is never 100%. The fact that the mathematical model is insufficient to identify the real problem, the number of predictions made when inputs are determined, and the power of the computer used for simulation can reduce the accuracy of the results. With the use of CFD simulations, however, it is possible to reduce the number of experiments and the total cost [104].

It is necessary to have some important knowledge about the flow to handle a problem using the computational fluid dynamics. For systems that are not steady or unsteady, the flow is compressible or incompressible, and the formation of laminar or turbulent profiles in single-phase or multiphase flows affects the success of the simulation. It is possible to say that modeling is easier in systems where there is no laminar flow, single phase and chemical reactions [104].

The first step for simulation is to create a mathematical model. Fort his purpose, the proper flow model should be chosen and the forces that cause motion and the geometry of the calculation must be determined. At the last stage, mass, momentum and energy conservation equations should be formulated and boundary conditions defined. In order to solve the functions and partial differentials found in the equations of the model with computer software,

these equations need to be transformed into a form that the computer can process. The process of transforming partial differential equations into a group of algebraic equations is called "discritization" [105].

There are four basic methods of discritization that are used to solve engineering problems: finite difference method (FDM), finite element method (FEM), boundary element method (BEM) and finite volume method (FVM). In the finite element method (FEM), the intermediate values of the physical variables are located on the solution domain. Boundary conditions are fully provided, while field equations are approximate [105]. Today, there are many commercial CFD software such as COMSOL, FLUENT and ANSYS CFX. FLUENT uses finite volume method, while discritization is performed by the finite element method in ANSYS and COMSOL software [103,106]. Computational fluid dynamics are important in spatial approaches Periodic discritization, mesh (network structure) selection and installation equations. Detailed information is provided in the following sections.

2.3.2. Spatial Discritization

Simultaneous solution of partial differential equations is carried out in researches on three dimensional transport. While there is no analytical solution to all equations, the use of complex techniques for analytical solutions is also unnecessary. Numerical techniques enable more direct and faster solution. However, with numerical techniques, approximate results are achieved instead of actual results. For an accurate solution, the following steps must be fully implemented in all CFD simulations: (i) the creation of geometry accurately, (ii) the division of the system into a correct and feasible number of elements so that numerical calculations can be performed, (iii) choice of mathematical models that estimates the system best, (iv) the computational fluid dynamics in tissue engineering, appropriate boundary conditions [107].

In order to apply numerical methods, it is necessary to divide the system area into smaller pieces. The process of discritizing the solution area into smaller nodes is called "hanging" or "grid production" in numerical calculation and CFD language. Using discretized states of the conservation equations, solutions are made for each node in the system according to the conditions of the environmental nodes [105].

2.3.3. Determination of Mesh Size and Asymmetrical Meshing

The computational fluid dynamics technique is based on partitioning of the solution area into smaller elements and analyzing each element separately, according to the conditions of the neighboring elements. In plane problems; Triangular, quadrilateral, polygonal elements are used, and the edges of these elements can have a straight or curved shape. Four-sided, six-sided, and parallel prism elements are commonly used in three-dimensional problems [107]. Figures 2.6 a and b show examples of elements used for 2D and 3D systems.
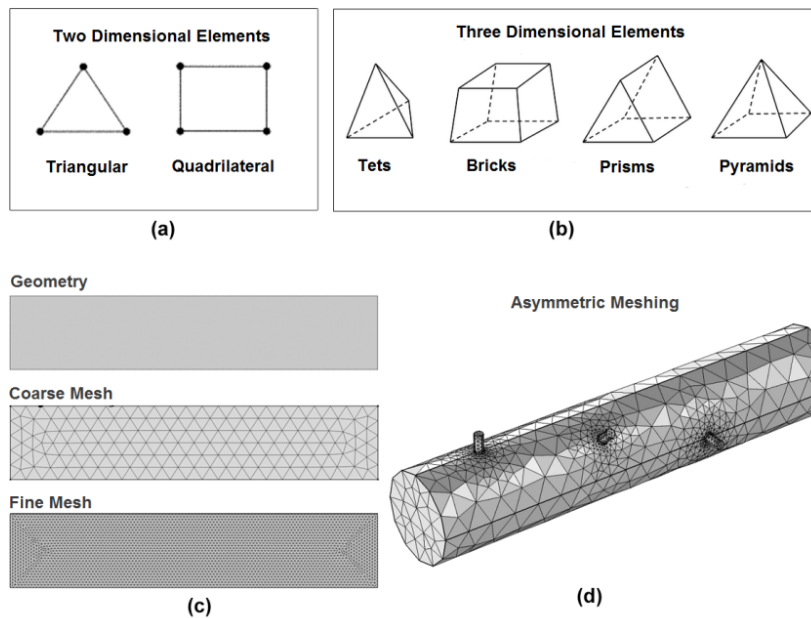
Figure 2.6; Two dimensional elements in CFD (a), three dimensional elements in CFD (b), mesh types in CFD (c), an example of asymmetric meshing (d). [108]

The accuracy of computational fluid dynamics simulations depends on the degree of discritization of the solution. The use of large mesh sizes leads to inaccurate, misleading and inadequate solutions. The reason for this is that when the element size is large, the system areas where the solution is constructed are far from each other. By reducing the element size, more localized solutions can be obtained so that the accuracy of the calculations and the resolution area have sufficient resolution. Although small mesh sizes allow us to achieve more accurate and accurate results, the availability of more elements in the system area increases the number of calculations required to achieve results, and therefore the need for computational

resources. For this reason, it is necessary to determine the most suitable mesh size in terms of resolution as well as the required source [37]. Figure 2.6.c shows images of the lattice structures obtained by using large and small elements of the rectangular geometry created in a 2D system. Because of the high aspect ratio of the tissues in general, the possibility of asymmetric meshing in CFD applications is very important in terms of tissue engineering researches. When asymmetric meshing is used, large elements are used in low-activity (low-gradient) regions, while regions where rapid change occurs can be divided into smaller elements (Figure 2.6 d).

2.3.4. Grid Independence

Grid independence is a matter of direct mesh size selection. Mesh size selection is a trial-and-error procedure without exact rules, so when selecting the node size, a good prediction is needed and the results are not guaranteed to be correct. For this reason, it is necessary to repeat the solution by reducing the mesh size and to compare the obtained results with the previous ones. If the difference between the two solutions is within a certain range of tolerance, then the ideal mesh size is reached. Thanks to the latest developments in CFD packages such as COMSOL, mesh selection can be done automatically. New meshing algorithms can detect areas that require higher resolution within the solution area and can re-adjust mesh size.

2.3.5. Periodic Discritization and Time Sequence

Due to its inherent transitional process, in studies on tissue regeneration, solutions are needed that can show the system change over time. This need makes periodic discritization as important as at least spatial discritization. The more critical the mesh size selection is to reach the right solutions, the more the time step values are determined. Incorrectly chosen time steps lead not only to incorrect solutions, but also to problems of convergence and unreasonable results such as negative concentration [107]. The time step (Δt) has been investigated deeply in the CDF literature for non-decentralized solutions and various rules have been established in order to be able to find the maximal Δt as a function of the mesh size.

The most general suggestions are:

(i) a typical particle moving in the system domain should not pass from one element to another within a time step,

(ii) a particular particle should not be diffused farther than an element in a time step,

(iii) momentum should not diffuse farther than an element in a time step.

In addition to these rules, maximum time step values can be calculated from the setup equations. For systems with transient behavior, the time step value should be optimized separately from the mesh size [107].

2.3.6. Determination of Installation Equations

Many researchers have benefited from the CFD to be able to examine the effects of flow field distributions in bioreactors. In addition to these workflows, where flow profiles and shear stresses are often computed, more recently, more complex approaches have been developed to account for changes in the permeability of scaffolds, cell growth kinetics and different geometric configurations due to tissue formation. The selection of the mathematical model is extremely important because it expresses the events taking place in the system. A model with unknown parameters or an incorrectly selected model can cause both invalid results and invalid solutions.

2.3.6.1. Flow Characteristics

In bioreactors, knowing the range of values of typical operating parameters such as pressure drop and flow rate is of great benefit in that optimum values can be found. Due to the characterization of flow characteristics, optimal values for cell migration, differentiation and extracellular matrix accumulation can be selected and shear stress, mass transfer and flow fields can be calculated. These approaches are also very important for bioreactor design. The bioreactor geometry can be determined using the computational fluid dynamics, and the positions and sizes of the inputs and outputs can be optimized.

Navier-Stokes equations (Equation 2.1) are used for the characterization of flow in bioreactors.

$$-\frac{\nabla p}{\rho} + \nabla.\left(\frac{\eta}{\rho}\nabla u\right) - u.\nabla u = \frac{\partial u}{\partial t} \qquad \text{(Equation 2.1)}$$

η represents dynamic viscosity (Pa·s); u reperesents the linear flow velocity in open channel (m/s); ρ represents the density of the fluid (kg/m^3) and p represents the pressure (Pa). The Navier-Stokes equations for the laminar flow profile in perfusion bioreactors and rotary bioreactors are easily applied. However, turbulent flow generally occurs in confounding cap bioreactors. Various approaches are used to model the effect of turbulence in the computational fluid dynamics. Studies conducted with the k-w model or other Reynolds Stress Models (RSM) developed to add the kinetic energy and propagation of turbulence to the account have been published [31,107].

2.3.6.2. Porous Media

Simultaneous modeling of free and porous media effects in the characterization of flow is a widely used approach because of the usage of porous tissue scaffolds in tissue engineering bioreactors. The most common method for matching flows in free and porous media is the use of Darcy equation [41,107]. In low Reynolds numbers in porous media, the Darcy equation connecting the drive power and the flow for laminar single-phase flow is given in Equation 2.2.

$$u = \frac{\kappa}{\eta}\nabla p \qquad \text{(Equation 2.2)}$$

κ represents, the permeability (m^2) of the porous media.

In Darcy's law, there are no viscous effects caused by the free-air flow, which can show various effects on the interface of free and porous media. For this reason, Darcy equation can reduce the flow model very much, depending on the properties of the fluid, the size and distribution of the pores. Brinkman equations are anticipated as an extension of Darcy's law and allow continuity for velocity and shear stresses at interfaces [41,107]. The Brinkman equation given in Equation 2.3 includes both viscous and drag forces. Thus, when permeability reaches infinity in the free environment, equation becomes Navier-Stokes equality.

$$\frac{\eta}{\varepsilon_p}\nabla^2 u - \frac{\eta}{\kappa}u = \nabla p \qquad \text{(Equation 2.3)}$$

ε_p represents porosity (non-dimensional).

2.3.6.3. Modelling of Nutrient Transport

One of the most fundamental aims of tissue engineering bioreactors is to renew the culture medium and provide the necessary nutrients to developing cells and tissues. Mass transfer in bioreactors occurs through two mechanisms depending on flow characteristics: convection and diffusion. In systems where the flow dominates, the mass transfer can be modeled by the convective-diffusion equation given in Equation 2.4. According to this equation, the concentration changes are not only due to diffusion, but also due to the larger gradients at which the flow is caused. The convective-diffusion equations (Equation 2.4) are combined with the Navier-Stokes equations (Equation 2.1) in order to find the nutrient distribution in the bioreactor.

$$\nabla.\left(-D_{A,B}\nabla c\right) + u.\nabla c = r_A \qquad \text{(Equation 2.4)}$$

c represents concentration (mol/m^3); $D_{A,B}$ represents the diffusion coefficient (m^2/s); r_A represents the net reaction rate for the component.

The reaction rate constant given in Equation 2.4 shows the rate of food consumption in the reactor. Several studies have been conducted to investigate cell population dynamics or oxygen consumption in porous media [107]. In some studies, the metabolic rate of consumption of glucose, lactate, or oxygen was found in the Michaelis-Menten equation (Equation 2.5).

$$-r_A = \frac{V_m c_A}{K_m + c_A} \qquad \text{(Equation 2.5)}$$

V_m represents the maximum rate of consumption (mol/m^3·s); K_m represents the Michaelis-Menten constant (mol/m^3).

However, in order to benefit from the Michaelis-Menten equation in computational fluid dynamics models, the cell properties (V_m, K_m) that are studied must be achieved by using experimental methods.

2.3.7. Computational Fluid Dynamics Applications in Tissue Engineering

In order to better understand the effects of different flow regimes and shear stresses on the cell proliferation and osteogenic differentiation behavior in the bioreactor, the hydrodynamic conditions of the bioreactors should be quantified and evaluated together with the experimental data. The ability to establish a relationship between the operational parameters of bioreactors and cell migration / differentiation using CFD is of great importance in terms of in vitro production of functional tissues as a tissue engineering product [26]. Although there are experimental techniques such as LDA (Laser Doppler Anemometer) or PIV (Particle Image Velocimetry) to characterize the flow within a bioreactor, CFD is considered as one of the most important techniques in terms of being able to simulate 3D flow in a short time and to be expressed with visual arguments. In this method microenvironments affecting tissue scaffolds and cells can be identified by taking advantage of the basic mass and momentum equations [31, 33].

Maes et al. (2009) compared the wall shear stresses of scaffolds with different porosity properties in the perfusion bioreactor using the CFD model [90]. Yan et al. (2011) modeled the flow in two different bioreactors, both perfused and non-perfused, based on a tissue scaffold produced by rapid prototyping. While high shear stress values are calculated in the perfusion system due to the flow through the pore, it has been found that the pores of the scaffold are exposed to very small shear stresses in the perfusion-free system where the culture medium is drained around the tissue scaffold [109]. In a study investigating the effect of flow on cell adhesion, the complex mechanical properties of cells were simplified through a linear elastic model, and the effect of varying flow rate on the perfusion bioreactor on the disruption of the cell surface was investigated [110]. In 2009, Cinbiz et al. published the CFD model using the Fluent software and evaluated the results obtained from the model with the experimental results and discussed the usefulness of the rotary wall bioreactor for cartilage tissue engineering [33]. It is important to calculate the gas and nutrient concentrations as well as the effect of flow and mechanical stimulation in the computational fluid dynamics models.

Model validation is also possible by adapting appropriate sensor systems to bioreactors [111].

Table 2.5 provides examples of CFD approaches used in tissue engineering applications

Table 2.5 CFD approaches used in tissue engineering applications in related literature.

Study	Conclusion	Reference
The flow in a percolation porous structure by direct simulation was performed.	The impact of stagnant zones within an irregular scaffold structure was modelled and found to influence the overall flow field of the system.	112
Multiple numerical simulations in conjunction with their experiments to verify the orbit of microcarrier beads within a rotating bioreactor vessel was performed.	Managed to establish a basic relationship between the density of the microcarrier beads, the surrounding fluid's density, and the resulting orbits of the beads.	113
Applied Fluent CFD models to calculate flow fields, shear stresses, and oxygen profiles around nonporous constructs which simulated cartilage development in a concentric cylinder bioreactor.	From these computational modelling studies they concluded that these values are above oxygen concentrations in cartilage in vivo, suggesting that bioreactor oxygen concentrations likely do not affect chondrocyte growth.	32
Developed equations based on the level-set principle to model fluid flow as well as to estimate soft tissue growth within a bioreactor.	The level-set method provided higher levels of accuracy, proved to be quite complex and not always feasible to apply.	114
Experimented on the CFD model based on the bi-axial bioreactor rotation.	Demonstrated that bi-axial bioreactor rotation enhances fluid flow within the vessel and the scaffolds positioned within the vessel.	115
Experimented on the CFD model based on a home made wavy-walled spinner flask in order to evaluate its functionality.	Verified the efficacy of a home made wavy-walled spinner flask using CFD by investigating and characterizing the flow regimes within their system, which were found to support cell proliferation by enhancing fluidic transport and stimulating matrix deposition of chondrocytes.	116
Developed a CFD model of culture medium flowing through a 3D scaffold of homogeneous geometry, with the aim of predicting the shear stresses acting on cells as a function of other parameters, such as scaffold porosity and pore size, as well as medium flow rate and the diameter of the perfused scaffold section.	The shear stress field is mapped for each fluid domain obtained from the histological images. The simulations showed that the pore size is a variable that strongly influences the predicted shear stress level, whereas the porosity is a variable that strongly affects the statistical distribution of the shear stresses, but not their magnitude.	117
Experimented on FEMLAB to utilize the distribution of the nutrients in the culture medium.	Utilized a FEMLAB code to model the rate of nutrient uptake in the culture of bone tissue with respect to their hollow-fibre membrane bioreactor.	118
Stated that vortex breakdown flows may enhance the mixing of culture media by presented a different perspective on the fluid-mixing phenomena within a spinner flask .	Discovered that profile and intensity of these fluid recirculation regions are highly Reynolds number dependent	119
Experimented on a comprehensive tissue-growth model in order to overcome the problem of the complexity of the biological processes and a relative lack of experimental data needed for validation,	Presented a 3D model based on cellular automata able to simulate the all he of a cell population taking into account cell division, migration, different seeding modes and contact inhibition.	120
Experimented on the environment all he cartilage constructs by redefining the geometries all he spinner flask and two different configurations of the wavy-walled bioreactor.	Characterized the complex hydro dynamic environment and examined the changes in the flow field due to the different positions of tissue-engineered cartilage constructs.	121

(Continuation) Table 2.5 CFD approaches used in tissue engineering applications in related literature.

Experimented on the development of a CFD model coupled with the cellular automation algorithm based on this background.	Succeeded in creating a model that studies in vitro tissue growth and is able to account for both cell migration and the cellular microenvironment, as created by the perfusion bioreactor system (e.g. nutrient and oxygen transport, mechanical stimuli).	122
Combined partial differential equations and the mixture theory, which was originally derived from the general theory of multiphase porous flow, where tissue, water and solid scaffold are modelled as different phases.	Successfully created a model that is able to account for tissue–tissue, tissue–water and tissue–scaffold interactions that makes it possible to acquire a viable alternative to tissue-growth models based on cellular automata which leads to the conclusion of the mentioned approach constituting a viable alternative to tissue-growth models based on cellular automata,	123
To construct the model geometry with μCT data and to calculate the all shear stresses affecting tissue scaffolds in the perfusion bioreactor.	The importance of all sheer stress has been emphasized. When it comes to evaluate all of the μCT data, the consumption of excessive time and resources has been verified. It has been discovered that when there are cells on the scaffold, the change in the flow can be neglected.	124
Calculation of the shear stresses that is affecting the cells in chitosan tissue scaffolds cultured in a rotating all bioreactor.	The shear stress values in the rotating bioreactor were found to be low, consistent with the literature. The lateral regions of the tissue scaffolds were found to be subjected to high shear stress, while the upper surfaces were found to undergo lower shear stress. The advantages of the bioreactor in the oxygen transfer model operating in continuous operations have been observed.	33
To demonstrate the advantages of the rectangular channel and the uniform distribution of forces and flow on the cylindrical cartridge structure in conventional perfusion reactors.	More uniform flow and shear stress were obtained in the rectangular channel. In perfusion reactors, it has been found that the flow must reach a certain distance before it reaches the scaffold. It is stressed that Stokes and Darcy equations are difficult to apply together and that Brinkman is a better model.	125
Characterization of flow in the scaffold under the conditions of perfusion and non-perfusion systems.	Lower shear stress is obtained in non-perfusing systems. It has been discovered that the flow model is much easier to create on CAD-designed scaffolds. The shear stresses and velocity profiles varied as the size of the geometry changed.	109
The characterization of the flow in the spinner flask bioreactor was evaluated by means of two different meshing methods and collecting the experimental data by using μPIV.	PIV data appeared to be more consistent with the immersed solid mesh method. The importance of evaluating different turbulence and meshing methods for turbulence has been emphasized. It has been seen that PIV is an important technique for model validation.	126
Investigation of the effect of media flow rate and pore size on cell adhesion and cell surface removal in a perfusion bioreactor.	A realistic mathematical model was created using experimental data. It has been found that the disconnection of the cell from the surface is inversely proportional to the flow velocity and to the pore size. It is emphasized that the model can be used for optimizing the operating parameters in perfusion reactor studies.	110

3. RESEARCH METHODOLOGY AND THEORY

In this section, the information about the experimental studies carried out within the scope of thesis is presented. In the first chapter, the information about the chemical and biological materials used in the studies was given. In the second chapter, general information about the production procedure of chitosan-HA SPHCs and the cell model used in experimental studies are presented. In the third and fourth chapters, components of the perfusion bioreactor and different mechanisms established for cell culture are described and sterilization studies are presented. In the fifth chapter, cell seeding and culture studies for human mesenchymal stem cells were carried out with tissue scaffolds of different sizes (P3D-6 and P3D-10) in the perfusion bioreactor have been included. Finally, in the last chapter, information about the modeling of computational fluid dynamics for the simulation of flow and mass transfer in perfusion bioreactor is presented.

3.1. Materials Used in Experimental Studies

Chitosan (75-85% deacetylation) was obtained from Aldrich (Germany). Glyoxal 40% aqueous solution (Aldrich, Germany) was used as the cross-linker, and sodium bicarbonate (NaHCO$_3$) was used as the gas foaming agent (Merck, USA). Acetic acid was obtained from Riedel de Haen (USA), spherical hydroxyapatite (HA) particles ranging in size from 55 to 110 µm were obtained from Science Application Industries, France. Sterile Dulbecco's Phosphate Buffered Saline (DPBS, pH:7.4), Minimum Essential Medium Alpha Modification (α-MEM) cell culture medium, fetal bovine serum (FBS), trypsin/EDTA solution and amphotericin-B (pH 7.4) which are used in cell culture were obtained from Hyclone (ABD). MTT (3- (4,5-dimethylthiazol-2-yl)-2,5-diphenyltetrazolium bromide) solution used for cell viability analysis, penicillin-streptomycin, β-glycerol phosphate salt, L-ascorbic acid and dexamethasone were purchased from Sigma (Germany). Twentyy-four well tissue culture polystyrenes (TCPS) were purchased from Nunclon Delta Surface (Denmark).

In all experimental studies conducted, hMSCs which were in stock and readily available in our laboratory were used. The hexamethyldistilazane (HMDS) used for sample preparation for SEM analysis were obtained from Sigma, (Germany). Cell culture dishes of 75 cm^2 and 150 cm^2 were obtained from Orange Scientific (Belgium). Samples for RT-PCR analysis were
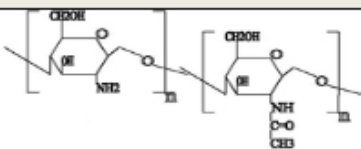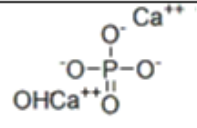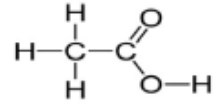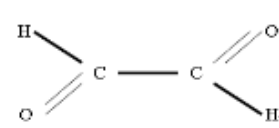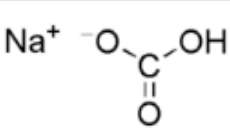
stored in Trizol (Invitrogen, USA) at -80 ° C until the analysis took place. Expression levels of Col 1, RUNX2, OCN, and OPN were determined by RT-PCR analysis to determine osteogenic differentiation.

3.2. Production and Characterization of Chitosan-HA SPHCs

Chitosan-HA tissue scaffolds were produced using microwave effect and gas foaming method [32]. A 2% (w/v) chitosan solution for the production of tissue scaffolds was obtained by dissolving chitosan solution in 1% (v/v) acetic acid for 1 day using a magnetic stirrer. After addition of HA microspheres (50 mg/mL) to the chitosan solution, homogeneous distribution of the HA particles in the solution was achieved by mechanical stirring. Subsequently, glyoxal (2 µL/mL) was added as a cross-linker and $NaHCO_3$ (3 mg/mL) as a foaming agent and the homogenization of the contents was achieved with a mechanical stirrer. The resulting mixture was dispersed in the wells of multi-well culture vessels and then quickly put into a microwave synthesis oven (Milestone, Italy) for 60-90 s and programmed at 90 Watt (W). At the end of the specified time period, foam formation and gelation were observed. Ethanol, 96% (v/v), was added to the specimens so that the removal of the hydrogels from the wells were facilitated. As the water molecules in the hydrogels transposed with the alcohol molecules which led to a diminution in volume the shrinking hydrogels were easily removed from the wells. Hydrogels which removed from the wells were swollen in pure water to remove unreacted cross-linker and other impurities. The resulting hydrogels were kept at -20 ° C for 1 day and then lyophilized for 4 days at -80 ° C in a freeze-drying apparatus (Christ, Germany) for complete drying, and then were allowed to stand overnight in 96% ethanol (v/v) to stabilize them. The hydrogels were then dried for an additional 1 day to remove ethanol from the constructions. After the hydrogels were completely dried, they were cut to have a diameter of 6 mm, a height of 3 mm and a diameter of 10 mm and a height of 3 mm, respectively, according to the dimensions of the perfusion ring (P3D-6 and P3D-10). The materials used in the production of chitosan-HA tissue scaffolds are summarized in Table 3.1, and the chitosan-HA production steps are schematically summarized in Figure 3.1

Table 3.1. Chitosan-HA SPHC Production Materials and Quantities

Name of the Chemical	Purpose of Use	Chemical Structure	Amount
Chitosan (75%-85% deacetylated)	Polymer		2% (w/v) Chitosan Solution
Hydroxyapatite (HA) (55-110 μm)	Composite agent		50 mg/mL
Acetic acid	Solvent		100 mL
Glyoxal (40% aqueous solution)	Cross-linker		2 μL/mL
Sodium bicarbonate (NaHCO₃)	Foaming agent		3 mg/mL

Chitosan Solution
Hydroxyapatite
Glyoxal
NaHCO₃

Microwave-Assisted Fabrication of Chitosan-Hydroxyapatite Super Porous Hydrogel Composites (Chitosan-HA SPHCs)

24-Well Tissue Culture Plate

Microwave
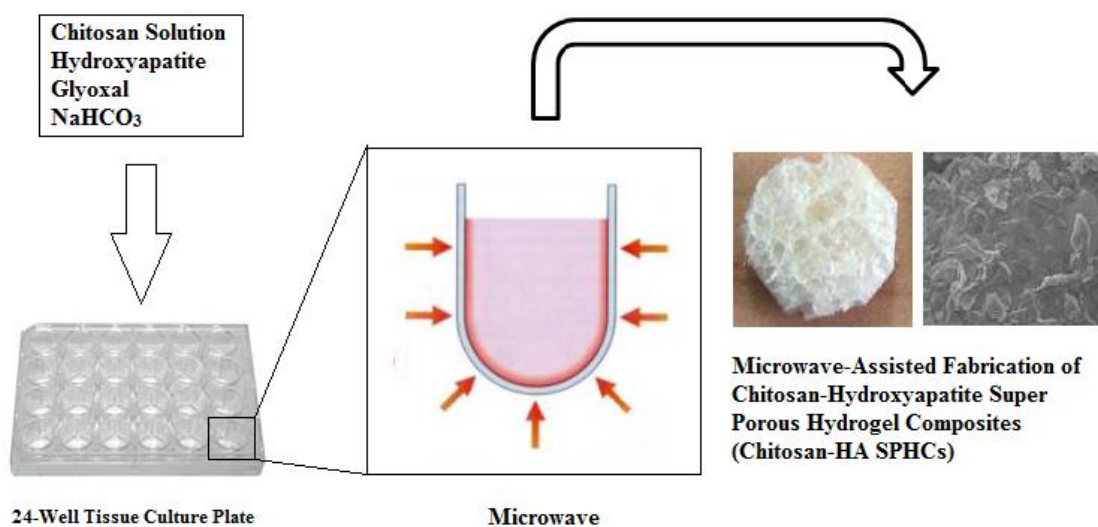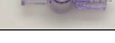
Figure 3.1 Production stages of chitosan-HA tissue scaffolds

Characterization studies of synthesized hydrogels have been carried out within the scope of previous publications of our group [32]. In this study, the polymer-particle interactions of the hydrogels were investigated in terms of pore sizes, densities, void fraction, swelling ratio, compression modulus, decomposition temperature, mechanical lutaral with ATR-FTIR (Attenuated Total Reflectance Fourier Transform Infrared) and the HA incorporation properities were investigated with Micro-Computerized Tomography (μCT).

3.3. Installation of Perfusion Bioreactor System

The perfusion bioreactor system is designed in a structure that can overcome mass transfer problems and prevent leaks for a long-term usage in vitro culture studies that require dynamic cell cultivation and sustainable sterility. New Era (USA) multichannel syringe pump, which allows the flow rate and direction of the bioreactor setup to be programmed, alongside with P3D-6 and P3D-10 perfusion circles, which are designed from transparent material specially developed for cylindrical tissue scaffolds by EBERS (Spain), where tissue scaffolding will be installed, ready sterile and easily integrated into the system, providing a safe environment for manipulation during application and tissue scaffolding, disposable sterile materials and autoclavable parts ensure that the system is handled conveniently. All the parts of the perfusion bioreactor assembly are presented in detail with their visuals, intended use and suppliers in Table 3.2.

Table 3.2 Perfusion Bioreactor Parts

Eqipment (Visual)	Material	Company	Purpose of Use
	Syringe Pump	New Era (USA)	The main part that provides control of the media flow rate and direction. Allows to work with 8 lines.
	Perfusion Chambers (P3D-6, P3D-10)	EBERS (Spain)	Provides a sterile and safe culture environment for tissue scaffolding through its sterility, contamination prevention, leakage inhibition, transparent structure, manipulation and ease of placement in the system fort he cylindrical scaffolds.
	Platinized silicon tubings (0.76 mm and 1.6 mm inner diam.)	Cole Parmer (USA)	Provides the connection between the system components. The lengths are arranged according to the distances between the perfusion ring and other system components.
	Female and male luer locks (suitable for tubes with 0.76 and 1.6 mm inner diam.)	Value Plastics (USA)	Provides connectivity to other components of the system. Female and male luer locks are connected to each other and provide sealing to the system.
	Luer Lock Syringe	Fisher Scientific (USA)	Gives sealing to connections in system via luer lock and prevents the deterioration of the sterility.
	Needle-free valve (Smartsite)	Smiths Medical (USA)	Allows the system to remain sterile during media change and manipulation of links.
	One-way valve	Fisher Scientific (USA)	Prevents the uncontrollable flow of the culture medium when the pump is switched off.

(Continuation) Table 3.2 Perfusion Bioreactor Parts

	Four-way valve	Fisher Scientific (USA)	Used to place hydrophilic and hydrophobic filters in the perfusion line.
	Hydrophobic filter	MilliPore (USA)	Enables the removal of air bubbles from the system and enables gas exchange in the ambient reservoir.
	Hydrophilic filter	MilliPore (USA)	Hydrophilic filters are used to keep the culture medium sterile during cell culture.
	Falcon 50 mL conical tube	Fisher Scientific (USA)	Serves as a reservoir for the pumped and withdrawn culture medium for bi-directional perfusion system

3.4. Sterilization Procedures

For sterilization of tissue scaffolds, the size of the perfusion ring was taken into account and the samples cut at 6 mm diameter and 3 mm height and at 10 mm diameter and 3 mm height were stored in 70% (v/v) ethanol. The samples washed with sterile DPBS (pH: 7.4) were then treated with UV light for 30 minutes each side. Sterilized hydrogels were conditioned for 1 night in α-MEM containing 10% (v/v) FBS and 1% (v/v) penicillin-streptomycin and were made ready for cell culturing. All procedures requiring sterile media were carried out in a laminar flow cabinet (Bioair, Type II Laminer Flow Cabinet, Italy).

The luer-tipped syringes used in the perfusion bioreactor assembly, single and four-way valves, smart-site needle-free valves, hydrophilic and hydrophobic filters, perfusion rings and luer-ended syringe needles were commercially obtained in sterile packages. Platinized silicon tubings were cut in the appropriate length prior to the experiment and sterilized by autoclave for 20 min at 121 ° C in autoclave bags with female/male luer lock connections as required by the perfusion line.

3.5. Cell Seeding and Cell Culture Studies

In the experimental studies that are carried out under static and dynamic conditions, chitosan-HA SPHCs were used as tissue scaffolds. Cell seeding and culture studies for human mesenchymal stem cells were carried out with tissue scaffolds of different sizes (P3D-6 and P3D-10). Cell seeding studies were carried out statically in TCPS and human mesenchymal

stem cells were seeded in growth medium for 5 days. Afterwards, the growth medium was replaced with the differentiation medium. Cell culture studies were divided into three main categories: monolayer, static and dynamic cell culture. All cell seeding and cell culture studies were performed within the scope of the thesis are summarized in Figure 3.2.
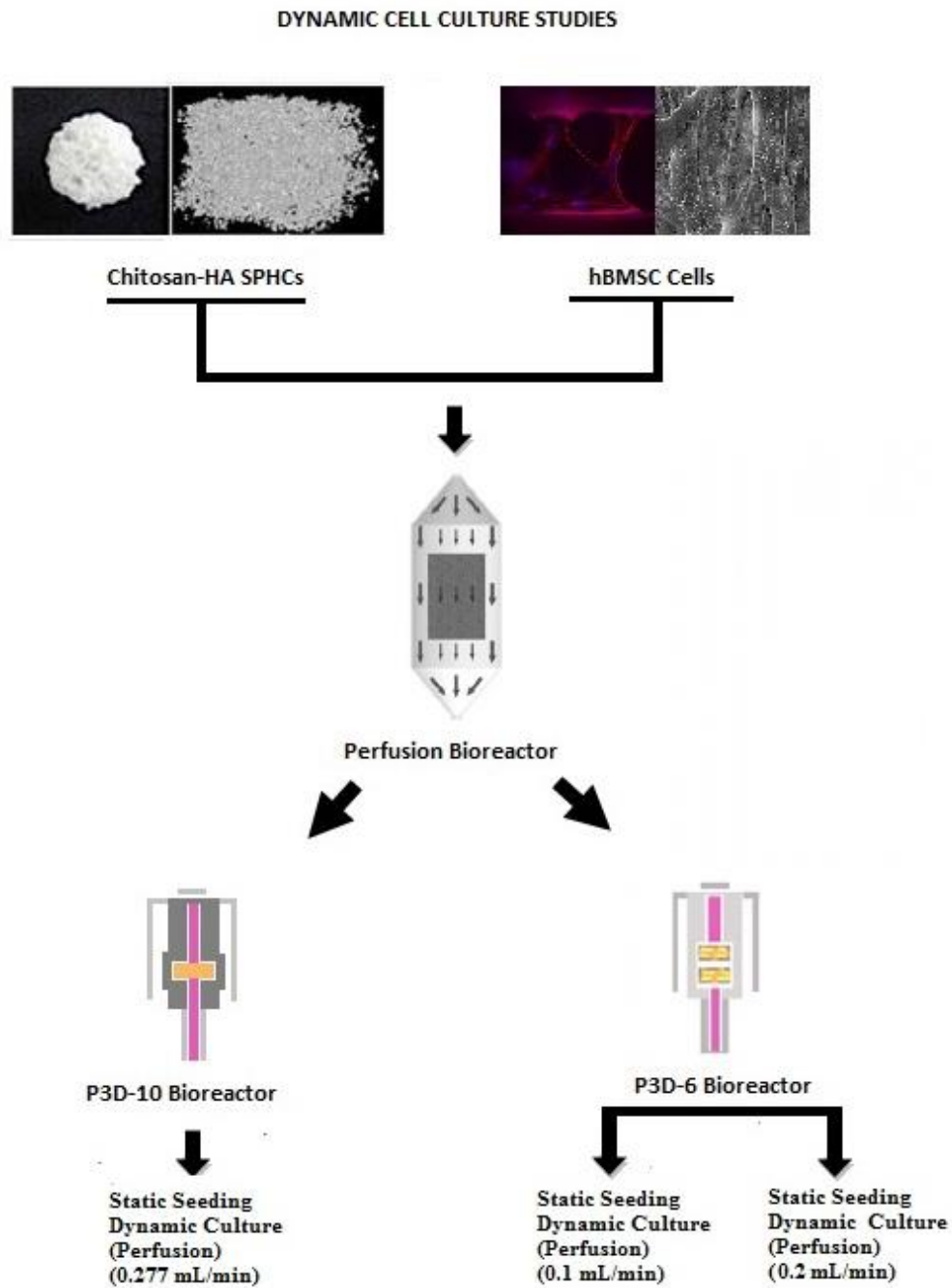
Figure 3.2. Cell culture studies within the scope of the thesis.

3.5.1. Static Cell Seeding Studies

Static cell seeding studies were performed in 24-well TCPSs. The 8th passage of hMSCs which were stocked in the liquid nitrogen tank, were seeded in flasks in a cell-growth medium consisting of hMSCs, α-MEM, 10% (v/v) FBS, 1% (v/v) penicillin-streptomycin and $0.04\,\mu L$ bFGF (Basic fibroblast growth factor).

When cells formed the saturation layer they were detached from the surface by trypsinization process. Then, cells were counted via hemocytometer after staining with trypan blue.

Cell counting was performed to distribute 50 µL cell suspension to each scaffold, with the required dilutions giving an inoculation density of 5×10^5 cells/scaffold. Samples were cultured at 37 ° C in a CO_2 incubator.

After 3 h of incubation for cell adhesion, 1 mL fresh medium was added to the seeded cells. Mitochondrial activities of cells were evaluated by MTT assay, cell adhesion and morphology were visualized by SEM analysis.

3.5.2. Cell Culture Studies

3.5.2.1. Monolayer Cell Culture Studies

To examine the proliferation behavior of the cells in monolayer cultures, the hMSCs in passage 8 were seeded with 24-well TCPS surfaces at an inoculation density of 1×10^4 cells/well and cultured for 26 days. Cell culture was carried out using growth medium in stationary conditions and starting from day 5, osteogenic differentiation medium (0.05 mM L-ascorbic acid, 10 mM beta glycerol phosphate salt, 100 nM dexamethasone, 10% (v/v) FBS and 1% (v/v) penicillin-streptomycin, and alpha-MEM containing 0.6% (v/v) L-glutamine, 0.4% (v/v) gentamycin, 0.4% (v/v) amphotericin B) replaced the culture media. Cell viability was monitored by MTT assay every 7 days throughout the culture period, while cell morphology was visualized by optical microscopy.

3.5.2.2. Static Cell Culture Studies

Static cell culture studies were performed in 24-well TCPS. The seeding of hMSCs in passage 8 was performed as the cell density in the chitosan-HA tissue scaffolds was $5\text{x}10^5$

cells/scaffold. On the 5th day of culture, 1 mL of osteogenic differentiation medium was added to each well, and the culture medium was replaced with fresh medium every 3 days for 21 days. MTT analysis was performed every 7 days to follow the change of cell viability during culture. Cell adhesion and proliferation were visualized by SEM analysis. The gene expression levels of the cells were determined by Real Time Polymerase Chain Reaction (RT-PCR) analysis.

3.5.2.3. Dynamic Cell Culture Studies Using Perfusion Bioreactor

For dynamic cell culture studies conducted in a perfusion bioreactor, at the end of day 5, the cells cultured in stationary conditions are combined with the necessary components in sterile conditions and the schematic bioreactor setup is presented for dynamic cell culture (Figure 3.3 and Figure 3.4). Ten mL of differentiation medium was then applied to the 10 mL luer tip syringe to be placed in the pump. After the completion of the perfusion bioreactor setup, the syringe pump was programmed for P3D-6 scaffolds at a flow rate of 0.1 mL/min and a flow rate of 0.2 mL/min, respectively, and the working volume was set at 6 mL. For P3D-10 scaffolds, the flow rate was set at 0.1 mL/min and the working volume was set at 10 mL. The syringe pump was kept in room conditions, the hydrophilic and hydrophobic filter systems which were connected to the 4-way valve, the perfusion ring and the ambient reservoir were placed in the CO_2 incubator. MTT analysis was performed every 7 days to follow the change of cell viability during culture. Cell morphology was visualized by SEM analysis. The gene expression levels of the cells were determined by RT-PCR analysis.
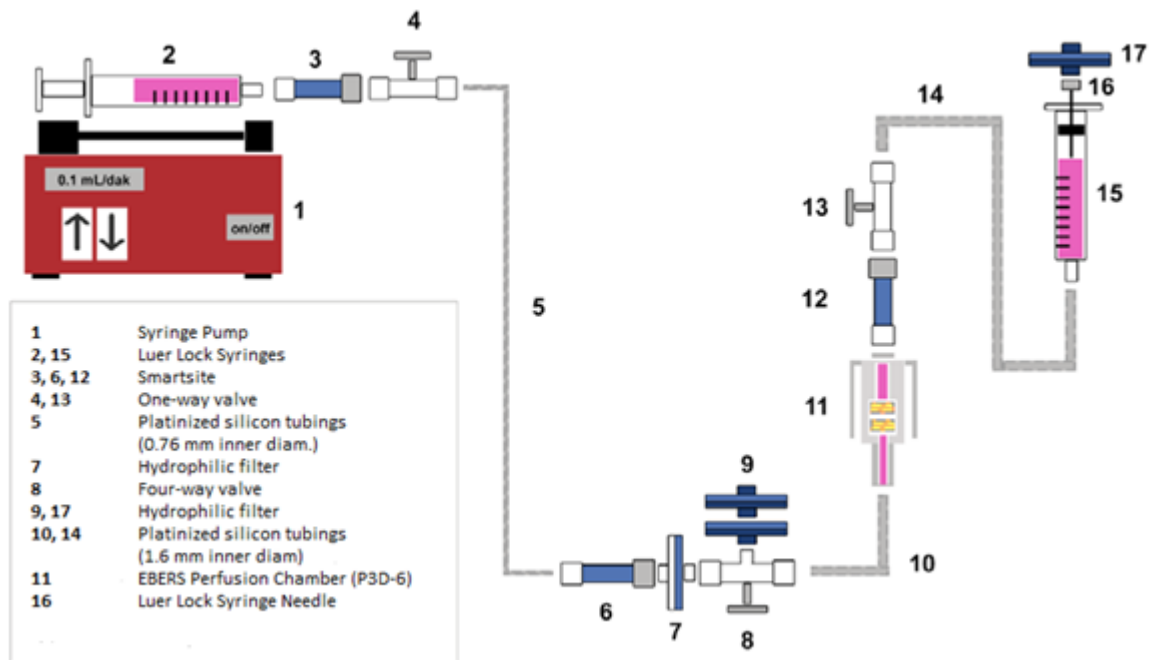
Figure 3.3. Schematic of the perfusion bioreactor setup used in dynamic cell culture studies for P3D-6 scaffolds.
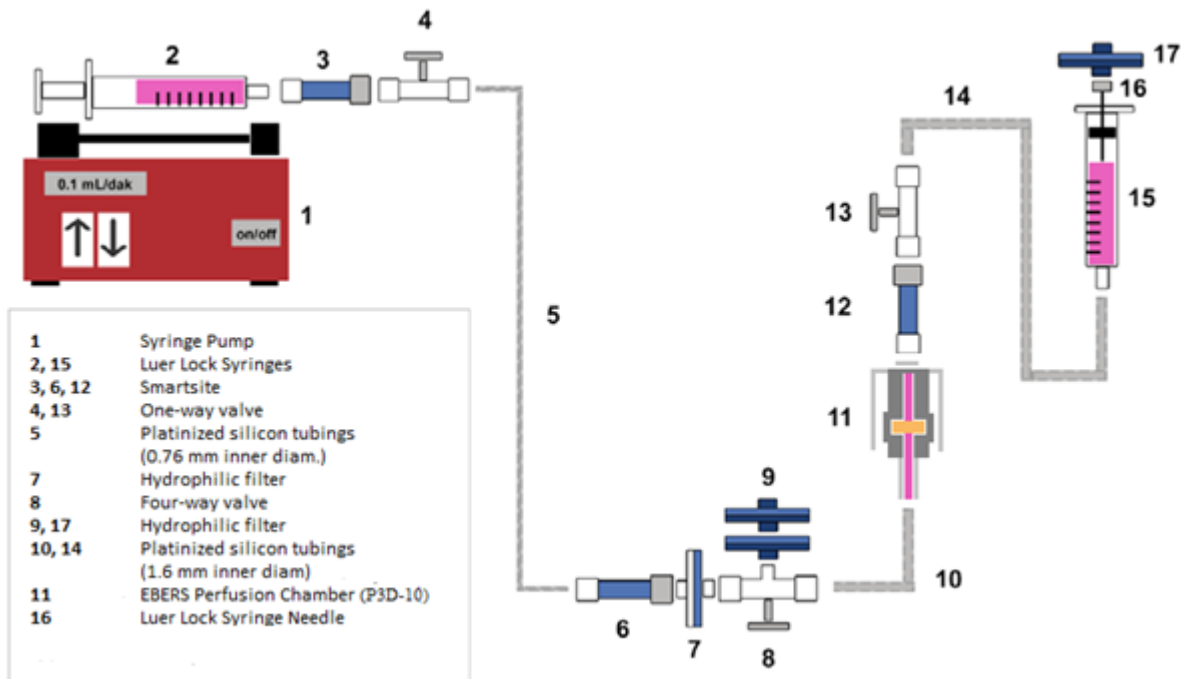
Figure 3.4. Schematic of the perfusion bioreactor setup used in dynamic cell culture studies for P3D-10 scaffolds.

3.5.3. Characterization Tests

In order to acquire the quantitative determination of mitochondrial activities of hMSCs on scaffolds, the study of adhesion, the spreading behavior and the morphology on tissue scaffolds and observations of gene-level effects of osteogenic differentiation, MTT analysis, SEM analysis and RT-PCR analysis were performed in the culture days of 7, 14 and 21. The following sections provide detailed information on the analyzes.

3.5.3.1. MTT Analysis

The viability of hMSCs on chitosan-HA SPH scaffolds was quantitatively determined by MTT analysis on days 7, 14 and 21. In the mitochondria of living cells, the MTT solution is converted to water-insoluble purple formazan crystals. The solution absorbance obtained by dissolving the crystals is directly proportional to cell viability. For the analysis, the culture medium on the specimens was first removed and 600 µL of serum-free medium and 60 µL of MTT (2.5 mg/mL PBS) solution were added to each well after placing the scaffolds of the different specimens in a new 24-well TCPS. Tissue scaffolds were incubated for 3 h at 37 ° C in an incubator. At the end of incubation, 400 µL of acidic isopropanol (0.04 M HCl) was added into each well in order to dissolve the formazan crystals. The optical density was determined spectrophotometrically by taking 200 µL of the resulting solution, using a microplate reader (Asys UVM 340, Austria) at 570 nm with 690 nm reference.

3.5.3.2. SEM Analysis

Samples taken on different days of the cultures were examined with SEM (Zeiss Evo50, Germany) to display the tendency and morphology of attachment and spreading of cells on chitosan-HA scaffolds. In the studies carried out within the scope of the thesis, the samples were displayed on the days 7th, 14th and 21st of cultures. The cell culture medium was removed from the scaffolds to be examined and then washed with DPBS (pH: 7.4). The washed tissue scaffolds were fixed in 1 mL of 2.5% (v/v) lutaraldehyde solution in the dark and at room temperature and maintained at 4°C in DPBS until analysis. Immediately prior to the analysis, chitosan-HA scaffolds were subjected to dehydration treatment using ethanol solution at different concentrations. The cells were kept for 2 min in 30%, 50%, 70%, 90% and 100% (v/v) ethanol solutions, respectively, and then kept in HMDS for 5 min. For SEM analysis, the

specimens were completely dried in room conditions, then divided into 3 parts as bottom, top and cross-section, placed on a special plate for analysis and after being coated with gold-palladium the imaging took place.

3.5.3.3. Real-time Polymerase Chain Reaction (RT-PCR) Analysis

The gene level of osteogenic differentiation of samples cultured in vitro on chitosan-HA scaffolds was determined by RT-PCR analysis. For this purpose, expression levels of alkaline phosphatase (ALP), collagen type 1 (Col1A1), runt related transcription factor 2 (RUNX2), osteocalcin (OCN) and osteopontin (OPN) genes which are indicators of osteogenic differentiation have been determined. β-actin was used as the housekeeping gene for the relative gene expression. For the RT-PCR analysis, the scaffolds on the 7th, 14th and 21st days of culture were taken and washed with DPBS (pH 7.4) and transferred to DNAse and RNAse microplates. Two hundred μL Trizol (Invitrogen, USA) was added to the samples that were broken down using microscissors and the samples mixed with vortex were stored at -80 $^{\circ}$ C until analysis. Immediately prior to analysis, 125 μL of chloroform was added to the samples dissolved at room temperature to isolate the RNA by the Trizol method, and the resultant was gently shaken. Subsequently, the samples were centrifuged at 4 $^{\circ}$ C for 10 min at 13,000 rpm and the liquid phase (300 μL) was transferred to the Rnase-free tube. The same amount of liquid phase (300 μL) was then added to the 70% ethanol samples and transferred to the columns after pipetting. After the transfer, the pellet was removed by centrifugation at 13,000 rpm for 1 min at 4 $^{\circ}$ C. Seven hundred μL of RW1 buffer was added to the remaining liquid phase and the pellet was removed by centrifugation at 13,000 rpm for 30 s at 4 $^{\circ}$ C. After this step, the remaining liquid phase was centrifuged at 500 rpm in RPE buffer at 4 $^{\circ}$ C for 30 s at 13,000 rpm to remove the pellet. This step has been repeated twice. The sample collection tubes were then changed, the capped tubes and collection tubes were centrifuged at 13,000 rpm for 1 min at 4°C. 50 μL Rnase free water was added to the samples and centrifuged at 13,000 rpm for 1 min at 4 $^{\circ}$ C and RNA isolation was completed. The concentrations of pure RNAs isolated (NanoDrop2000c Thermoscientific, USA) were measured and averaged and calculations have been made according to the lowest amount of RNA. Quantities of RNA determined from the lowest concentration were placed in equal amounts throughout the Eppendorf tubes. Reaction Mix was prepared in accordance with

manufacturer's protocol using cDNA for cDNA synthesis from isolated RNA (Applied Biosystem Kit cDNA, USA). Reaction Mix contains water, dNTP, random hexamer, reverse transcriptase and RNAse inhibitor. The prepared reaction solution was centrifuged for 1-2 s. 6.8 µL of the solution was added to all Ependorf tubes containing RNA in equal amounts and the bubbles were bursted out by spinning. CDNA synthesis was then completed by incubation at 25 ° C for 10 min, at 40 ° C for 120 min and at 85 ° C for 5 min in a thermal cycler (Roche Light Cycler® Nano, Germany). RT-PCR analysis was performed using SolisBioDyne 5xHot FirePol® EvaGreen® qPCRMix Plus (Estonia) kit. PCR Mix contains DNAase water, reverse primer (Table 3.3), forward primer (Table 3.3). For each sample from the synthesized cDNA, 2 µL of ependorf tubes were taken and 18 µL of the PCR Mix prepared above was distributed. The solution was centrifuged and made ready for use. The PCR analysis was then carried out with the activation step at 95 ° C for 15 min, the extension step at 95 ° C for 15 s, at 60 ° C for 20 s, at 72 ° C for 20s, the amplification step at at 60 ° C for 20 s and 20 s and the separation step at at 60 ° C for 4 s and at 95 °C for 20 s was carried out in 45 cycles.

Table 3.3. Genes and primers of genes whose expressions are measured in RT-PCR analysis

Gene	Primer
β-actin	F-5'-GTGCTATGTTGCCCTAGACTTCG-3' R-5'-GATGCCACAGGATTCCATACCC-3'
COL1	F-5'-CAAGATGTGCCACTCTGACT-3' R-5'-TCTGACCTGTCTCCATGTTG-3'
OCN	F-5'-CTTTCTGCTCACTCTGCTG-3' R-5'-TATTGCCCTCCTGCTTGG-3'
RUNX2	F-5'-GCATGGCCAAGAAGACATCC-3' R-5'-CCTCGGGTTTCCACGTCTC-3'
OPN	F-5'-CACTTTCACTCCAATCGTCCCTAC-3' R-5'-ACTCCTTAGACTCACCGCTCTTC-3'

3.5.4. Statistical Analysis

Data acquired from studies were statistically evaluated using the GraphPad Software Instat program. The data are presented with mean ± standard deviation values for three parallel samples. One-way ANOVA was used together with the Tukey-Kramer post hoc test for statistical comparison of the different groups and it was considered significant that the p-value was less than 0.05. Student's t-test was used for the statistical analysis of the results of cell seeding studies with the number of groups are deemed as 2 and it was considered significant that the p-value was less than 0.05.

3.6. Computational Fluid Dynamics Modelling Studies

In this section of the thesis, we use computational fluid dynamics approaches to study flow and mass transfer simulations in high and low flow perfusion bioreactors.

3.6.1. Method

For computational fluid dynamics (CFD) modeling studies, COMSOL software, which is licensed by Middle East Technical University (Ankara), is used. COMSOL is a multi-physics and finite element analysis (FEA) software. The modeling process in COMSOL can be done quickly with predefined physics interfaces and has a wide range of applications from heat transfer to flow problems, from structural mechanics to electromagnetic analysis [97]

The completed modeling works using COMSOL software in the scope of the thesis can be listed as follows:

- Flow model in perfusion bioreactor without scaffold
- Flow model in perfusion bioreactor in the presence of non-porous scaffold
- Flow model in perfusion bioreactor in the presence of permeable scaffold
- Mass transfer model in perfusion bioreactor in the presence of permeable scaffold

Pre-defined interfaces of COMSOL software are used in modeling studies. For the simulation of the flow, the modules found in the COMSOL "Computational Fluid Dynamics Module" are used. The "Free and Porous Media Flow" model was used in simulation studies (permeability model 3 and 4) for perfusion bioreactor with permeable tissue scaffold while "Laminar Flow"

model was preferred for other studies (models 1 and 2). Figure 3.5 shows the use of the COMSOL program for modeling flow in a perfusion bioreactor without tissue scaffolding on the program page.
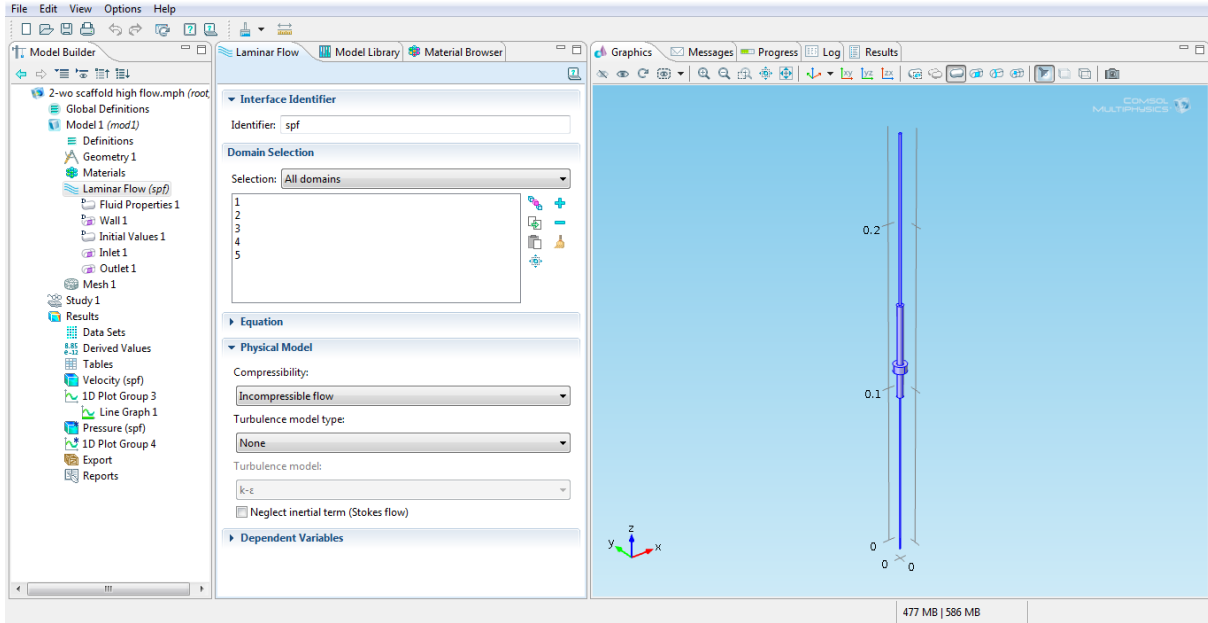
Figure 3.5. The use of the "Laminar Flow Model" in the COMSOL program for flow modeling in a perfusion bioreactor without a tissue scaffold.

The Navier-Stokes equations are used for the incompressible flow in the laminar flow model. The momentum transfer equation is given in Equation 3.1 and the continuity equation is given in Equation 3.2 for incompressible fluids.

$$\rho \frac{\partial u}{\partial t} + \nabla.\left[-\eta \left(\nabla u + (\nabla u)^T \right) + pl \right] = -\rho (u.\nabla) u \tag{3.1}$$

$$\nabla.u = 0 \tag{3.2}$$

η represents dynamic viscosity (Pa · s); u represents the linear flow velocity in open channel (m/s); ρ represents the density of the fluid (kg/m^3) and p represents the pressure (Pa). Brinkman equation (Equation 3.3) was used in the simulation of momentum transfer in the

permeable tissue scaffold (porous media) while the flow in the bioreactor (free environment) was solved with Navier-Stokes equations in the "Free and Porous Media Flow" model.

$$\frac{\rho}{\varepsilon_p}\frac{\partial u}{\partial t}+\nabla.\left[-\frac{\eta}{\varepsilon_p}\left(\nabla u+\left(\nabla u\right)^T\right)+pl\right]=-\frac{\eta}{\kappa}u \tag{3.3}$$

ε_p represents porosity (dimensionless); and κ represents permeability of the porous medium (m^2). The boundary conditions used in the flow models are as follows:

$$u.n=u_0 \qquad\qquad\qquad\qquad \text{(Inflow)}$$

$$u=0 \qquad\qquad\qquad\qquad \text{(No Slip)} \qquad (3.4)$$

$$p=0,\eta\left(\nabla u+\left(\nabla u\right)^T\right)n=0 \qquad\qquad\qquad\qquad \text{(Outflow)}$$

In order to model the flow in porous tissue scaffolds, the scaffold permeability must be accurately calculated. The permeability of a porous medium is a geometric feature and is influenced by the morphology and topology of the pores making right angles to the flow direction. Different equations have been proposed in the literature to account for the permeability values of tissue scaffolds with different pore structures [101]. In one approach, it is assumed that freeze-drying of aqueous solutions results in the formation of cylindrical pores located in the flow direction. The permeability value in texture scaffolds with this pore structure can be calculated with Equation 3.5. Since this approach is suitable for chitosan-HA SPHCs produced in the thesis study, the permeability of the tissue scaffold in the "Free and Porous Media Flow" model in simulation studies is calculated by Equation 3.5.

$$\kappa=\frac{\pi}{128}nD^4 \tag{3.5}$$

ε_p represents the permeability (m^2) of the porous medium, n represents the number of pores in the unit perpendicular to the flow ($1/m^2$), and D is the pore diameter (m).

The "Transport of Dilute Species" model in the "Chemical Reaction Engineering Module" of COMSOL software was used to model mass transfer. The established mass balances for

diffusion and convection of mass transfer in a perfusion bioreactor and consumption of oxygen and glucose in cells are given in Equations 3.6 and 3.7.

$$\nabla.\left(-D_{A,B}\nabla c_A\right)+u.\nabla c_A = r_A \qquad (3.6)$$

$$N_A = -D_{A,B}\nabla c_A + uc_A \qquad (3.7)$$

cA represents the concentration (mol/m^3); $D_{A,B}$ represents diffusivity coefficient (m^2/s); r_A represents the net reaction rate for the component (mol/m^3.s); and N_A represents, flow (mol/m^2·s).

The boundary conditions used in the mass transfer models are given as follows:

$$c_A = c_{A0} \qquad \text{(Inflow)}$$

$$n.\left(-D_{A,B}\nabla c_A + c_A u\right) = 0 \qquad \text{(Zero Flux)} \qquad (3.8)$$

$$n.\left(-D_{A,B}\nabla c_A + c_A u\right) = n.c_A u \qquad \text{(Outflow)}$$

3.6.2. Bioreactor Geometry and Meshing

For the simulation of flow and mass transfer in the perfusion bioreactor system used in experimental studies, the bioreactor geometry was first modeled in the COMSOL program. The cylinders were assembled by considering the actual dimensions of the system except for the lengths of the silicon tubes (Figure 3.6). The parts of the reactor that the cylinders represent are described in Figure 3.6.

44
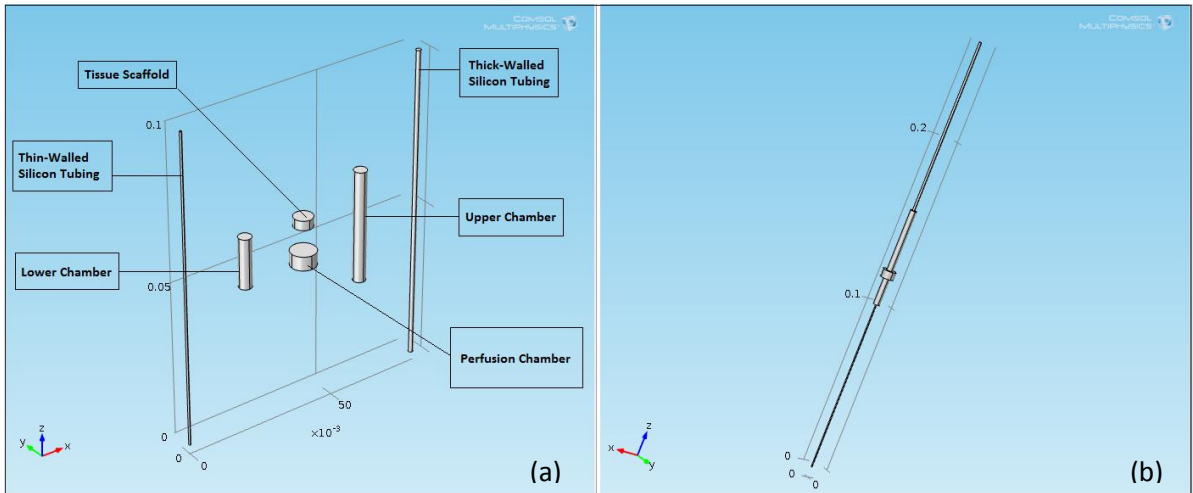
Figure 3.6 Modeling of the geometry of the perfusion bioreactor using COMSOL (a) general view, (b) reactor parts represented by the cylinders.

In order to apply the finite element analysis in COMSOL, it is necessary to create the final number of meshes to be solved. In the modeling studies carried out within the scope of the thesis, the reactor geometry was divided into pieces using free tetrahedral meshes. In the models studied, however, mesh size and number of elements vary depending on differences in geometry and simulation approaches. The images of the mesh formed for the perfusion bioreactor without tissue scaffold are shown in Figure 3.7.
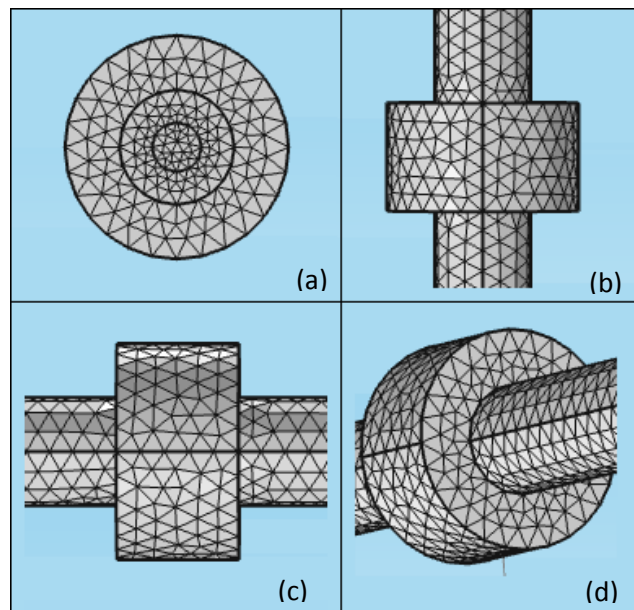
Figure 3.7 The free tetrahedral mesh for the perfusion bioreactor (a) an x-y axis image (b) a y-z axis image, (c) an x-z axis image (d) an x-y-z axis image

3.6.3. Simulation Parameters

The operating and design parameters used in the studies for the simulation of flow and mass transfer in the perfusion bioreactor are given in Table 3.4

	Reactor Component	Diameter (m)	Lenght (m)
Dimensional values of the perfusion bioreactor	Thin Tubing	0.00076	0.1
	Lower Chamber	0.004	0.016
	Perfusion Chamber	0.008	0.004
	Upper Chamber	0.004	0.036
	Thick Tubing	0.016	0.1
Temperature, T	$37°C$		
Density of culture medium, ρ	1000 kg/m^3		
Viscosity of the culture medium, η	0.0007 Pa.s		
Scaffold Size (P3D-6)	$D = 6 \text{ mm}$ $H = 3 \text{ mm}$		
Scaffold Size (P3D-10)	$D = 10 \text{ mm}$ $H = 3 \text{ mm}$		
Porosity (ε) and permeability (κ) values	$\varepsilon_p = \%78$ $\kappa = 6.13 \times 10^{-9} \text{ m}^2$		
Scaffold Pore Size	$D_{pore} = 500 \text{ μm}$		
The volumetric flow rates (Q) in the perfusion bioreactor	$Q_{Low\ Velocity} = 0.1 \text{ mL/min}$ $Q_{High\ Velocity} = 0.277 \text{ mL/min}$		
Reynolds Number in the perfusion without tissue scaffold	$N_{RE,\ Low\ Velocity} = 0.0317$ $N_{RE,\ High\ Velocity} = 4$		
Parameters related to oxygen transfer; diffusion coefficient (D), concentration ®, and reaction value ®	$D_{o2,H2O} = 3 \times 10^{-9} \text{ m}^2/\text{s}$ $R_{MSC,O2} = 98 \times 10^{-15} \text{ mol/h.cell}$ $C_{O2,Inflow} = 0.2 \text{ mol/m}^3$		
Parameters related to glucose transfer; diffusion coefficient (D), concentration ®, and reaction value ®	$D_{Glucose,H2O} = 6.6 \times 10^{-10} \text{ m}^2/\text{s}$ $R_{MSC,\ Glucose} = 342 \times 10^{-15} \text{ mol/h.cell}$ $C_{Glucose,\ Inflow} = 5.56 \text{ mol/m}^3$		

4. RESULTS AND DISCUSSION

In this section, the results obtained from experimental studies carried out have been presented in order to determine the reproductive and osteogenic differentiation potentials of human mesenchymal stem cells in different operating parameters and varying scaffold sizes in perfusion bioreactors supplemented with chitosan-HA scaffold. In the first part, results of cell culture studies performed with static and dynamic approaches are presented alongside the stationary cell seeding studies carried out with the hMSCs. In the second part of the study, information was provided about the characterization of cell seeding and cell culture results. In the last section, the results and discussions of CFD modeling studies are presented in order to determine the flow and mass transfer profiles in the perfusion bioreactor.

4.1. Cell Culture Studies

4.1.1. Monolayer Cell Culture Studies

The viabilities of hMSCs in monolayer cultures were measured by MTT analysis and the results are presented in Figure 4.1. Results from the first day of culture showed that the cells attached to the TCPS surface and maintained their viability. A significant increase was detected between days 1 and 4 of the culture due to cell proliferation. From the 5th day of culture, it was expected that the growth rates would gradually decrease due to the differentiation of the cells in the osteogenic differentiation medium. During the first 21 days, mitochondrial activity was found to increase due to the increase in the number of cells. On the 28th day of culture, the decrease in activity was explained by the effects of cells reaching saturation in monolayer culture and contact inhibition.
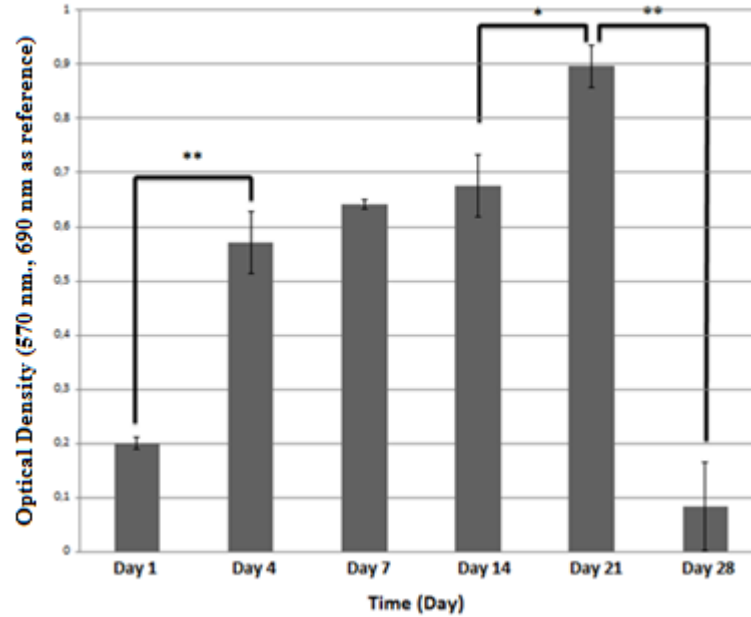
Figure 4.1 Mitochondrial activities of hMSCs cultured on TCPS surfaces for 28 days under static conditions (* $p < 0.05$, ** $p < 0.01$).

Morphologies of the monolayer culture of human MSCs were visualized by an optical microscope on the fourth day of culture. In Figures 4.2-a and b, it is seen that the cells are in fibroblastic morphology and they are healthy. The spindle formation and the viability of the cells have been observed.
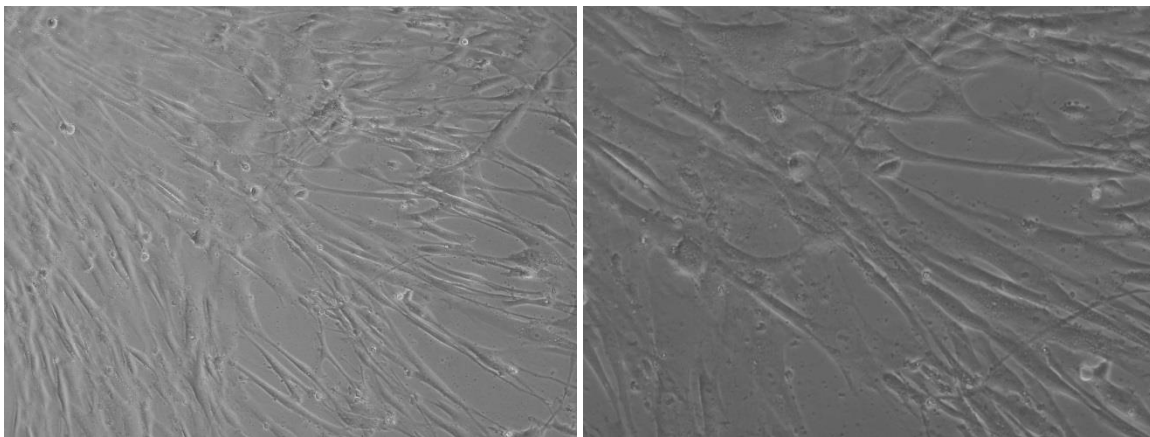
Figure 4.2. Optical microscope images of hMSCs cultured monolayer on TCPS surfaces: (a) 20 X, (b) 40 X.

4.1.2. Static Cell Culture Studies

Static cell culture studies were conducted to determine the morphology and proliferation behavior of human MSCs on chitosan-HA scaffolds, and the results of the MTT analysis are presented in Figure 4.3. As seen in Figure 4.3, the highest mitochondrial activity in culture was encountered on day 1. However, an increase from the 4th day to the 14th day was observed, and a continuous decrease was detected in the following days. From the 5th day of culture, it was expected that the d rates would decrease gradually due to the differentiation of the cells in the osteogenic differentiation medium. Mitochondrial activity falls on days 21 and 28 of the culture, but this decrease was not found to be statistically significant.

SEM photographs on days 7, 14 and 21 of the culture study carried out in static conditions are presented in Figure 4.4. SEM images show that chitosan-HA SPHCs support hMSC adhesion. At the top of the scaffold, it was determined that the cells have maintained their spherical formations and a significant increase in the distributions of the cells were detected as the days progressed. Sections taken from the tissue scaffolds show that the amount of the cells that advances into the central area are infrequent, but maintain their spherical forms. It is noted that the cells have attached much more intensively in the lower regions of the scaffolds compared to the upper and central regions. Cells which are held individually on the HA particles can be recognized on images taken at high magnifications. However, it was observed that the cells maintained their spherical form and did not spread alongside the walls of the scaffolds. It has been interpreted that cells can not be homogeneously distributed in chitosan-HA SPHCs by static culture method because of the variable attachment rates which are highest in the upper and lower regions of the scaffold, but lesser in the central region. As a result of the obtained SEM images, it can be seen that the cellular activity and viability continued despite the declines in mitochondrial activity.
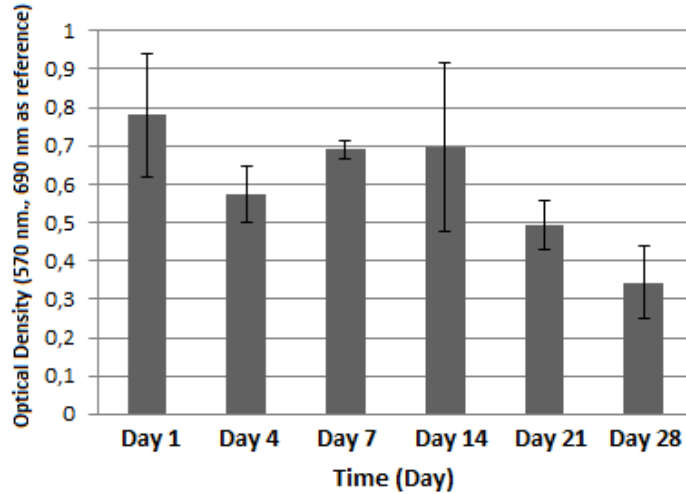
Figure 4.3. Mitochondrial activities of hMSCs cultured on chitosan-HA tissue scaffold for 28 days in static conditions.
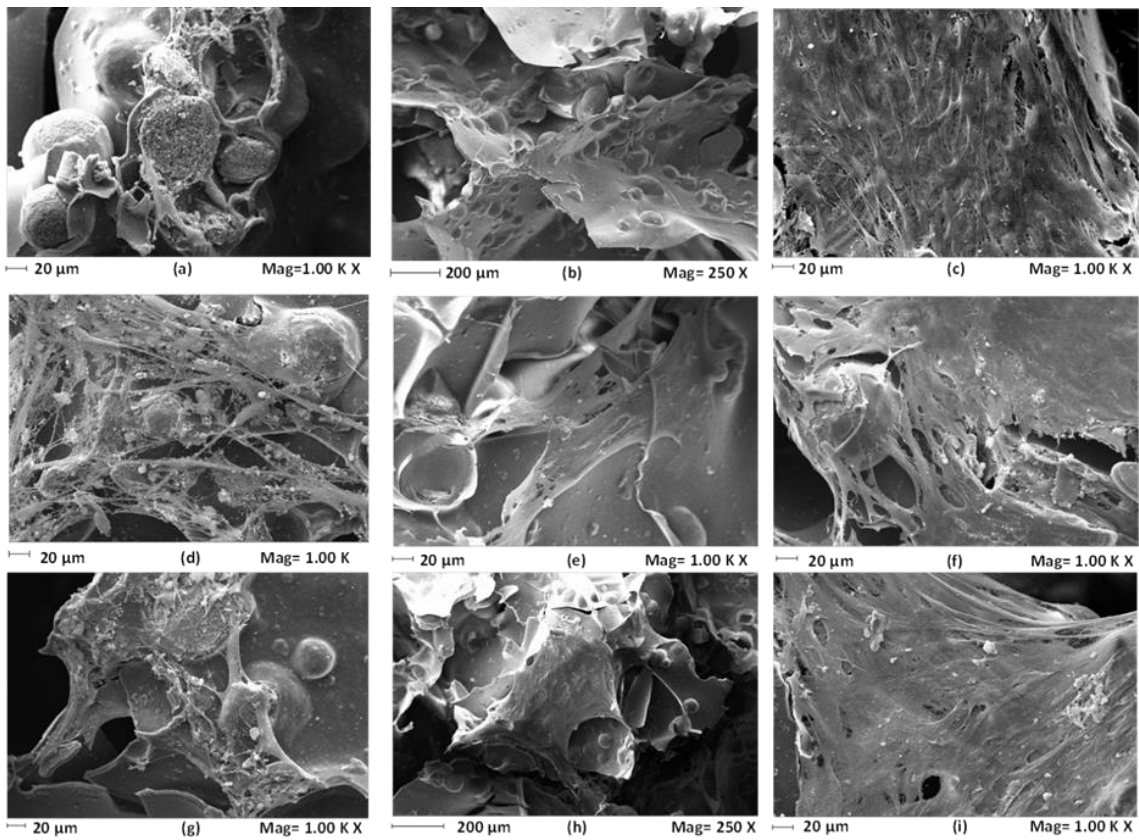
Figure 4.4. SEM images of day 7 of hMSCs in chitosan-HA SPHCs under static culture conditions. Bottom: (a) 1.00 K X, Cross-section: (b) 250 X, Top: (c) 1.00 K X; Day 14 SEM images. Lower: (d) 1.00 K X, Cross-section: © 1.00 K X, Upper: (f) 1.00 K X .; Day 21 SEM images. Bottom: (g) 1.00 K X, Cross section: (h) 250 X, Top: (i) 1.00 K X.

4.1.3. Dynamic Cell Culture Studies in Perfusion Bioreactor at 0.1 mL/min Flow Rate

After studying the behavior of human MSCs on chitosan-HA tissue scaffolds under stationary conditions, culture studies were performed in a perfusion bioreactor at a flow rate of 0.1 mL/min in order to increase cell viability. The results of the MTT analysis are presented in Figure 4.5 and Figure 4.6. Figure 4.5 shows that a high level of cell activity was reached at the onset of culture and mitochondrial activity declined between days 7 and 14, and this decrease was statistically significant. The observed rise from day 14 to day 21, while not being statistically significant, presents the continuation of the cell viability which has been shown at the SEM images presented in Figure 4.7. Considering the total culture period, it has seen that the perfusion bioreactor does not have a positive effect on cell viability that is statistically significant. Zhao et al states that stem cells have a high proliferation and flexibility potential, such as hMSC, are highly sensitive to environmental factors, and the effects of culture parameters are more prominent in stem cells due to ECM production and differentiation of a large part of the development [13]. Grayson et al. reported a prominent elevation in osteoblast proliferation and mineral content at a flow rate range of 0.3-3 mL / min [14]. Therefore, a change in flow rate is predicted to affect the results significantly.

Figure 4.5 Mitochondrial activities of hMSCs for 21 days in chitosan-HA SPHC at a flow rate of 0.1 mL/min in a bi-directional perfusion bioreactor (Statistically significant difference: * p <0.05).

Figure 4.6. The comparison of mitochondrial activities of static and dynamic culture resuşts at a flow rate of 0.1 mL/min. (Statistically significant difference: * p <0.05).

SEM images of hMSCs on chitosan-HA SPHCs cultured bidirectionally at a flow rate of 0.1 mL / min in a perfusion bioreactor are presented in Figure 4.7. The images show that the cells at the top of the scaffold retain their spherical forms and attach to the pores and continue to proliferate in groups. When the sections of the tissue scaffolds are examined, it is noticed that in the dynamic culture, the cells are held at a higher density in the central part of the scaffold, contrary to the static culture. Dynamic culture has advantages in terms of mass transfer compared to the stationary culture and it has been found that shear stresses imposed by the flow imitate the physiological environment in the body to support the resultant osteogenic differentiation and these results are found to show parallelism with related literature [15-18]. When the images of the lower part of the scaffolds were examined, it has been seen that the cells proliferate in a similar way to the static culture, while maintaining their spherical forms, and proceeded to spread in the following days. In higher magnifications, cells that attach to the pores and their proliferation can be distinguished.

Figure 4.7. SEM images of hMSC cells in chitosan-HA SPHC cultured bi-directionally at a flow rate of 0.1 mL / min in a perfusion bioreactor, Day 7. Bottom: (a) 1.00 K X, Cross-section: (b) 250 X, Top: (c) 1.00 K X; Day 14 SEM images. Lower: (d) 1.00 K X, Cross section: © 1.00 K X X, Top: (f) 1.00 K X. 21. Day SEM images. Bottom: (g) 1.00 K X, Cross section: (h) 250 X, Top: (i) 1.00 K X.

4.1.4. Dynamic Cell Culture Studies in Perfusion Bioreactor at 0.2 mL/min Flow Rate

After studying the behavior of human MSCs in a perfusion bioreactor at a flow rate of 0.1 mL/min, culture studies were performed in a perfusion bioreactor at a flow rate of 0.2 mL/ min in order to evaluate and compare the effects of the flow rate on the cell viability.

The results of the MTT analysis are presented in Figure 4.8 and Figure 4.9. Figure 4.8 shows that a high level of cell activity was reached at the onset of culture and a strong decline has been observed in the   ermeable   ial activity of the cells during the culture. While being statistically insignificant, the ongoing cell viability has been shown at the SEM images presented in Figure 4.10. Considering the total culture period, it has seen that the perfusion bioreactor does not have a positive effect on cell viability that is statistically significant.
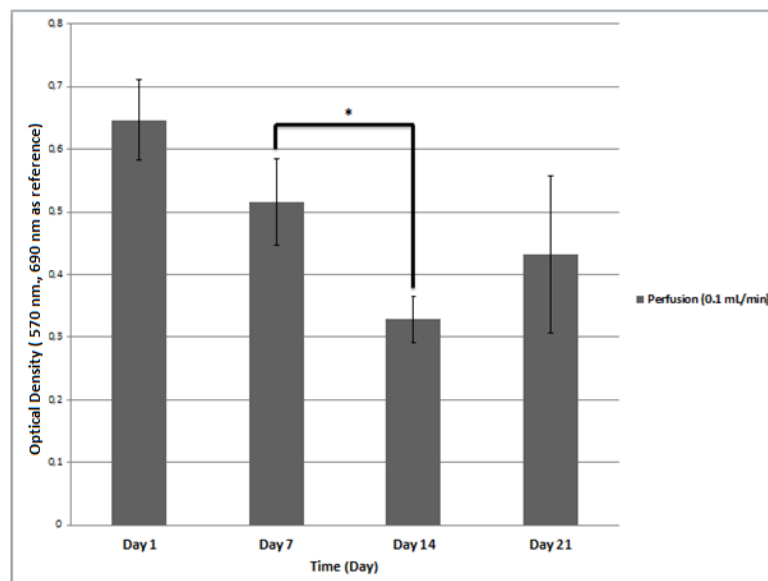
53
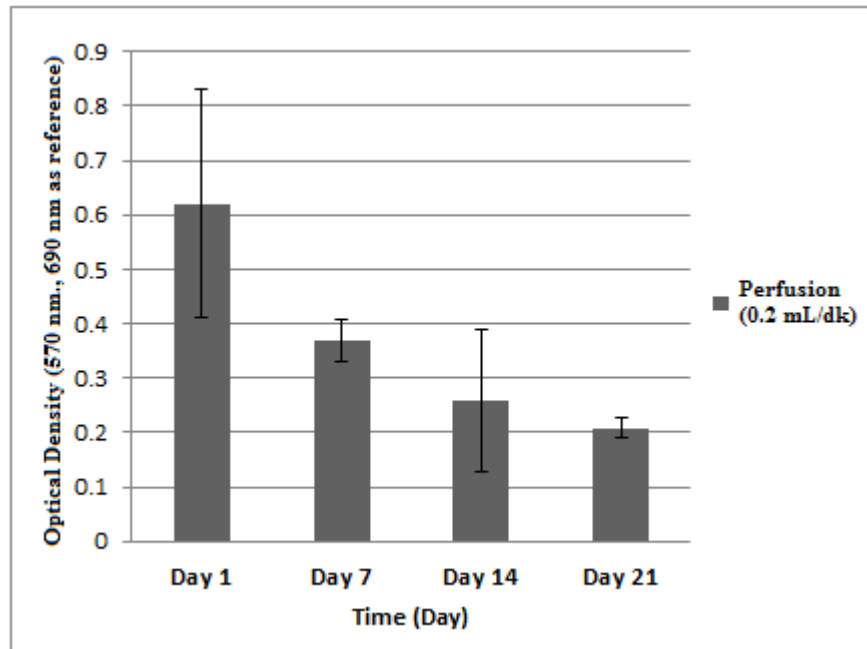
Figure 4.8. Mitochondrial activities of hMSCs cultured for 21 days in chitosan-HA SPHC at a flow rate of 0.2 mL / min in a bi-directional perfusion bioreactor (Statistically significant difference: * p <0.05).

Figure 4.9 also presents a strong decline in the   ermeable   ial activity during the culture after a high level of cell activity at the onset of culture while the mentioned decline being much more prominent for perfusion bioreactor at 0.2 mL/min flow rate than static culture as shown in Figure 4.9. A significant statistical difference was observed on day 14 with an asterisk, and on days 7 and 21 with two asterisks, which further supports the claim that the perfusion bioreactor has a negative effect on cell viability that is statistically significant.
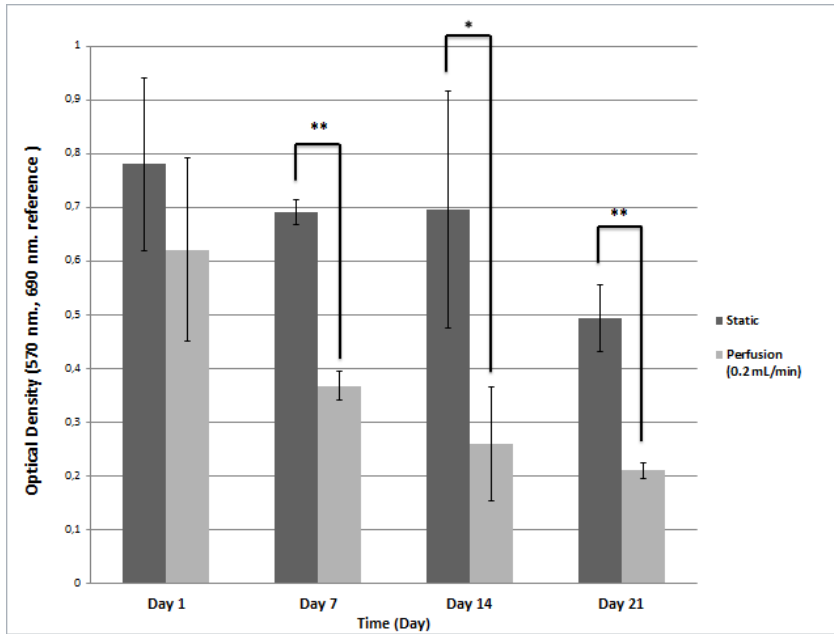
Figure 4.9. The comparison of mitochondrial activities of statically cultured hMSCs for 21 days in chitosan-HA SPHC at a flow rate of 0.2 mL/min in a bi-directional perfusion bioreactor (Statistically significant difference: * p <0.05, ** p<0.01).
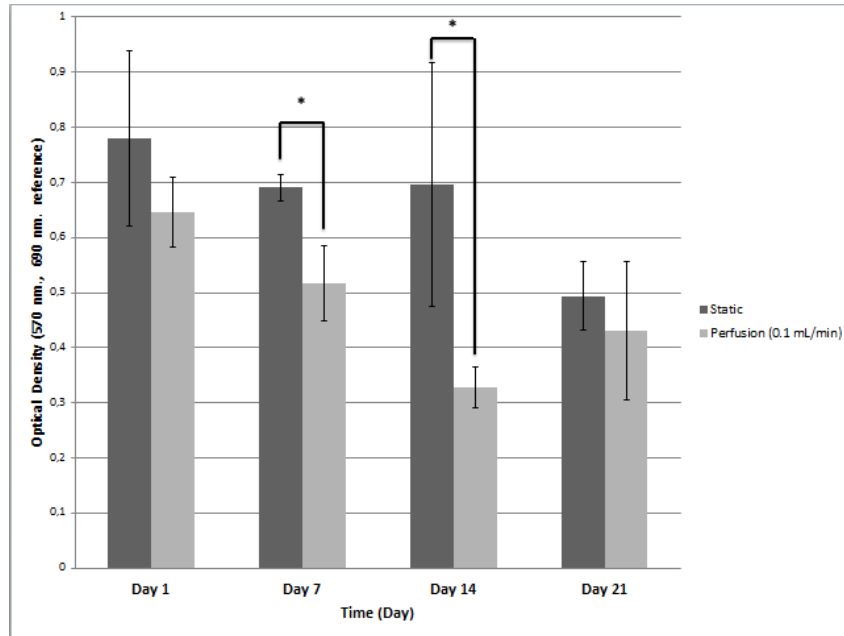
SEM images of hMSCs on chitosan-HA SPHCs cultured bidirectionally at a flow rate of 0.2 mL/min in a perfusion bioreactor are presented in Figure 4.10. The images show that the density of cells on chitosan-HA tissue scaffolds was lower than expected. The cells at the top of the scaffold retain their spherical forms and attach to the pores and continue to proliferate in groups. When the middle sections of the tissue scaffolds are examined, it can be noticed that in the dynamic culture, the cells are held at higher density in the central part of the scaffold, contrary to the static culture. Dynamic culture has advantages in terms of mass transfer compared to static culture and it has been found that shear stresses imposed by the flow imitate the physiological environment in the body to support the resultant osteogenic differentiation and these results are found to show parallelisms with related literature [15-18]. When the images of the lower part of the scaffolds were examined, it has been seen that the cells proliferate in a similar way to static culture while maintaining their spherical forms, and proceeded to spread in the following days. In high scale magnifications, cells that attach to the pores and their proliferation were distinguishedIn conclusion, it was interpreted that cells maintained their viability at a flow rate of 0.2 mL/min but the cell surface interaction was weakened by the effect of flow rate.
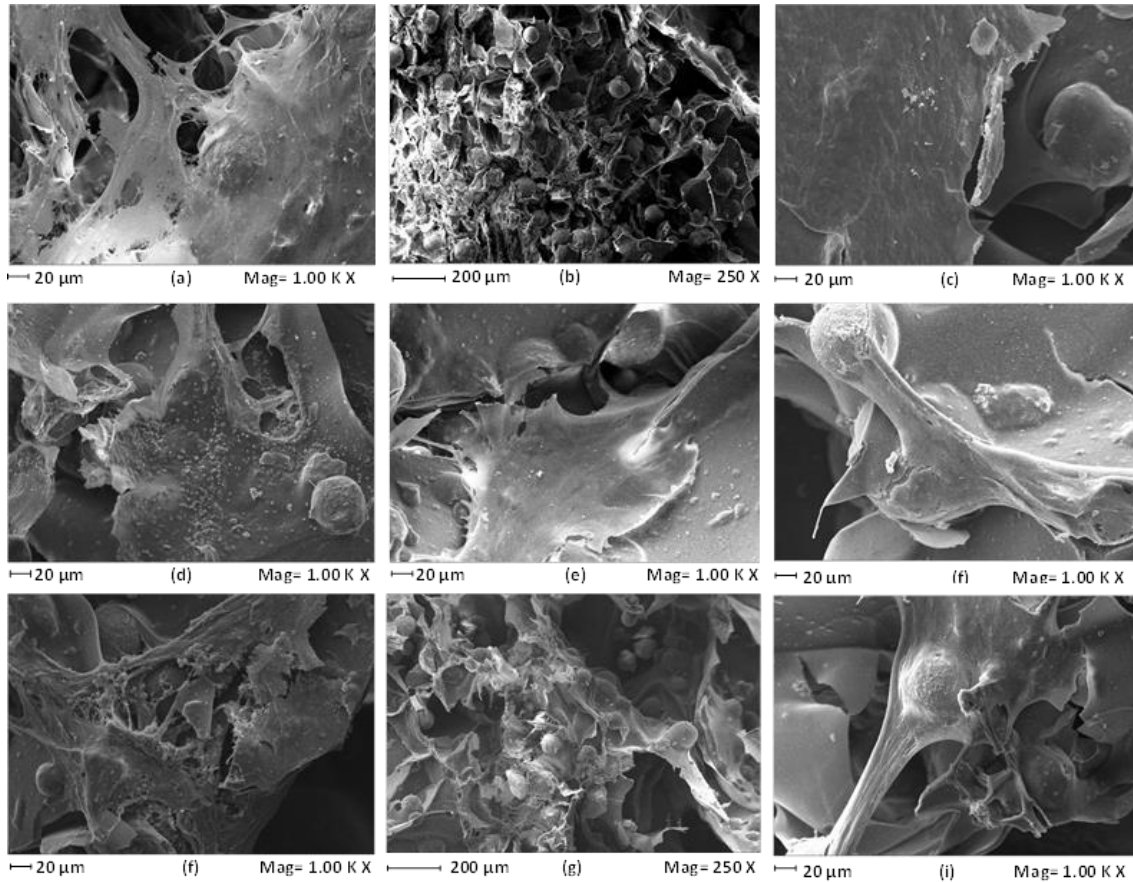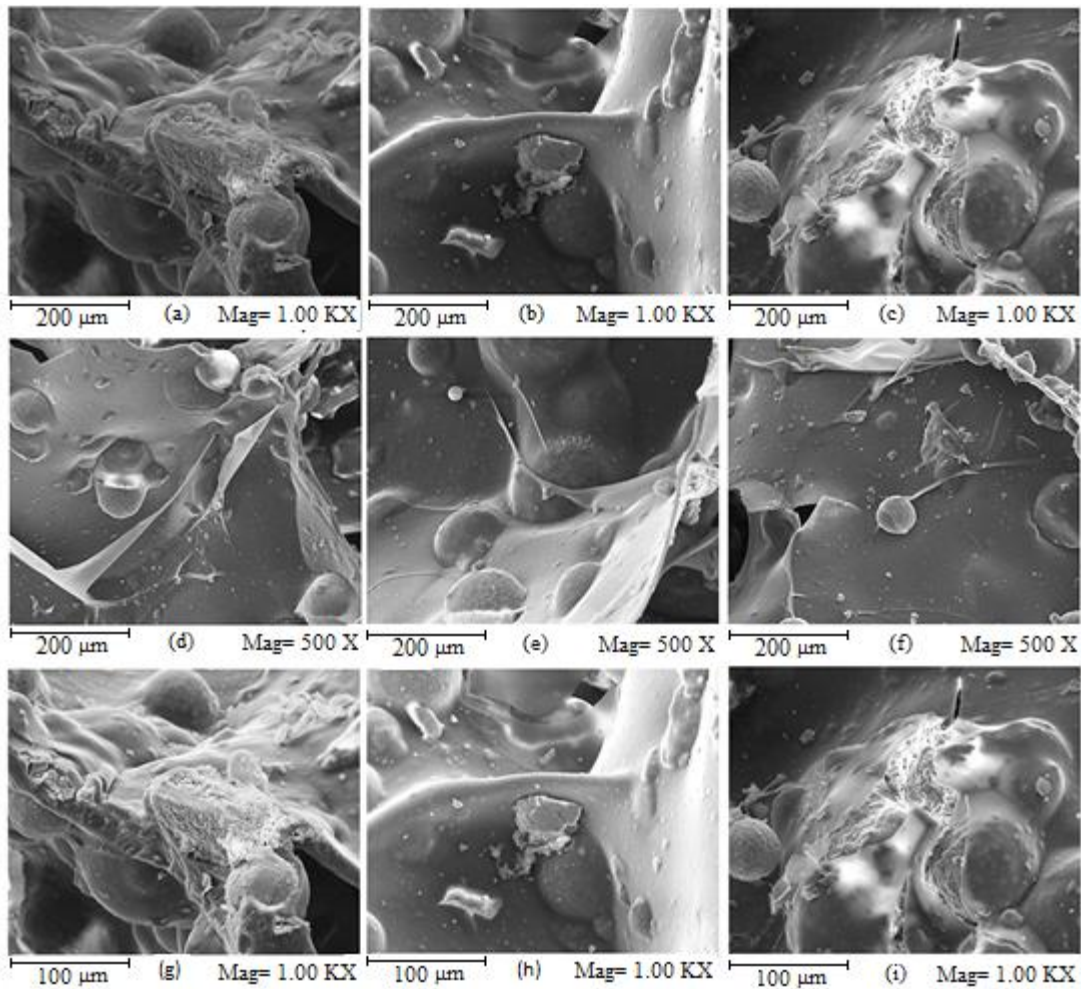
Figure 4.10 SEM images of hMSCs in chitosan-HA SPHC cultured bi-directionally at a flow rate of 0.2 mL / min in a perfusion bioreactor, Day 7 SEM images Bottom: (a) 1.00 KX, Cross-section: (b) 1.00 KX, Top: (c) 1.00 K X; Day 14 SEM images. Lower: (d) 500 X, Cross section: © 500X, Top: (f) 500 X. Day 21 SEM images. Bottom: (g) 1.00 KX, Cross section: (h) 1.00 KX, Top: (i) 1.00 KX.

4.1.5. Effect of Flow Rate on Perfusion Bioreactor

Considering the cell culture studies carried out with hMSCs; it has been observed that the static culture conditions presented better results in terms of mitochondrial activity than the dynamic culture for 21 days (Figure 4.11). Moreover, it has been determined that this activity presented a decline that is statistically significant. However, SEM images and the finding in the related literature clearly show that the cell type is a determinant factor in cell viability: Cartmell et al. found a significant increase in osteoblast-like cell growth at lower flow rates (0.01 mL/min) compared to the static control, but they also found a significant decrease in cell

56

viability at flow rates between 0.01 and 1 mL/min [84], yet Grayson et al. proved otherwise [27]. These discrepancies can be explained by varying behaviors of different cell types, as well as by the fact that the variations encountered in the system geometries and the designs of the scaffolds that are exposed to similar volumetric flow rates, resulting in completely separate shear stresses [27].
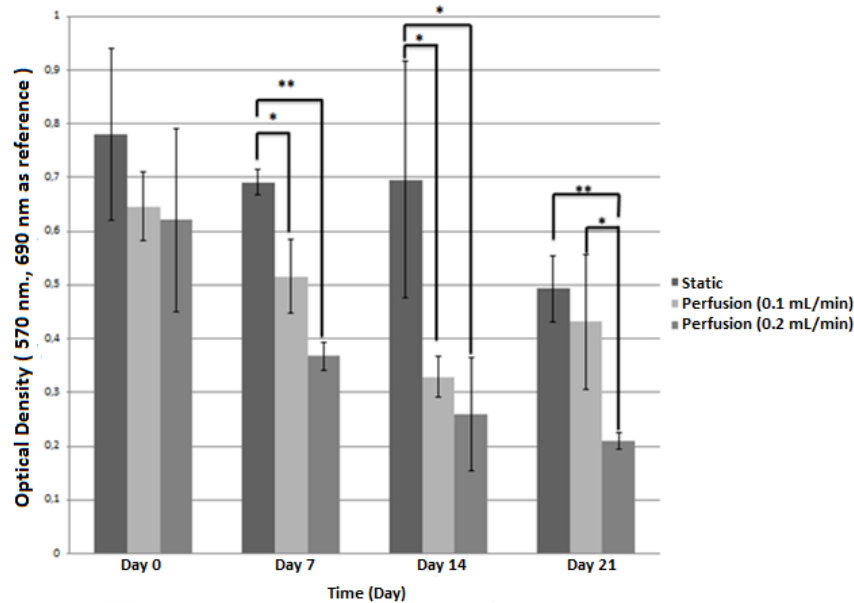
Figure 4.11 Comparison of the effects of different culture conditions on mitochondrial activities of hMSCs on chitosan-HA tissue scaffolds (Statistically significant difference: * p <0.05, ** p<0.01).

To investigate the effects of different culture conditions on osteoblastic differentiation of hMSCs, RT-PCR analysis was performed on samples cultured in static conditions and dynamically cultured samples at a flow rate of 0.1 mL/min. The results obtained are presented in Figure 4.12-a-d. The relative expression of the ALP gene from early markers of osteoblastic differentiation was found to increase starting from day 14 in static culture conditions. However, it was ermeabl that the mentioned increase in perfusion culture started on the 7th day and reached its highest value on the 14th day. Compared to ALP relative gene expressions in static and perfusion culture samples on the 14th day of dynamic culturing, perfusion cultures were found to be statistically significant and higher. In Figure 4.12-b, the COL1A1 relative gene expression of the early markers has also been evaluated comparatively between static and dynamic cultures. Similar to the results for the ALP gene, the expression of COL1A1 was

found to be statistically significantly higher in perfusion culture performed at a flow rate of 0.1 mL / min on day 14. In the relative expressions of the RUNX2 gene, one of the most important markers of osteoblastic differentiation, and the OPN gene, which is one of the indicators that the matrix produced by the cells that are ready for mineralization, perfusion culture on the 14th day of culture again enabled the culture medium to establish a higher expression. The results obtained from the RT-PCTR analysis have shown that perfusion cultures support osteoblastic differentiation of hMSCs better than stationary cultures.
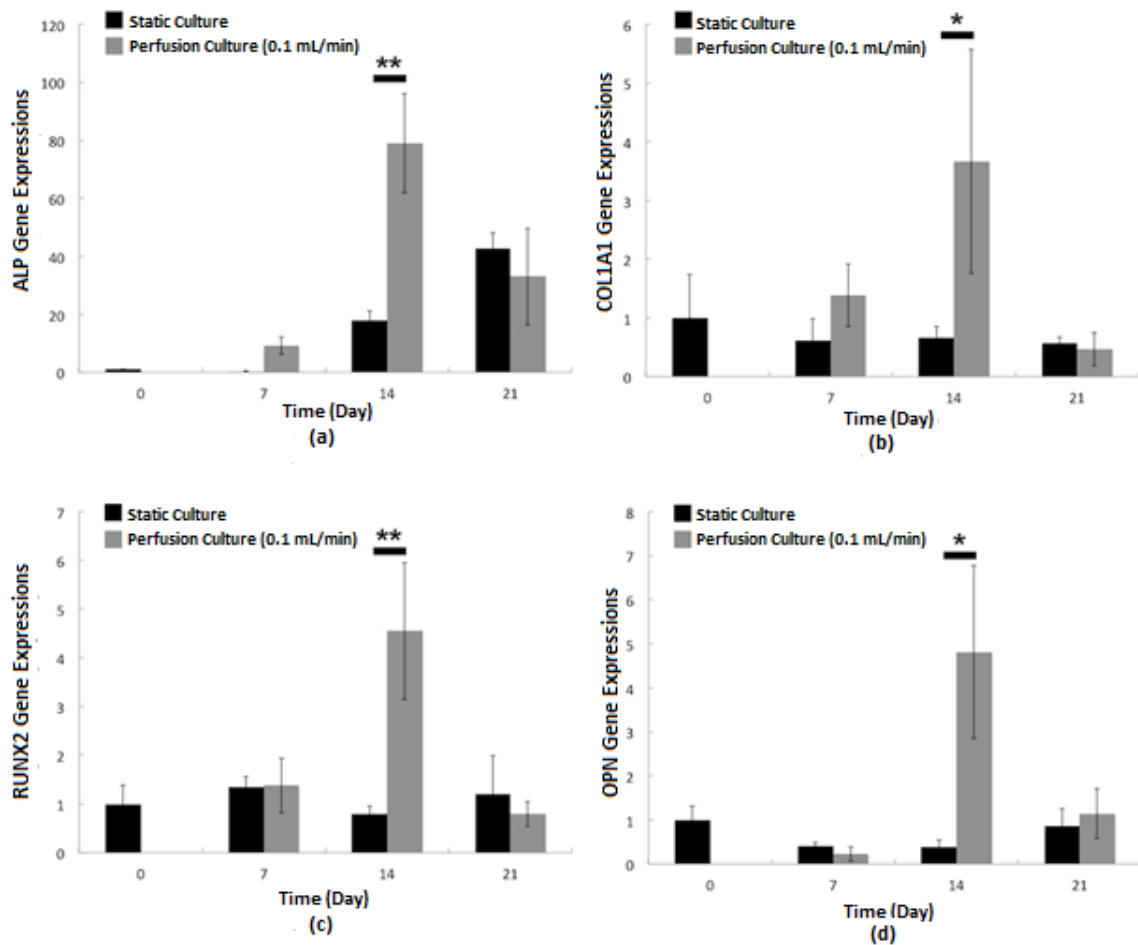
Figure 4.12. Effect of bidirectional perfusion flow at 0.1 mL/min flow rate on gene expressions of hMSCs cultured on chitosan-HA SPHCs, (a) *ALP*, (b) *COL1A1*, (c) *RUNX2* ve (d) *OPN* (n = 3, * p <0.05, ** p <0.01 represent statistical significance).

4.1.6. Dynamic Cell Culture Studies in Perfusion Bioreactor at 0.27 mL/min Flow Rate

Dynamic cell culture studies based on P3D-10 perfusion chambers have been carried out to establish the dynamic environment created by the flow rate of 0.1 mL/min that allows the

production of larger bone patches by evaluating the findings obtained from culture studies with hMSCs. Based on the analytical calculations performed, the linear velocity value of the P3D-6 perfusion chamber generated by the volumetric flow rate of 0.1 mL/min was calculated and the volumetric flow rate was increased to 0.27 mL/min for this linear velocity to be obtained in the P3D-10 chamber. The mitochondrial activities of the cells were measured by MTT assay and the results are presented in Figure 4.13. Activity values measured before perfusion culture indicate that hMSCs are efficiently planted in larger tissue scaffolds and the viability of the cells have been preserved. Preservation of the cell viability on the 7th and 14th days of perfusion cultures corresponds with previous results. The morphology of the cells on the chitosan-HA scaffold was examined by SEM analysis and the images obtained are shown in Figure 4.14. Images have shown that cell density in static cultured tissue scaffolds is less than that of previous studies (Figure 4.14-a-f). The results obtained from the perfusion culture are given in Figure 4.14-g-ı and it has been found that the cell density was lower than that of previous studies. The decrease in cell density in perfusion culture studies carried out in the P3D-10 chamber is thought to be related to the variation in flow profile. Simulation studies of computational fluid dynamics have been carried out in order to clarify the reasons for the mentioned problem.
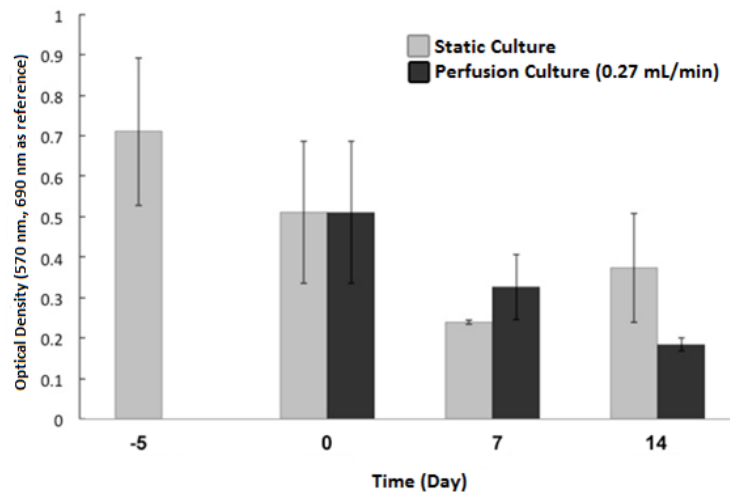
Figure 4.13. Comparisons of mitochondrial activities of hMSCs cultured for 14 days on a bidirectional flow at 0.27 mL/min flow rate in P3D-10 perfusion chambers on chitosan-HA SPHCs after static culture and a five day pre-culture period (No statistically significant difference was observed)
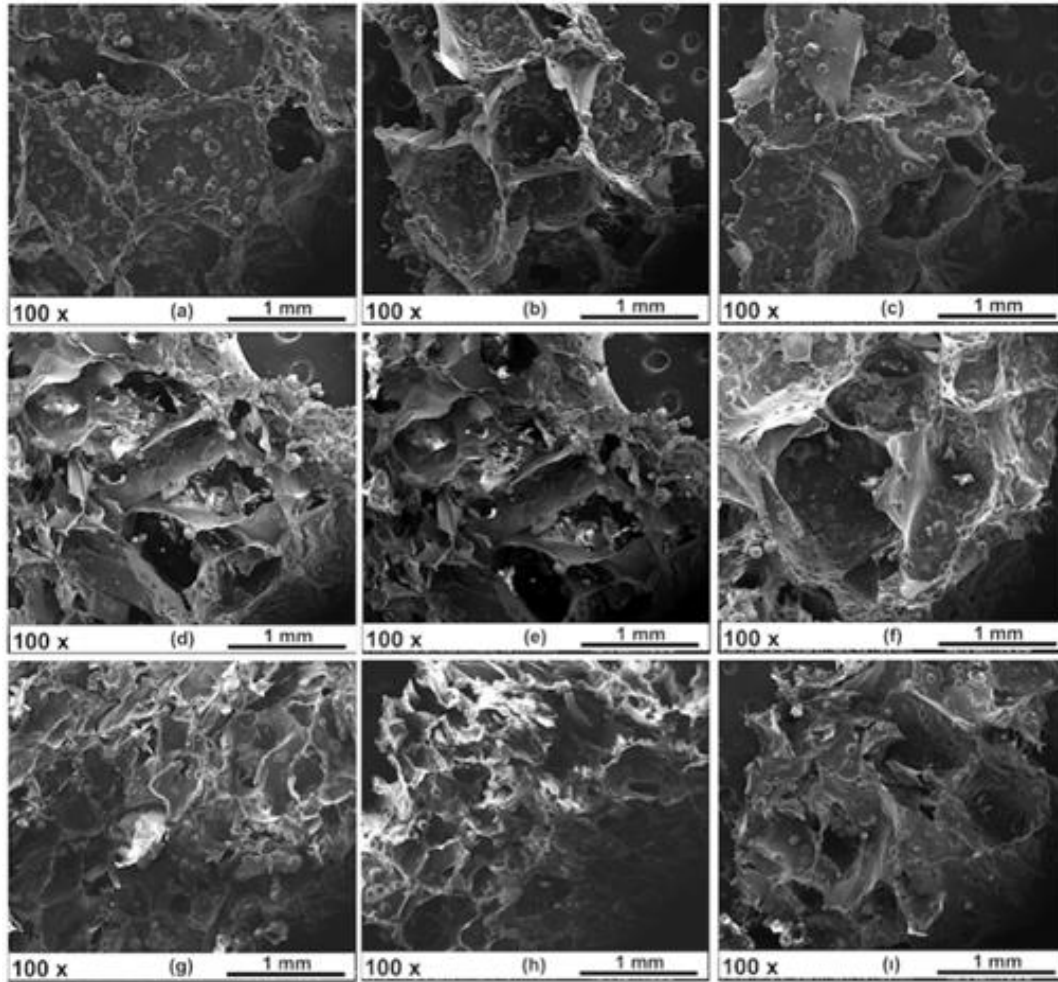
Figure 4.14. SEM images of hMSCs in chitosan-HA SPHC cultured bi-directionally at a flow rate of 0.2 mL/min in a P3D-10 perfusion bioreactor chamber, SEM images of static culture Day 1. Top: (a) 100 X, Cross-section: (b) 100 X, Bottom: (c) 100 X; SEM images of static culture Day 7. Top: (d) 100 X, Cross section: © 100 X, Bottom: (f) 100 X. SEM images of perfusion culture Day 7 Top: (g) 100 X, Cross section: (h) 100 X, Bottom: (i) 100 X.

4.2. Computational Fluid Dynamics Modelling Studies

In this section of the thesis, the results of simulation studies for modeling flow rate and mass transfer in a perfusion bioreactor operating at different flow velocities and tissue scaffolds of different sizes are discussed. In the modeling studies using COMSOL software with the methods described in Section 3.6, flow simulation was performed for the perfusion bioreactors without tissue scaffold in the first stage. On the ongoing studies, various models have been created by considering non-porous scaffolding and permeable scaffolding as primary scaffold

types. In addition, simulations of glucose and oxygen transfer were made using a permeable scaffold model in order to determine the shear stresses affecting the cells.

4.2.1. Perfusion Bioreactor Flow Model Without a Tissue Scaffold

As a first step in modeling studies, flow simulation was performed in a perfusion bioreactor without a tissue scaffold. For this purpose, the laminar flow model presented in the CFD module of COMSOL software has been utilized.

As it was stated in Section 3.6.2, the bioreactor geometry was obtained by combining 5 cylinders of different diameters and lengths, each representing a component in the reactor system. All components except the silicone tubes are modeled according to their actual measurements. The length of the silicone tubes at the entrance and exit of the perfusion chamber was determined to be 10 cm in order to shorten the calculation period and to facilitate the post-model data.

Perfusion bioreactor without tissue scaffold was discretized by COMSOL using calibrated free four-sided mesh for fluid dynamics problems (Figure 4.15). It is envisaged to use a smaller mesh structure in the areas where the gradient is expected to be large, and a larger mesh structure in the other regions, and therefore the use of asymmetric meshing has been found suitable.
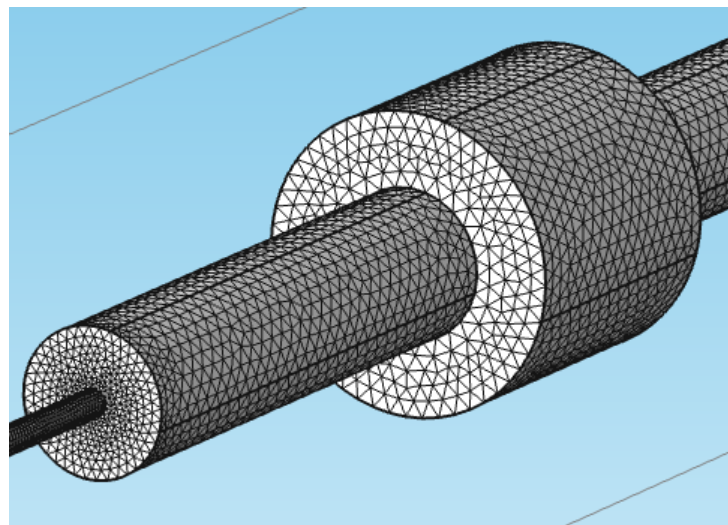
Figure 4.15. Use of free four-sided mesh in a perfusion bioreactor model without tissue scaffold.

Images of the velocity profile in the perfusion bioreactor are presented in Figure 4.16-a. The blue regions are the areas where the velocity is low and the red regions are the areas where the highest velocity is present. The color-velocity relationship on the scale is presented separately for each shape. The highest velocity in the reactor was reached at the inlet tube by 8.0914×10^{-3} m/s. The parabolic velocity profile due to the laminar flow appears in Figure 4.17. In the perfusion circle, it was determined that the linear velocity decreased with the increase of the diameter and it was noted that due to the sudden expansion in the circle, the dead zones in the corners were observed (Figure 4.16-b).

(a)   (b)
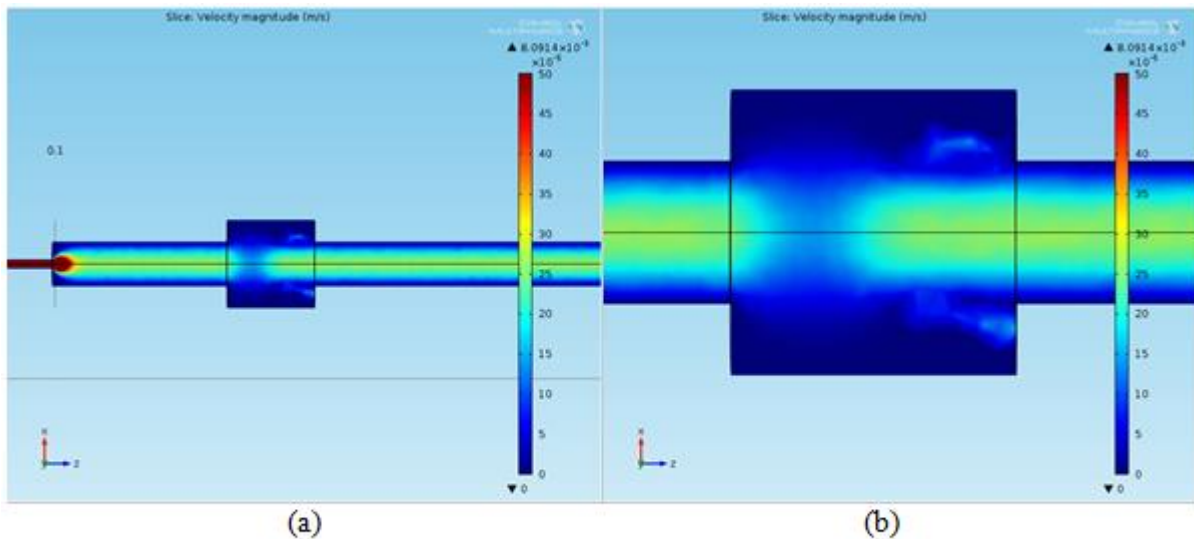
Figure 4.16. Velocity profiles in the perfusion bioreactor without tissue scaffold: (a) overview, (b) detailed view of the perfusion chamber.

An imaginary line passing through the center of the perfusion bioreactor is defined in the model to assess how the linear velocity changes along the reactor. Figure 4.17 shows the change in velocity along the horizontal axis. The graph confirms that the information obtained from Figure 4.16 as it represents the increase in velocity at the inlet and outlet of the silicon tubes. In Figure 4.17-b, the flow rate in the perfusion chamber changes from 0.25×10^{-3} m/s to 0.26×10^{-3} m/s.

(a)   (b)
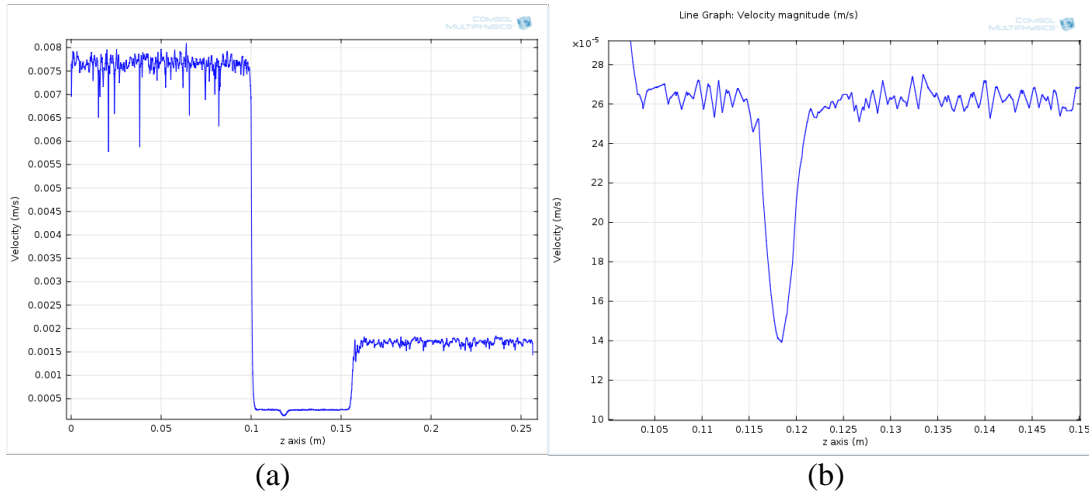
Figure 4.17. Velocity profile in the perfusion bioreactor without tissue scaffold: (a) the change in velocity in the reactor along the z-axis, (b) the change in velocity along the z-axis within the perfusion chamber.

By determining the flow rate and velocity profile in the perfusion bioreactor without a tissue scaffold, COMSOL Laminar Flow Model has found a suitable basis for the construction of the CFD model of the bioreactor that is presented. Due to the expected shape of the flow fields, it is thought that realistic results will be achieved as to how the tissue scaffold placed in the perfusion chamber will affect the flow fields.

4.2.2. Perfusion Bioreactor Flow Model with Non-Porous Tissue Scaffold

The chitosan-HA tissue scaffolds used in experimental studies are three-dimensional and porous structures. In order to have a preliminary study on simulations to be carried out in the presence of tissue scaffold, the assumption of nonporous tissue scaffold is made in this section and the system geometry given in Figure 4.18 is created in COMSOL. Models for permeable and porous tissue scaffolds in the continuing sections have also been included since the thesis study aims to identify the micro-environments and mechanical forces to which the cells in the tissue scaffold are exposed.

<div align="center">(a)   (b)</div>
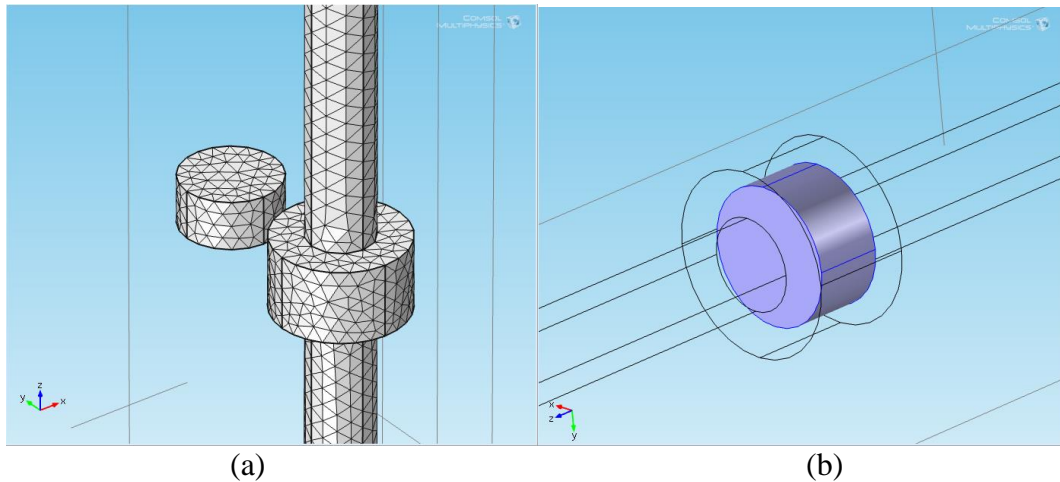
Figure 4.18. (a) Use of free four-sided mesh in the model of non-porous tissue scaffold and perfusion bioreactor, (b) location of tissue scaffold in the perfusion chamber.

Figure 4.19 shows images of the velocity profiles in the system that contains a rigid scaffold. In Figure 4.19-a, the highest flow rate was found to reach the inlet tube (8.0983×10^{-3} m/s). It has been shown that the model is reliable to reach the results which are compatible with the values obtained in the reactor without the tissue scaffold. In Figure 4.19-b it is clearly seen that the rigid tissue scaffold changes the speed profile. It has been determined that the velocity of the medium flow has been found to achieve very low values on the surface of the tissue scaffold that meets the flow. Moreover, it has been observed that the velocity increases in the regions where the upper and lower parts of the chamber are close to the scaffold, depending on the flow that is running around the scaffold. The velocity profile in the bioreactor is shown numerically by the graphs given in Figure 4.19. Flow has stopped in the tissue scaffold due to the absence of the pores, and the velocity has decreased to 0 m/s at certain points , which are shown in Figure 4.19-a and b. The linear velocity on the surface of the tissue scaffold was found to be 3.8×10^{-5} m/s.

(a)   (b)
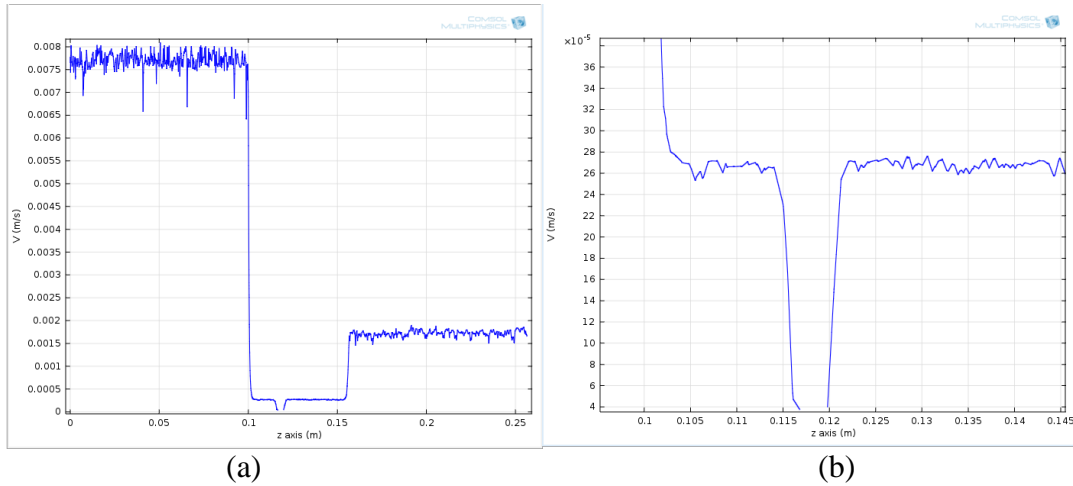
Figure 4.19. The velocity profile in the perfusion bioreactor in the presence of a non-porous tissue scaffold, (a) the change in velocity in the reactor along the z-axis; (b) the change in velocity along the z-axis within the perfusion chamber.

The shear rate profiles were used to calculate the shear stresses acting on different surfaces of the nonporous tissue scaffold. Since it is assumed that the culture medium is an incompressible fluid, shear stress values are calculated by multiplying shear rate and medium viscosity. In Figure 4.20, the shear velocity profiles that are applied for the anterior and posterior sides of the scaffold are provided. Depending on the design of the perfusion chamber, the direct flow of the center of the tissue scaffold causes the forces in these regions to be higher than those in the lateral zones. The highest shear stress acting on the center of the scaffold was calculated as 4.3064×10^{-4} dyne / cm^2.

(a)   (b)
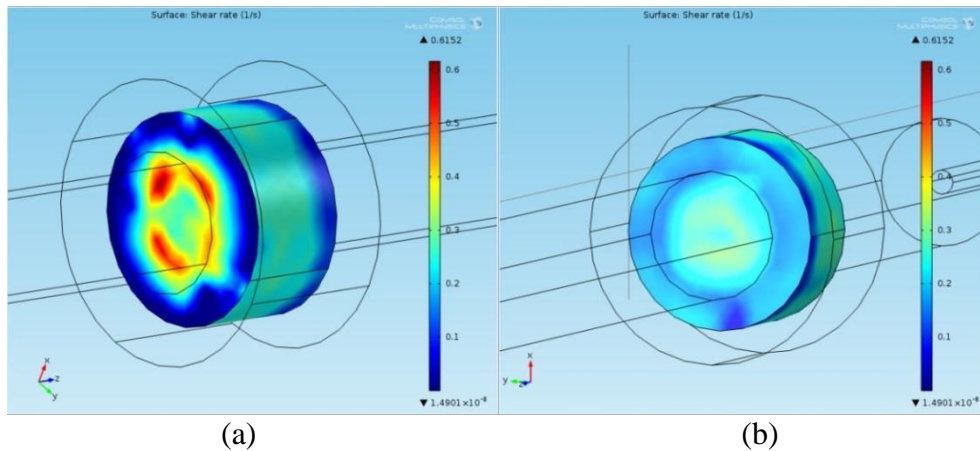
Figure 4.20. Shear rate profiles affecting non-porous tissue scaffold in perfusion bioreactor: (a) anterior side (b) posterior side.

In the models obtained for the perfusion bioreactor with a rigid scaffold, the graph varying with the horizontal axis of shear rates in the perfusion chamber are presented in Figure 4.21. The scaffold was found to have a higher shear rate on the surface that meets the flow.
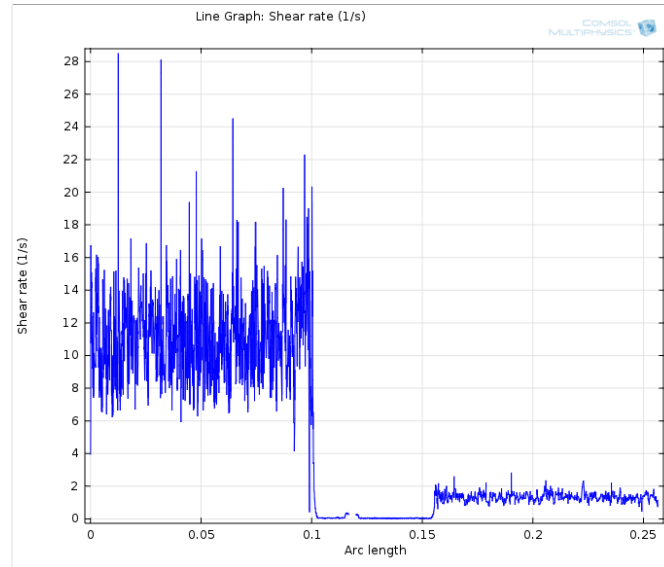
Figure 4.21. Shear rates affecting non-porous tissue scaffold in perfusion bioreactor.

4.2.3. Perfusion Bioreactor Flow Model at Flow Rate of 0.1 mL/min in the Presence of a P3D-6 Permeable Tissue Scaffold

One of the most important goals of the studies aimed at the production of bone grafts with the tissue engineering approach is to achieve homogeneous tissue formation in three dimensional, porous tissue scaffolds. Perfusion bioreactors are systems that provide intra-pore flow to promote nutrient and oxygen transfer to the cells in the inner regions of tissue scaffolds, as well as to promote osteogenic differentiation by applying shear stress to the cells. In the computational fluids dynamics model of the thesis study, simulations were carried out with permeable tissue scaffolds using the "Free and Porous Media Flow Model" in COMSOL's CFD module to develop a more realistic approach that shows parallelism with the experimental conditions and a free four-sided mesh was used to create this model. Properties of permeable tissue scaffold are given in Table 3.6.3. The calculation method of the permeability in the porous scaffolds is based on the doctoral dissertation of I.G. Beskardes [32]. The porosity value has been found to be 78% and the permeability has been calculated as 6.13×10^{-9} m^2. Figure 4.22 presents images of the velocity profile in the perfusion bioreactor

which contains a permeable tissue scaffold. It is seen that the permeable scaffold does not affect the flow in the thin tube and the highest linear velocity was reached in the thin tube by 7.8952×10^{-3} m/s (Figure 4.22-a). The flow velocity has been found to decrease at the surface of the permeable tissue scaffold. However, due to the penetration of the culture medium into the scaffold, a velocity profile in the tissue scaffold can be observed in Figure 4.22-b. Futhermore, it is also observed that the culture media flowed through both the permeable tissue scaffold and the periphery before leaving the perfusion chamber.

(a)   (b)
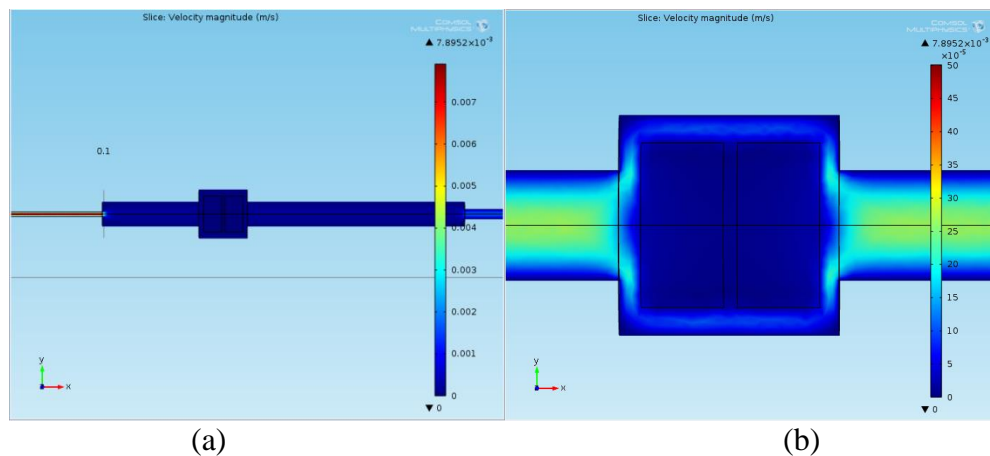
Figure 4.22. Velocity profile in perfusion bioreactor at flow rate of 0.1 mL/min in the presence of a P3D-6 permeable tissue scaffolds: (a) overview, (b) detailed view of the perfusion chamber.

Due to the porosity and permeability properties, the fluid movement in the tissue scaffold continued. Figure 4.23 shows how the velocity profile changes along the horizontal axis. The linear velocity in the internal region of the first permeable tissue scaffold changed from 0.023×10^{-3} to 0.001×10^{-3} (Figure 4.23-b), and the second permeable scaffold changed from 0.0103×10^{-3} to 0.0252×10^{-3}. Expectations have been confirmed that these values would be lower than the linear velocities obtained for the empty perfusion chamber.

(a)   (b)
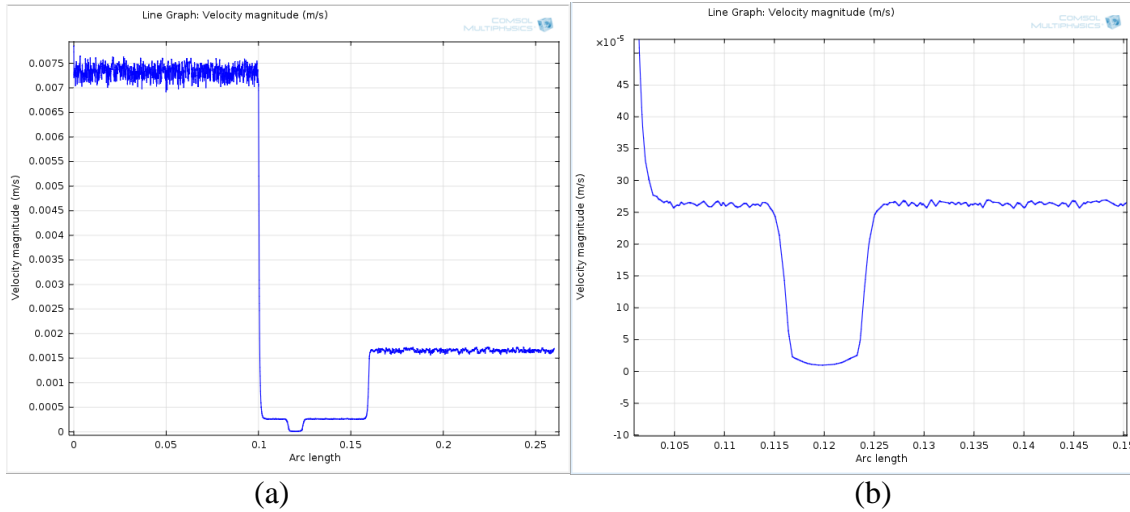
Figure 4.23. Velocity profile in perfusion bioreactor at flow rate of 0.1 mL/min in the presence of a P3D-6 permeable tissue scaffolds: (a) the change in velocity in the reactor along the z-axis, (b) the change in velocity along the z-axis within the perfusion chamber.

The shear stress profiles acting on the surface of the permeable tissue scaffold are presented in Figure 4.24. High shear stress values are observed on the anterior side of the scaffold (Fig. 4.24-a). The physical forces acting on the lateral zones were found to be lower than those acting on the posterior surface (Figure 4.24-b).

(a)   (b)
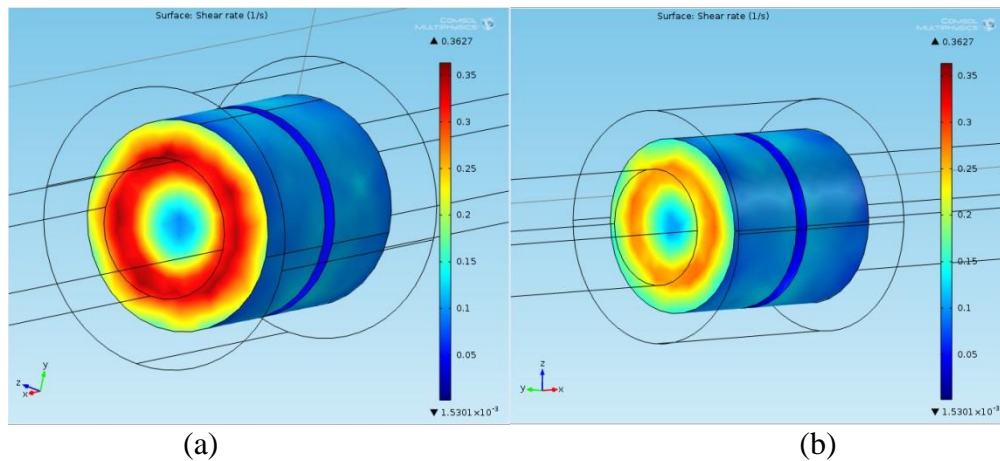
Figure 4.24. Shear rate profiles affecting P3D-6 permeable tissue scaffolds in perfusion bioreactor at flow rate of 0.1 mL/min: (a) anterior side (b) posterior side.

The design of the perfusion chamber plays a major role in imitating the physical forces that affect the tissue scaffolds. In this model, due to the fact that the scaffold does not cause a tight settlement in the chamber, lateral zones are prevented from being exposed to high shear stresses when they contact with freely flowing fluid. However, in order for the scaffold not to

move in the chamber, it is necessary to make the distance between the lower and upper parts of the chamber narrower than the diameter of the tissue scaffold. This causes the center portions of the tissue scaffold to be affected by higher shear stresses. The graph presented in Figure 4.25 shows that the highest shear stress acting on the anterior region of the scaffold in the bioreactor was calculated as 2.5389 x 10^{-4} dyne/cm^2. When these results are evaluated, it can be implied that the increased flow rate in the perfusion bioreactor achieves the resultant increase in shear stresses acting on the cells. It was also found that these values were lower when compared with the results obtained from the studes with the rigid tissue scaffold. It has been concluded that assumptions made in the CFD approaches have a decisive influence on the results and that the pore structure can change the physical forces affecting the cells.
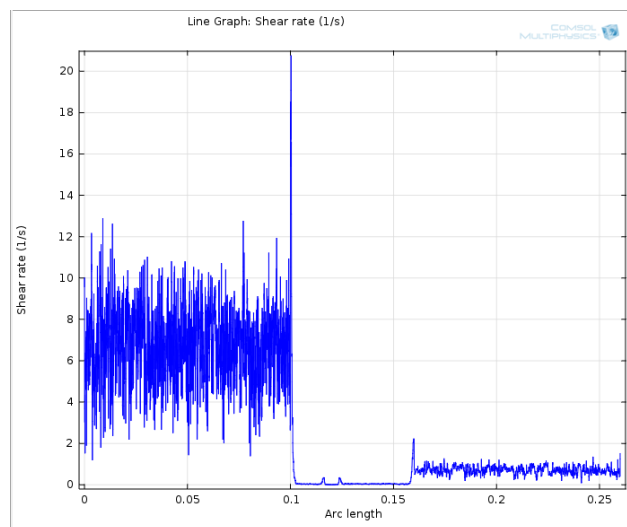
Figure 4.25. Shear rates affecting P3D-6 permeable tissue scaffolds in perfusion bioreactor at flow rate of 0.1 mL/min.

4.2.4. Perfusion Bioreactor Mass Transfer Model at Flow Rate of 0.1 mL/min in the Presence of a Pemeable Tissue Scaffold

The COMSOL Chemical Reaction Engineering Module's "Transport of Diluted Species Models" section has been selected for the simulation of glucose and oxygen transport in the perfusion bioreactor and the tissue scaffold. For the joint evaluation of momentum and mass transfer, "Transport Model of Dilute Species" is mapped to "Free and Porous Media Flow Model". Since the mass transfer is carried out by a permeable tissue scaffold, the mesh structure and features described in Section 4.2.3 are also applicable for this section.

The parameters used for the simulation of glucose and oxygen transfer are presented in Table 3.6.3. From the experimental results, it is assumed that there are 5×10^5 cells in the tissue scaffold and it is also assumed that the glucose and oxygen consumption reactions occur homogeneously in a 3-dimensional tissue scaffold.

The data obtained from the simulations performed for the glucose concentrations are presented graphically in Figure 4.26.

| (a) | (b) |

Figure 4.26. Glucose transport profile P3D-6 perfusion bioreactor in the presence of permeable tissue scaffolds at flow rate of 0.1 mL/min: (a) overview, (b) detailed view of the perfusion chamber.

Using Figure 4.26-a it was determined that the glucose concentration is high in the thin silicon tube and at the inlet of the perfusion chamber (5.5627 mol/m^3). However, glucose concentration was also found to be high in the culture medium surrounding the tissue scaffold in the perfusion chamber (Figure 4.26-b). On the posterior side of the first tissue scaffold, the concentration decreased to 5.33 mol/m^3. Furthermore the concentration rate was found to be 5.32 mol/m^3 on the anterior side of the second scaffold, and 5.078 mol/m^3 on the posterior side. The fact that this gradient is too small suggests that the use of a perfusion bioreactor effectively transfers glucose to the internal regions of the tissue scaffold.

In Figure 4.27-a, b, when the glucose concentration profile on the surface of the permeable tissue scaffold is taken into account, it is seen that the cells on the anterior side that meet the flow are exposed to a concentration of 5.5576 mol/m^3 and the cells on the posterior side have a concentration of about 5.0505 mol/m^3. Because of the fact that the concentration difference

between the anterior and posterior sides is very low, it can be pointed out that the cells in all regions of the tissue scaffold are exposed to similar conditions.

(a)   (b)

Figure 4.27. Glucose concentration profile on the surface of P3D-6 permeable tissue scaffolds in the presence of permeable tissue scaffolds at flow rate of 0.1 mL/min: (a) anterior side (b) posterior side.

The profile of the glucose concentration on the surface of the tissue scaffold system is given in (Figure 4.27). The graph presented in Figure 4.28 was used to examine the change in glucose concentration along the horizontal axis in the bioreactor. It appears that a small portion of the glucose that reaches the tissue scaffold is consumed by the cells. As a result, an increase in the glucose concentration has been detected at the outlet.

Figure 4.28. Change in glucose concentration in perfusion bioreactor in the presence of P3D-6 permeable tissue scaffolds at flow rate of 0.1 mL/min.

The model of glucose transport created by permeable tissue scaffold has shown that both the bioreactor and the gradient within the tissue scaffold are eliminated by increasing the flow rate. Moreover, it has been seen that the glucose level has not been reduced and a micro-environment that allows homogeneous tissue formation has been created successfully.

Another environmental component that is as important as glucose for the cells in tissue engineering is oxygen. In the relevant literature, it has been reported that diffusion coefficient of oxygen is 3-4 times higher than that of glucose [56, 101]. However, due to the lower solubility of oxygen, cells are known to be exposed to low concentrations of oxygen [9, 56].

The data obtained from simulations for oxygen transfer are presented in Figure 4.29. In Figure 4.29-a, the profile obtained was found to be high (0.2001 mol/m^3) at the inlet of the silicone tube, at the inlet of the perfusion chamber and around the scaffold, similar to glucose transfer model. With an efficient transfer system, the cells inside the tissue scaffold were also exposed to high oxygen values. The lowest oxygen concentration value in the scaffold was found to be 0.1214 mol/m^3 (Figure 4.29-b). The low gradient rate suggests that a perfusion bioreactor has created a microenvironment that supports homogenous tissue formation.

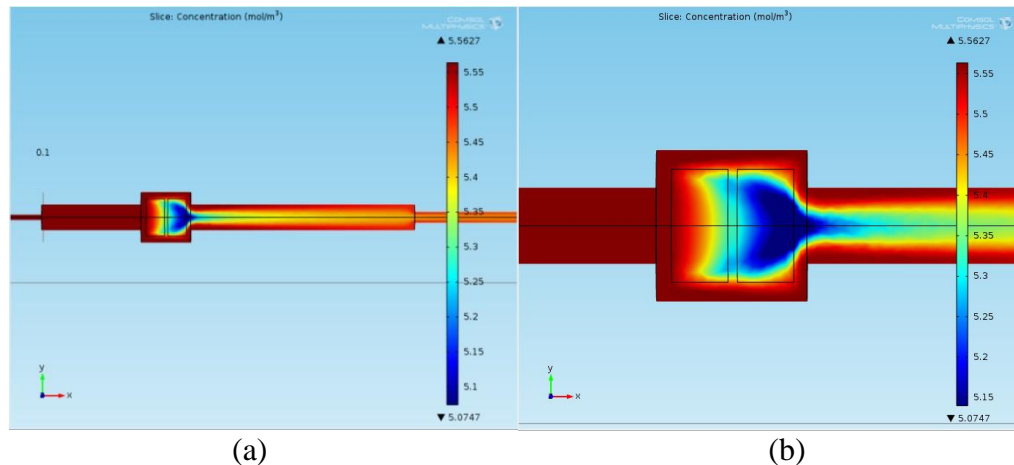(a)   (b)
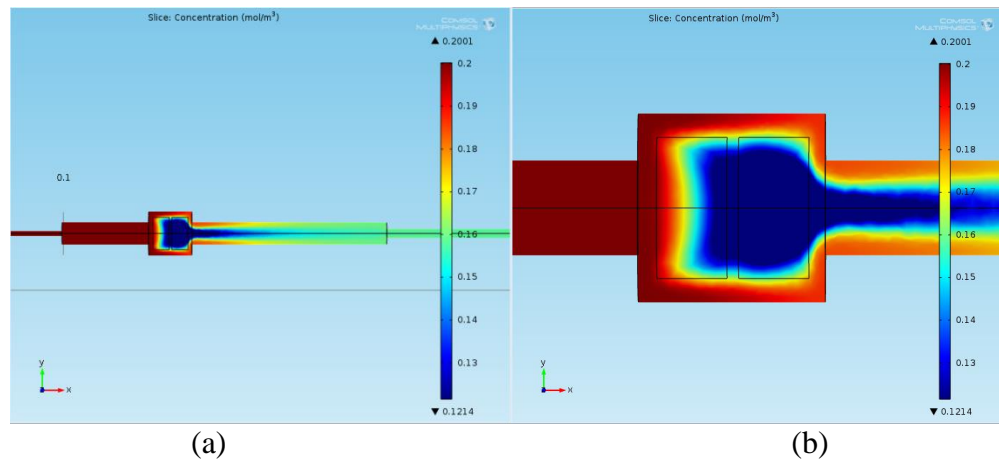
Figure 4.29 Oxygen transport profile P3D-6 perfusion bioreactor in the presence of permeable tissue scaffolds at flow rate of 0.1 mL/min: (a) overview, (b) detailed view of the perfusion chamber.

(a)　　　　　　　　　　　　(b)

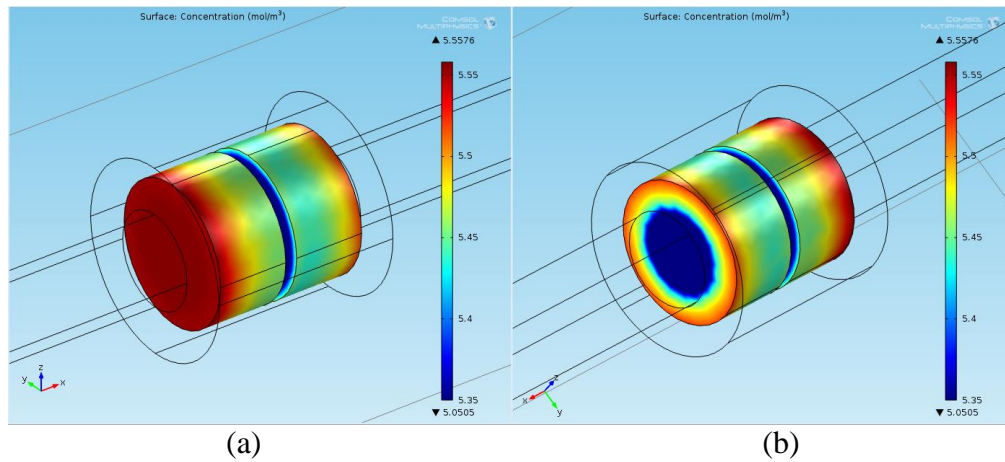Figure 4.30. Oxygen concentration profile on the surface of P3D-6 permeable tissue scaffolds in the presence of permeable tissue scaffolds at flow rate of 0.1 mL/min: (a) anterior side (b) posterior side.

Considering the profiles given in Figure 4.30, the result show that the anterior and posterior surfaces of the tissue scaffold are exposed to similar oxygen concentrations. As it is shown in Figure 4.31, In the perfusion system where the oxygen level in the bioreactor varied along the horizontal axis, only a small portion of the oxygen in the culture medium reaching the tissue scaffold in the system was consumed by the cells. These results have shown that cells will be exposed to sufficient oxygen concentrations even when the circulation of the medium is being performed. The bioreactor system used in the thesis study was found to provide an oxygen concentration of 0.1791 mol/m^3 at the center of the first scaffold, and 0.1278 mol/m^3 at the center of the second scaffold, respectively.
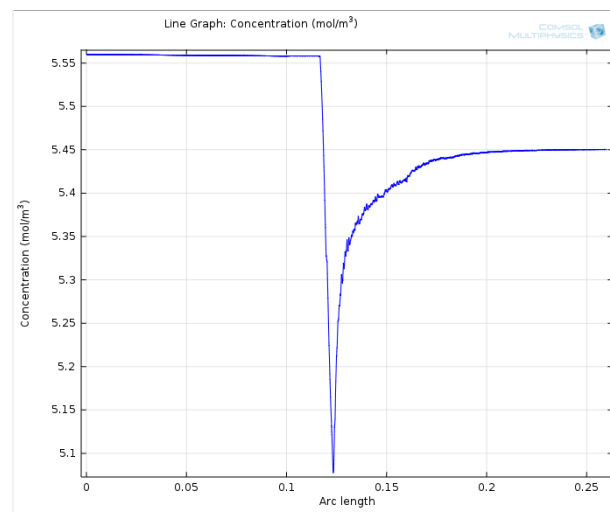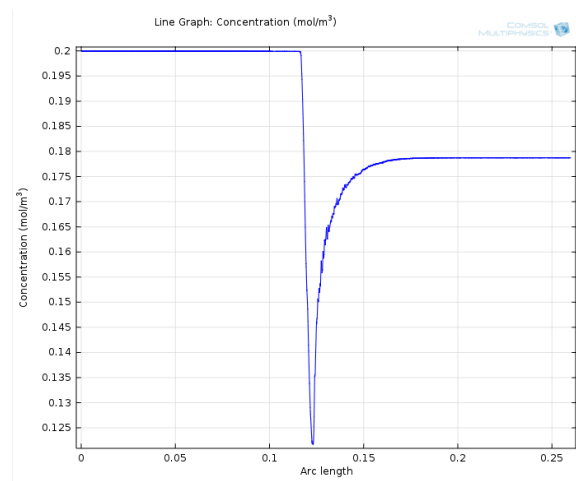

Figure 4.31. Change in oxygen concentration in perfusion bioreactor in the presence of P3D-6 permeable tissue scaffolds at flow rate of 0.1 mL/min.

73

4.2.5. Perfusion Bioreactor Flow Model at Flow Rate of 0.2 mL/min in the Presence of a P3D-6 Pemeable Tissue Scaffold

In this part of the modelling studies, a perfusion bioreactor flow model at the flow rate of 0.2 mL/min in the presence of the   ermeable tissue scaffold that has the same properties has been modelled in order to compare the findings with the perfusion bioreactor flow model at the flow rate of 0.1 mL/min. Figure 4.32 presents images of the velocity profile in the perfusion bioreactor which contains a permeable tissue scaffold. It is seen that the permeable scaffold does not affect the flow in the thin tube and the highest linear velocity was reached in the thin tube by 15.8×10^{-3} m/s (Figure 4.32-a). The flow velocity has been found to decrease at the surface of the permeable tissue scaffold. However, due to the penetration of the culture medium into the scaffold, a velocity profile in the tissue scaffold can be observed in Figure 4.32-b. Futhermore, it is also observed that the culture media flowed through both the permeable tissue scaffold and the periphery before leaving the perfusion chamber.

(a)   (b)

Figure 4.32. Glucose transport profile P3D-6 perfusion bioreactor in the presence of permeable tissue scaffolds at flow rate of 0.2 mL/min: (a) overview, (b) detailed view of the perfusion chamber.

Due to the porosity and permeability properties, the fluid movement in the tissue scaffold continued. Figure 4.33 shows how the velocity profile changes along the horizontal axis. In the perfusion system given, the linear velocity in the internal region of the first permeable tissue scaffold changed from 0.175×10^{-3} to 0.02×10^{-3} m/s (Figure 4.33-b), and the second permeable scaffold changed from 0.02×10^{-3} to 0.05×10^{-3} m/s. Expectations have been

confirmed that these values would be higher than the linear velocities obtained from the 0.1 mL/min model.

(a)   (b)
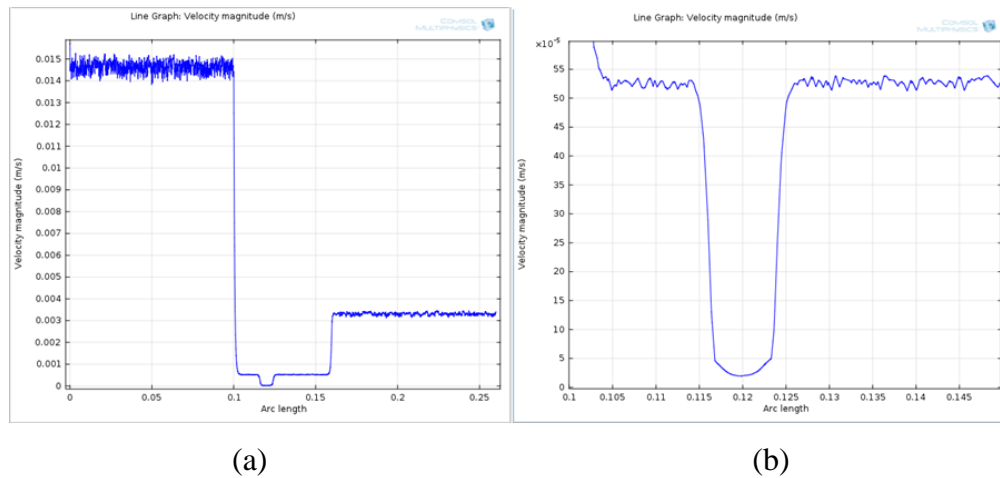
Figure 4.33. Velocity profile in perfusion bioreactor at flow rate of 0.2 mL/min in the presence of a P3D-6 permeable tissue scaffolds: (a) the change in velocity in the reactor along the z-axis, (b) the change in velocity along the z-axis within the perfusion chamber.

The shear stress profiles acting on the surface of the permeable tissue scaffold are presented in Figure 4.34. High shear stress values are observed on the anterior side of the scaffold (Fig. 4.34-a). The physical forces acting on the lateral zones were found to be lower than those acting on the rear surface (Figure 4.34-b).

(a)   (b)
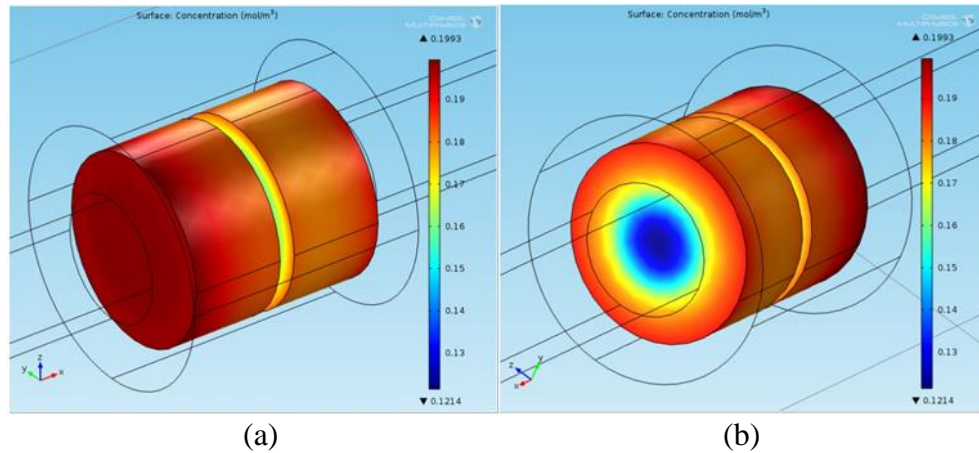
Figure 4.34. Glucose concentration profile on the surface of P3D-6 permeable tissue scaffolds in the presence of permeable tissue scaffolds at flow rate of 0.2 mL/min: (a) anterior side (b) posterior side.

The graph presented in Figure 4.35 show that the highest shear stress acting on the aneterior region of the scaffold in the bioreactor was calculated as 5.0708×10^{-4} dyne/cm^2. When these results are evaluated, it can be implied that the increased flow rate in the perfusion bioreactor achieves the resultant increase in shear stresses acting on the cells. It was also found that these values were higher when compared with the results obtained from the 0.1 mL/min model. It has been concluded that assumptions made in the CFD approaches have a decisive influence on the results and that the flow rate can change the physical forces affecting the cells.
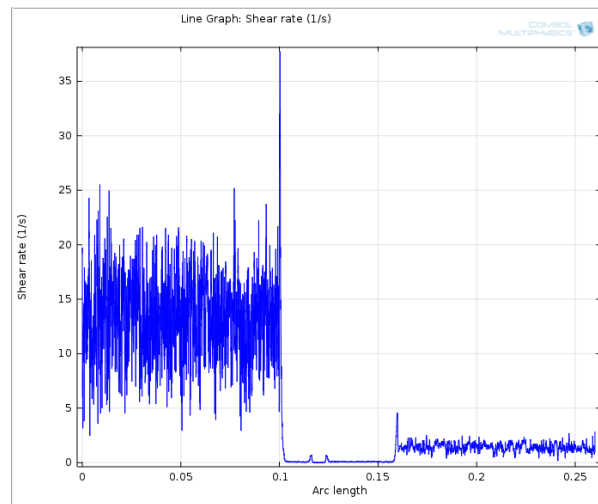
Figure 4.35. Shear rates affecting P3D-6 permeable tissue scaffolds in perfusion bioreactor at flow rate of 0.2 mL/min

4.2.6. Perfusion Bioreactor Mass Transfer Model at Flow Rate of 0.2 mL/min in the Presence of a Pemeable Tissue Scaffold

In this part of the modelling studies, a perfusion bioreactor mass transfer model at the flow rate of 0.2 mL/min in the presence of the permeable tissue scaffold that has the same properties has been modelled in order to compare the findings with the perfusion bioreactor flow model at the flow rate of 0.1 mL/min. From the experimental results, it is assumed that there are 5×10^5 cells in the tissue scaffold and it is also assumed that the glucose and oxygen consumption reactions occur homogeneously in a 3-dimensional tissue scaffold.

The data obtained from the simulations performed for the glucose conentrations are presented graphically in Figure 4.36.
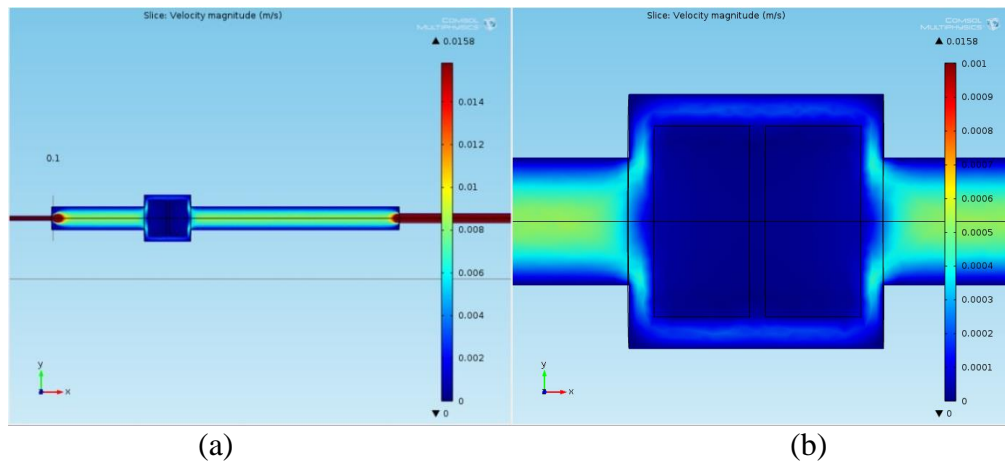
Figure 4.36. Glucose transport profile P3D-6 perfusion bioreactor in the presence of permeable tissue scaffolds at flow rate of 0.2 mL/min: (a) overview, (b) detailed view of the perfusion chamber.

As the Figure 4.36-a suggests, it was determined that the glucose concentration is high in the thin silicon tube and at the inlet of the perfusion chamber (5.5654 mol/m^3). However, glucose concentration was also found to be high in the culture medium surrounding the tissue scaffold in the perfusion chamber (Figure 4.36-b). On the posterior side of the first tissue scaffold, the concentration decreased to 5.558 mol/m^3. Furthermore the concentration rate was found to be 5.442 mol/m^3 on the anterior side of the second scaffold, and 5.325 mol/m^3 on the posterior side. The fact that this gradient is too small suggests that the use of a perfusion bioreactor effectively transfers glucose to the internal regions of the tissue scaffold.

In Figure 4.37, when the glucose concentration profile on the surface of the permeable tissue scaffold is taken into account, it is seen that the cells on the anterior side that meet the flow are exposed to a concentration of 5.5583 mol/m^3 and the cells on the posterior side have a concentration of about 5.2917 mol/m^3. Because the concentration difference between the anterior and posterior sides is very low, it can be pointed out that the cells in all regions of the tissue scaffold are exposed to similar conditions.

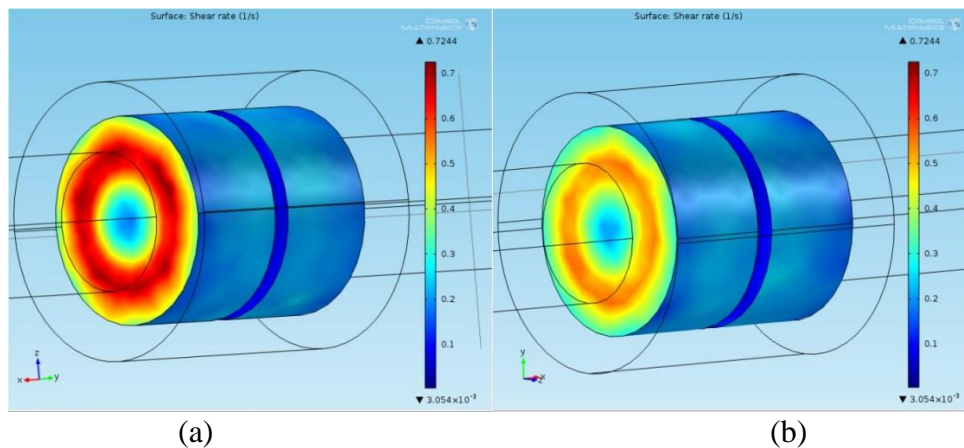(a)   (b)
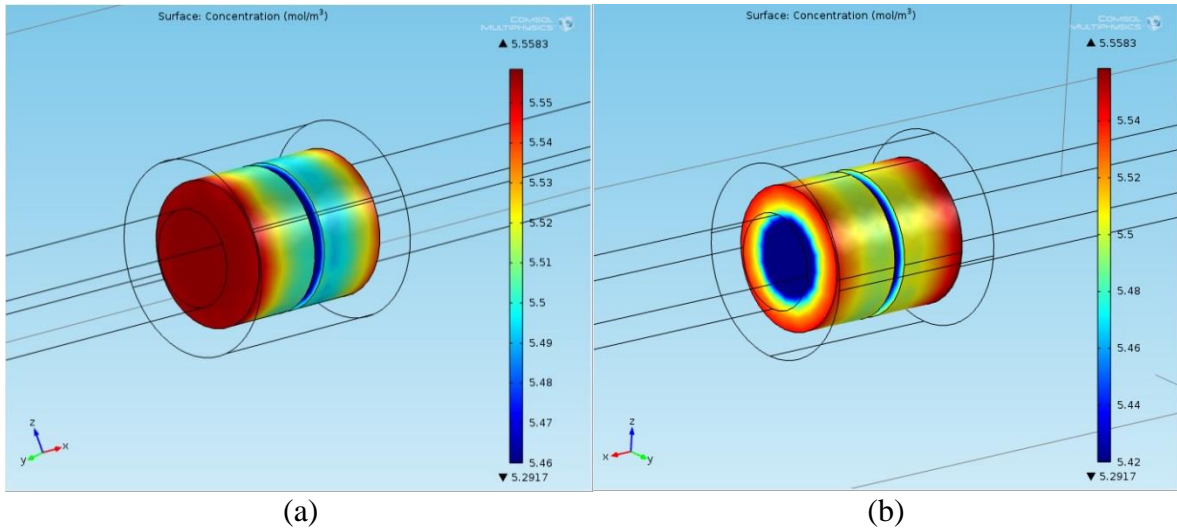
Figure 4.37. Glucose concentration profile on the surface of P3D-6 permeable tissue scaffolds in the presence of permeable tissue scaffolds at flow rate of 0.2 mL/min: (a) anterior side (b) posterior side.

The profile of the glucose concentration on the surface of the tissue scaffold system is given in Figure 4.38. The graph presented in Figure 4.38 was used to examine the change in glucose concentration along the horizontal axis in the bioreactor. It appears that a small portion of the glucose that reaches the tissue scaffold is consumed by the cells. As a result, an increase in the glucose concentration has been detected at the outlet.

Figure 4.38. Change in glucose concentration in perfusion bioreactor in the presence of P3D-6 permeable tissue scaffolds at flow rate of 0.2 mL/min.

78

The model of glucose transport created by permeable tissue scaffold has shown that both the bioreactor and the gradient within the tissue scaffold are eliminated by increasing the flow rate. Moreover, it has been seen that the glucose level has not been reduced and a micro-environment that allows homogeneous tissue formation has been created successfully.

The data obtained from simulations for oxygen transfer are presented in Figure 4.39. In Figure 4.39-a, the profile obtained was found to be high (0.2001 mol/m^3) at the inlet of the silicone tube, at the inlet of the perfusion chamber and around the scaffold, similar to the glucose transfer model. With the efficient transfer system, the cells inside the tissue scaffold were also exposed to high oxygen values. The lowest oxygen concentration value in the scaffold was found to be 0.1525 mol/m^3 (Figure 4.39-b). The low gradient rate suggests that the perfusion bioreactor has created a microenvironment that supports homogenous tissue formation.
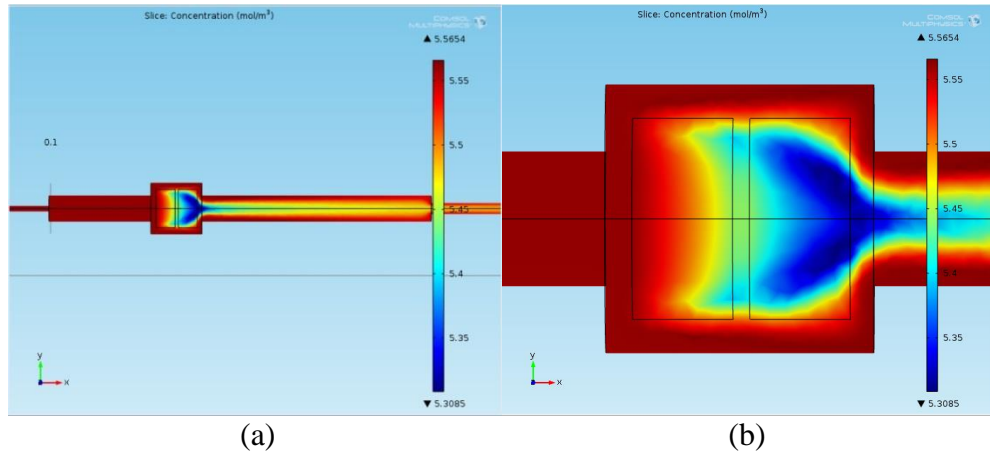

(a)   (b)
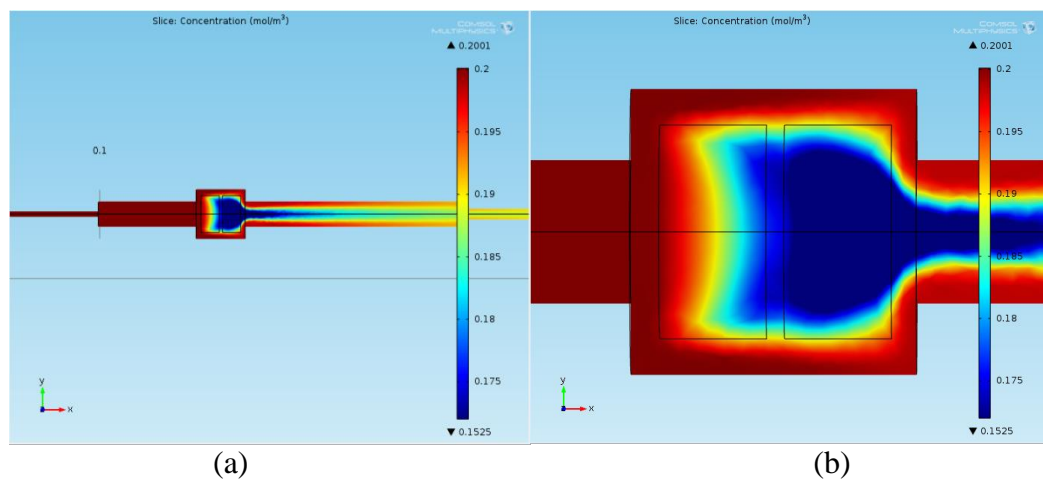
Figure 4.39 Oxygen transport profile P3D-6 perfusion bioreactor in the presence of permeable tissue scaffolds at flow rate of 0.2 mL/min: (a) overview, (b) detailed view of the perfusion chamber.

(a)   (b)
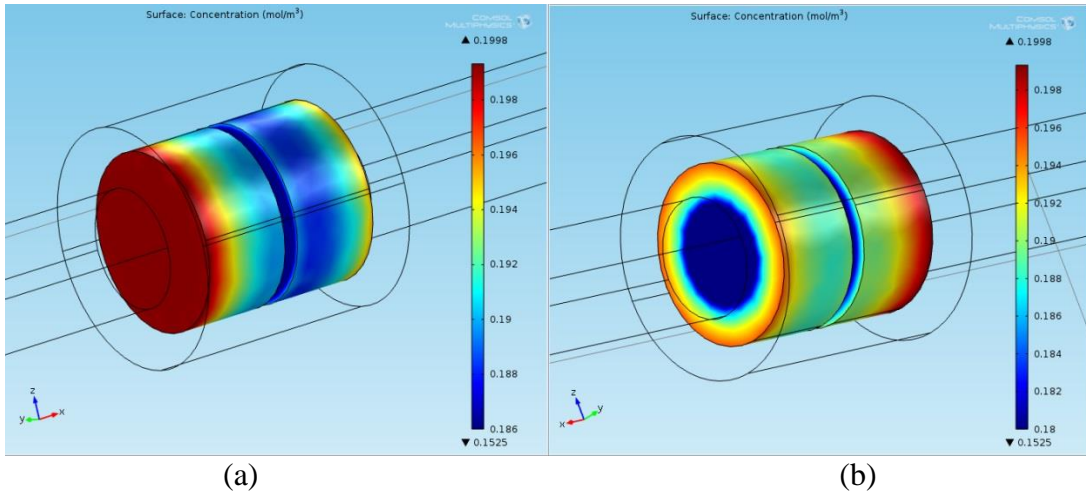
Figure 4.40. Oxygen concentration profile on the surface of P3D-6 permeable tissue scaffolds in the presence of permeable tissue scaffolds at flow rate of 0.2 mL/min: (a) anterior side (b) posterior side.

Considering the profiles given in Figure 4.40 and the graph given in Figure 4.41, the result show that the anterior and posterior surfaces of the tissue scaffold are exposed to similar oxygen concentrations. In the perfusion system where the oxygen level in the bioreactor varied along the horizontal axis, only a small portion of the oxygen in the culture medium reaching the tissue scaffold in the system was consumed by the cells. These results have shown that cells will be exposed to sufficient oxygen concentrations even when the circulation of the medium is being performed. The bioreactor system used in the thesis study was found to provide an oxygen concentration of 0.191 mol/m^3 at the center of the first scaffold, and 0.1614 mol/m^3 at the center of the second scaffold respectively.
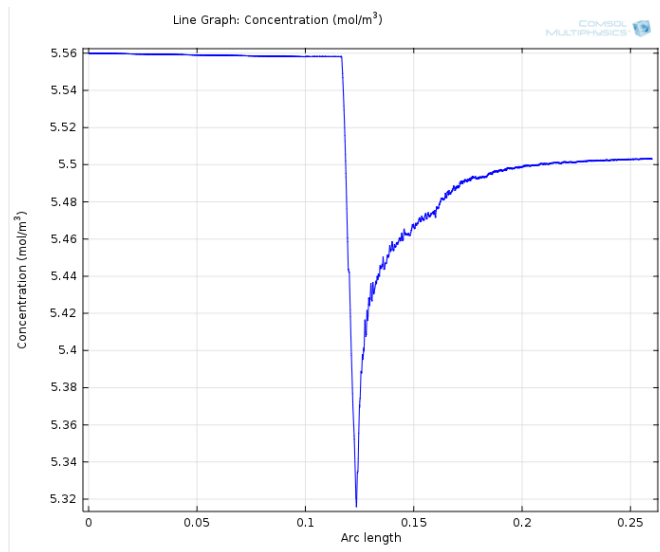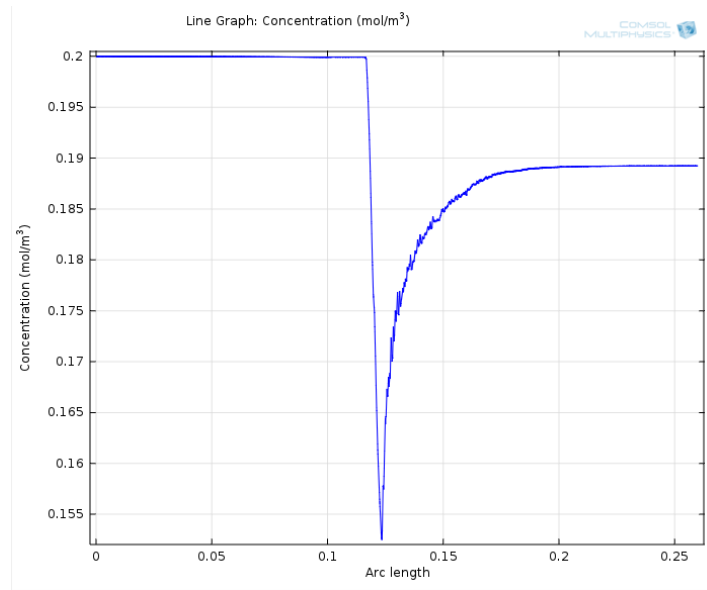
Figure 4.41. Change in oxygen concentration in perfusion bioreactor in the presence of P3D-6 permeable tissue scaffolds at flow rate of 0.2 mL/min.

4.2.7. Perfusion Bioreactor Flow Model at Flow Rate of 0.27 mL/min in the Presence of a P3D-10 Pemeable Tissue Scaffold

In this part of the modelling studies, a perfusion bioreactor flow model at the flow rate of 0.27 mL/min has been modelled in the presence of a P3D-10 pemeable tissue scaffold in order to investigate the availability of the production of larger bone grafts. The aim of the modelling study is to to investigate whether the culture conditions generated at a flow rate of 0.1 mL/min in the P3D-6 chamber show similar characteristics at a flow rate of 0.27 mL / min in the P3D-10 chamber. The geometry and mesh structure that are created in COMSOL for this purpose are given in Figure 4.42-a and 4.42-b. Figure 4.42-c shows the formation of a laminar flow in the chamber of the P3D-10 bioreactor. The linear velocity values (2.6×10^{-4} m/s) obtained as a result of the modeling studies for the anterior and posterior sides of the chamber were found to be very close to those obtained in the P3D-6 circles. However, the fact that the velocity values of the tissue scaffolds in figure 4.42-d are found to be approximately 1.6×10^{-4} m/s reveals that the culture conditions in the perfusion circles P3D-6 and P3D-10 are different from each other. It was found that higher flow rate is more likely to be more efficient fot the tissue scaffolds cultured in the P3D-10 perfusion chambers.
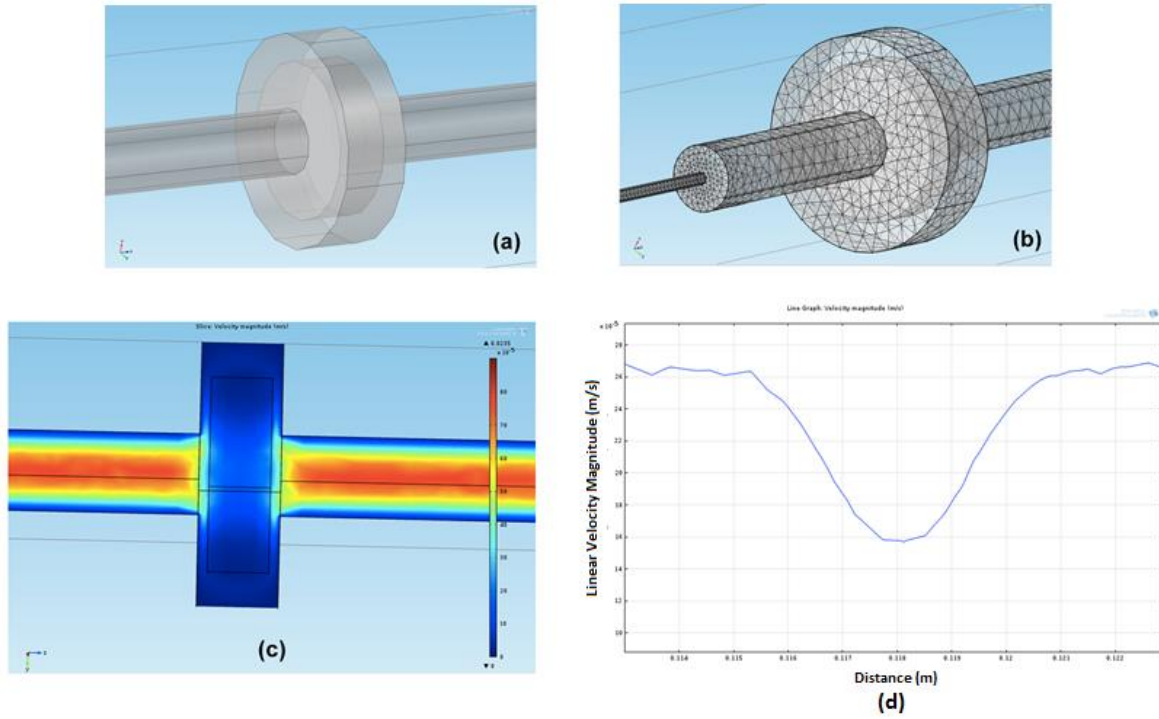
Figure 4.42. CFD Modelling studies with P3D-10 perfusion chamber: (a) perfusion chamber geometry (b) use of free tetrahydral mesh (c) flow profile in the P3D-10 perfusion chamber and tissue scaffold at a flow rate of 0.27 mL/min (d) variation of the linear velocity with the distance in the perfusion circle.

5. CONCLUSION

Within the scope of this thesis study, the osteoblastic differentiation potentials of human mesenchymal stem cells were investigated under the condition of being seeded into chitosan-HA tissue scaffolds in various sizes and cultured on perfusion bioreactors within different flow velocities. The results obtained from the experiments using the perfusion bioreactors were evaluated comparatively with the studies carried out under the static conditions. In the last part of the study, flow and mass transfer simulation studies were performed with COMSOL software for the characterization of the microenvironment to which the cells cultured in the perfusion bioreactor were exposed. Significant findings from the study are summarized below:

- Chitosan-HA SPHCs have been successfully produced by combining microwave radiation and gas foaming methods using glyoxal as a crosslinking agent, and sodium bicarbonate as ($NaHCO_3$) a foaming agent.

- In order to investigate the osteoblastic differentiation potentials of the hMSCs in the perfusion bioreactor, two different tissue scaffolds have been successfully constructed for dynamic approach and the setup of the experiment has been successfully completed.

- P3D-6 and P3D-10 perfusion chambers which are designed as porous tissue scaffolds and offered many advantages in terms of providing ease of operation were used for the bioreactor studies. The syringe pump was preferred for media flow, so that the flow rate could be controlled without any complications. A system has been established in which sterilization can be maintained in long-term in vitro cultures by the use of appropriate parts and filters.

- The installation of the perfusion bioreactor, a bioreactor type that offers many advantages for bone tissue engineering; prevents leakage and contamination during long-term operations and allows manipulation during environmental refinement has been successfully completed.

- Dynamic culture approach is used in the studies that were carried out in a perfusion bioreactor and the static cell seeding studies were carried out in 24-well TCPS and tissue scaffolds.

- Because the chitosan-HA SPHC tissue scaffolds support cell adhesion and can reach high swelling rates in a short time, the pipette-assisted cell suspension was evaluated to be high in optical density as a result of its absorptivity to the scaffold due to the abundance of pores.

- It has been observed that the flow rate and flow direction parameters have statistically significant effects on the adhesion of cells to the scaffold surfaces.

- It was determined that among the cell culture studies carried out under different conditions for 21-days in vitro, the highest cell viability that has been reached in the perfusion bioreactor was discovered to be under the static culture conditions in P3D-6 tissue scaffolds.

- Various simulation studies have been carried out using COMSOL software to characterize the micro-environment in which the cultured cells of the chitosan-HA SPHCs in the perfusion bioreactor are exposed at low (0.1 mL/min) and high (0.2 mL/min) flow rates.

- In order to verify the precision of the model, the velocity values in the flow model created in the system without a tissue scaffold was compared with the results obtained from the analytical trials.

- Simulations based on non-porous scaffolds have shown that non-porous structure changes the flow profile too much. As a more realistic approach, the permeable tissue scaffold model was used in order to evaluate the effect of flow and mass transfer models. It was found that the velocity profiles obtained from the model established by the assumption of permeable tissue scaffolds are compatible with the expected results. For this reason, simulations of glucose and oxygen transfer in the perfusion bioreactor and tissue scaffold were carried out using the permeable scaffold model.

- According to the outcome of the studies, it was determined that hMSCs cultured in dynamic conditions (P3D-6, 0.1 mL/min-0.2 mL/min) after static cell seeding supported the osteoblastic differentiation.

In the light of all the findings obtained in the thesis study, it has been seen that the dynamic culture approach performed in perfusion bioreactor with chitosan-HA tissue scaffolds is a suitable in vitro model for bone tissue engineering by means of supporting the osteogenic

differentiation, but not on cell viability. Computational fluid dynamics modelling studies have been considered to be a significant contribution in terms of evaluating experimental results and recommending appropriate operating parameters for bone tissue regeneration in dynamic cultures. Experimental studies and CFD simulations have shown that all parameters are critical for successfully achieving in vitro production of engineered bone grafts in thesis studies conducted with tissue scaffolds of different sizes and subjected to different flow rates.

6. REFERENCES

[1]   Lee, Na Kyung, et al. Endocrine regulation of energy metabolism by the skeleton. *Cell* 130.3: 456-469, **2007**.

[2]   Stevens, M., Biomaterials for bone tissue engineering, *Materials Today*, 11,18-25, **2008**.

[3]   Neovius, E., & Engstrand, T. Craniofacial reconstruction with bone andbiomaterials: Review over the last 11 years. *Journal of Plastic, Reconstructive and Aesthetic Surgery*, 63, 1615–1623, **2010**.

[4]   Holtorf, Heidi L., John A. Jansen, and Antonios G. Mikos. Modulation of cell differentiation in bone tissue engineering constructs cultured in a bioreactor. *Tissue Engineering*. Springer US, 225-241, **2006**.

[5]   Gaspar, Diana Alves, Viviane Gomide, and Fernando Jorge Monteiro. The role of perfusion bioreactors in bone tissue engineering. *Biomatter* 2.4: 167-175, **2012**.

[6]   Yu, Xiaojun, et al. Bioreactor-based bone tissue engineering: the influence of dynamic flow on osteoblast phenotypic expression and matrix mineralization. *Proceedings of the National Academy of Sciences of the United States of America* 101.31: 11203-11208, **2004**.

[7]   Hill, Nicola M., J. Geoffrey Horne, and Peter A. Devane. Donor site morbidity in the iliac crest bone graft. *Australian and New Zealand Journal of Surgery* 69.10: 726-728, **1999**.

[8]   Seiler 3rd, J. G., and J. Johnson. Iliac crest autogenous bone grafting: donor site complications. *Journal of the Southern Orthopaedic Association* 9.2: 91-97, **1999.**

[9]   Perez-Sanchez, M. J., Ramirez-Glindon, E., Lledo-Gil, M., Calvo-Guirado, J. L., &Perez- Sanchez, C. Biomaterials for bone regeneration. *Medicina OralPatologia Oral y Cirugia Bucal*, 15, 517–522, **2010**.

[10]   Garg, T., Singh, O., Arora, S., & Murthy, R. Scaffold: A novel carrier for celland drug delivery. *Critical Reviews in Therapeutic Drug Carrier Systems* 29, 1–63, **2012**.

[11]   Stodolak-Zych, E., Szumera, M., & Blazewicz, M. Osteoconductive nanocomposite materials for bone regeneration. *Materials Science Forum*, 730–732, 38–43, **2012**.

[12]   Barradas, A. M. C., Yuan, H., van Blitterswijk, C. A., & Habibovic, P. Osteoinductive biomaterials: Current knowledge of properties, experimental models and biological mechanisms. *European Cells and Materials* 21, 407–429, **2011.**

[13]   Fröhlich, Mirjam, et al. Bone grafts engineered from human adipose-derived stem cells in perfusion bioreactor culture. *Tissue Engineering Part A* 16.1: 179-189, **2009**.

[14]   Vunjak-Novakovic G, Meinel L, Altman G, Kaplan D: Bioreactor cultivation of osteochondral grafts. *Orthod Craniofac Res*, 8:209-218, **2005.**

[15] Marolt, Darja, Miomir Knezevic, and Gordana Vunjak-Novakovic. Bone tissue engineering with human stem cells. *Stem Cell Research & Therapy* 1.2: 10, **2010**.

[16] Mygind T, Stiehler M, Baatrup A, Li H, Zou X, Flyvbjerg A, Kassem M, Bunger C: Mesenchymal stem cell ingrowth and diff erentiation on coralline hydroxyapatite scaffolds. *Biomaterials*, 28:1036-1047, **2010**.

[17] Boukhechba, Florian, et al. Human primary osteocyte differentiation in a 3D culture system. *Journal of Bone and Mineral Research* 24.11: 1927-1935, **2009**.

[18] Turhani, Dritan, et al. Three-dimensional composites manufactured with human mesenchymal cambial layer precursor cells as an alternative for sinus floor augmentation: an in vitro study. *Clinical Oral Implants Research* 16.4: 417-424, **2005**.

[19] Meinel, Lorenz, et al. Bone tissue engineering using human mesenchymal stem cells: effects of scaffold material and medium flow. *Annals of Biomedical Engineering* 32.1: 112-122, **2004**.

[20] Chesnutt, Betsy M., et al. Composite chitosan/nano-hydroxyapatite scaffolds induce osteocalcin production by osteoblasts in vitro and support bone formation in vivo. *Tissue Engineering Part A* 15.9: 2571-2579, **2009**.

[21] Hofmann, Sandra, et al. Control of in vitro tissue-engineered bone-like structures using human mesenchymal stem cells and porous silk scaffolds. *Biomaterials* 28.6: 1152-1162, **2007**.

[22] Dalby, Matthew J., et al. The control of human mesenchymal cell differentiation using nanoscale symmetry and disorder. *Nature Materials* 6.12: 997-1003, **2007.**

[23] Comisar, Wendy A., et al. Engineering RGD nanopatterned hydrogels to control preosteoblast behavior: a combined computational and experimental approach. *Biomaterials* 28.30: 4409-4417, **2007**.

[24] Engler, Adam J., et al. Matrix elasticity directs stem cell lineage specification. *Cell* 126.4 : 677-689, **2006**.

[25] Karageorgiou, Vassilis, et al. Porous silk fibroin 3-D scaffolds for delivery of bone morphogenetic protein-2 in vitro and in vivo. *Journal of Biomedical Materials Research Part A* 78.2: 324-334, **2006**.

[26] Chao, Pen-hsiu Grace, Warren Grayson, and Gordana Vunjak-Novakovic. Engineering cartilage and bone using human mesenchymal stem cells. *Journal of Orthopaedic Science* 12.4: 398, **2007.**

[27] Grayson, Warren L., et al. Effects of initial seeding density and fluid perfusion rate on formation of tissue-engineered bone. *Tissue Engineering Part A* 14.11: 1809-1820, **2008.**

[28]   Sikavitsas, Vassilios I., et al. Mineralized matrix deposition by marrow stromal osteoblasts in 3D perfusion culture increases with increasing fluid shear forces. *Proceedings of the National Academy of Sciences* 100.25: 14683-14688, **2003**.

[30]   Sittichockechaiwut, Anuphan, et al. Use of rapidly ehavior ing osteoblasts and short periods of mechanical loading to accelerate matrix maturation in 3D scaffolds. *Bone* 44.5: 822-829, **2009**.

[31]   Hutmacher, Dietmar W., and Harmeet Singh. Computational fluid dynamics for improved bioreactor design and 3D culture. *Trends in Biotechnology* 26.4: 166-172, **2008**.

[32]   Gercek Beskardes, I., *Comparison of different bioreactor performances for osteogenic differentiation of mesenchymal stem cells*. Doctoral Disseration, Hacettepe University Institute of Natural and Applied Sciences, Ankara, **2014**.

[33]   Cinbiz, M.N., Tigli, R.S., Beskardes, I.G., Gumusderelioglu, M., Colak, U., Computational fluid dynamics modeling of momentum transport in rotating wall perfused bioreactor for cartilage tissue engineering, *Journal of Biotechnology*, 150, 389-95, **2010**.

[34]   Mravic, Marco, Bruno Péault, and Aaron W. James. Current trends in bone tissue engineering. *BioMed Research International*, **2014**.

[35]   Gümüşderelioğlu, M., Doku Mühendisliğinin Ürünleri. *Bilim ve Teknik Dergisi*, **2010**.

[36]   Amini, A.R., Laurencin, C.T., Nukavarapu, S.P., Bone tissue engineering: recent advances and challenges, *Critical reviews in Biomedical Engineering*, 40, 363-408, **2012**.

[37]   Zimmermann, C.E., Borner, B.I., Hasse, A., Sieg, P., Donor site morbidity after microvascular fibula transfer, *Clinical Oral Investigations*, 5, 214-9, **2001**.

[38]   Agarwal, R., García, J.A., Biomaterial strategies for engineering implants for enhanced osseointegration and bone repair, *Advanced Drug Delivery Reviews*, 12756, 1-10, **2015**.

[39]   Wua, S., Xiangmei, L., Kelvin, W.K., Changsheng, Y., Xianjin, Y.L., Biomimetic porous scaffolds for bone tissue engineering, *Materials Science and Engineering*, 80, 1-36, **2014**.

[40]   Rodrigues, A.V.C, Fernandes, T.G., Diogo, M.M., Stem cell cultivation in bioreactors, *Biotechnology Advances*, 29, 815-829, **2011**.

[41]   Schofer, M.D., Tunnermann, L., Kaiser, H., Roessler, P.P., Theisen, C., Heverhagen, J.T., Hering, J., Voelker, M., Agarwal, S., Efe, T., Fuchs-Winkelmann, S., Paletta, R.J., Functionalisation of PLLA nanofiber scaffolds using a possible cooperative effect between collagen type I and BMP-2: impact on colonization and bone formation in vivo, *Journal of Material Science*, 2227-2233, **2012**.

[42]   Villalona, Gustavo A., et al. Cell-seeding techniques in vascular tissue engineering. *Tissue Engineering Part B*: Reviews 16.3: 341-350, **2010**.

[43]   Wendt, D., Timmins, N., Malda, J., Janssen, F., Ratcliffe, A., Vunjak- Novakovic, G., Martin, I. Bioreactors for tissue engineering. *Tissue Engineering*, 1ˢᵗ ed., (eds: Van Blitterswijk, C.A.,), Academic Press, Canada, 483-506, **2008**.

[44]   Griffon, D.J., Abulencia, J.P., Ragetly, G.R., Fredericks, L.P., Chaieb, S., A comparative study of seeding techniques and three-dimensional matrices for mesenchymal cell attachment. *Journal of Tissue Engineering and Regenerative Medicine*, 5, 169-79, **2011**.

[45]   Ellis, M., M. Jarman-Smith, and J. B. Chaudhuri. Bioreactor systems for tissue engineering: a four-dimensional challenge. *Bioreactors for Tissue Engineering*. Springer Netherlands, 1-18, **2005**.

[46]   Frost, H.M., Skeletal structural adaptations to mechanical usage (SATMU): 2. Redefining Wolff's law: the remodeling problem, *The Anatomical Record*, 226, 414-22, **1990**.

[47]   Chen, Ching-Yun, et al. 3D porous calcium-alginate scaffolds cell culture system improved human osteoblast cell clusters for cell therapy. *Theranostics* 5.6: 643, **2015**.

[48]   Jaasma, M.J., Plunkett, A.N., O'Brien, F.J., Design and validation of a dynamic flow perfusion bioreactor for use with compliant tissue engineering scaffolds, *Journal of Biotechnology*, 133, 490-496, **2008**.

[49]   Moffat, K.L., Neal, A.R., Freed, E.L., Guilak F., Engineering functional tissues: in vitro culture parameters, *Principle of Tissue Engineering*, (eds: Lanza, R., Langer, R., Vacanti, J.P.), Boston, 237-259, **2013**.

[50]   Bhumiratana, Sarindr, et al. Principles of bioreactor design for tissue engineering. *Principles of Tissue Engineering*: 261-78, **2013.**

[51]   Grayson, Warren L., et al. Optimizing the medium perfusion rate in bone tissue engineering bioreactors. *Biotechnology and Bioengineering* 108.5: 1159-1170, **2011.**

[52]   Yeatts, Andrew B., and John P. Fisher. Bone tissue engineering bioreactors: dynamic culture and the influence of shear stress. *Bone* 48.2: 171-181, **2011.**

[53]   Salehi-Nik, Nasim, et al. Engineering parameters in bioreactor's design: a critical aspect in tissue engineering. *BioMed Research International*, **2013.**

[54]   Godara, P., McFarland, C.D., Nordon, E.R., Design of bioreactors for mesenchymal stem cell tissue engineering, *Journal of Chemical Technology Biotechnology*, 408-420, **2008**.

[55]   Sladkova, Martina, and Giuseppe Maria de Peppo. Bioreactor systems for human bone tissue engineering. *Processes* 2.2: 494-525, **2014.**

[56]   El Haj, A.J., Cartmell, H.S., Bioreactors for bone tissue engineering, *Journal of Engineering and Medicine*, 1523-1532, **2010**.

[57]   Marijanovic, Inga, et al. Bioreactor-Based Bone Tissue Engineering. *Advanced Techniques in Bone Regeneration*. InTech, **2016**.

[58]   Tığlı, R. Seda, and Menemşe Gümüşderelioğlu. Chondrogenesis on BMP-6 loaded chitosan scaffolds in stationary and dynamic cultures. *Biotechnology and Bioengineering* 104.3: 601-610, **2009.**

[59]   Sikavitsas, V.I., Bancroft, G.N., Mikos, A.G., Formation of three-dimensional cell/polymer constructs for bone tissue engineering in a spinner flask and a rotating wall vessel bioreactor, *Journal of Biomedical Materials Research*, 62, 136-48, **2002**.

[60]   Chen, Huang-Chi, and Yu-Chen Hu. Bioreactors for tissue engineering. *Biotechnology Letters* 28.18: 1415-1423, **2006**.

[61]   Bartnikowsk,I M., Klein, J.T., Melchels, F.P.W., Woodruf, M.A., Effects of scaffold architecture on mechanical characteristics and osteoblast response to static and perfusion bioreactor cultures, *Biotechnology and Bioengineering*, 1440-1451, **2014**.

[62]   Yeatts, Andrew B., et al. In vivo bone regeneration using tubular perfusion system bioreactor cultured nanofibrous scaffolds. *Tissue Engineering Part A* 20.1-2: 139-146, **2013.**

[63]   Kasper, F.K., Liao, J., Kretlow, J.D., Sikavitsas, V.I., Mikos, A.G., Flow perfusion culture of mesenchymal stem cells for bone tissue engineering, *StemBook*, **2008**.

[64]   Rauh, Juliane, et al. Bioreactor systems for bone tissue engineering. *Tissue Engineering Part B*: Reviews 17.4: 263-280, **2011.**

[65]   Yeatts, Andrew B., and John P. Fisher. Bone tissue engineering bioreactors: dynamic culture and the influence of shear stress. *Bone* 48.2: 171-181, **2011**.

[66]   Bancroft, Gregory N., et al. Fluid flow increases mineralized matrix deposition in 3D perfusion culture of marrow stromal osteoblasts in a dose-dependent manner. *Proceedings of the National Academy of Sciences* 99.20: 12600-12605, **2002**.

[67]   Datta, Néha, et al. In vitro generated extracellular matrix and fluid shear stress synergistically enhance 3D osteoblastic differentiation. *Proceedings of the National Academy of Sciences of the United States of America* 103.8: 2488-2493, **2006.**

[68]   Holtorf, Heidi L., et al. Flow perfusion culture of marrow stromal cells seeded on porous biphasic calcium phosphate ceramics. *Annals of Biomedical Engineering* 33.9: 1238-1248, **2005**.

[69]   Gomes, Manuela E., et al. Effect of flow perfusion on the osteogenic differentiation of bone marrow stromal cells cultured on starch-based three-dimensional scaffolds. *Journal of Biomedical Materials Research Part A* 67.1: 87-95, **2003**.

[70]   Gomes, Manuela E., et al. Influence of the porosity of starch-based fiber mesh scaffolds on the proliferation and osteogenic differentiation of bone marrow stromal cells cultured in a flow perfusion bioreactor. *Tissue Engineering* 12.4: 801-809, **2006.**

[71]   Holtorf, Heidi L., John A. Jansen, and Antonios G. Mikos. Flow perfusion culture induces the osteoblastic differentiation of marrow stromal cell-scaffold constructs in the absence of dexamethasone. *Journal of Biomedical Materials Research Part A* 72.3 326-334, **2005.**

[72]   Sikavitsas, Vassilios I., et al. Flow perfusion enhances the calcified matrix deposition of marrow stromal cells in biodegradable nonwoven fiber mesh scaffolds. *Annals of Biomedical Engineering* 33.1: 63, **2005**

[73]   Gomes, Manuela E., et al. In vitro localization of bone growth factors in constructs of biodegradable scaffolds seeded with marrow stromal cells and cultured in a flow perfusion bioreactor. *Tissue Engineering* 12.1: 177-188, **2006**.

[74]   Alvarez-Barreto, Jose F., et al. Flow perfusion improves seeding of tissue engineering scaffolds with different architectures. *Annals of Biomedical Engineering* 35.3: 429-442, **2007**.

[75]   Alvarez-Barreto, Jose F., and Vassilios I. Sikavitsas. Improved mesenchymal stem cell seeding on RGD-modified poly (L-lactic acid) scaffolds using flow perfusion. *Macromolecular Bioscience* 7.5: 579-588, **2007**.

[76]   Bjerre, Lea, et al. Flow perfusion culture of human mesenchymal stem cells on silicate-substituted tricalcium phosphate scaffolds. *Biomaterials* 29.17: 2616-2627, **2008**.

[77]   Sikavitsas, Vassilios I., et al. Influence of the in vitro culture period on the in vivo performance of cell/titanium bone tissue-engineered constructs using a rat cranial critical size defect model. *Journal of Biomedical Materials Research Part A* 67.3: 944-951, **2003.**

[78]   Grayson, Warren L., et al. Engineering anatomically shaped human bone grafts. *Proceedings of the National Academy of Sciences* 107.8: 3299-3304, **2010**.

[79]   Xie, Youzhuan, et al. Three-dimensional flow perfusion culture system for stem cell proliferation inside the critical-size β-tricalcium phosphate scaffold. *Tissue Engineering* 12.12: 3535-3543, **2006**.

[81]   Olivier, V., et al. In vitro culture of large bone substitutes in a new bioreactor: importance of the flow direction. *Biomedical Materials* 2.3: 174, **2007.**

[82]   Bernhardt, Anne, et al. Mineralised collagen—an artificial, extracellular bone matrix—improves osteogenic differentiation of bone marrow stromal cells. *Journal of Materials Science: Materials in Medicine* 19.1: 269-275, **2008.**

[83]   Pisanti, Paola, et al. Tubular perfusion system culture of human mesenchymal stem cells on poly-L-lactic acid scaffolds produced using a supercritical carbon dioxide-

assisted process. *Journal of Biomedical Materials Research Part A* 100.10: 2563-2572, **2012.**

[84]   Janssen, F. W., et al. Online measurement of oxygen consumption by goat bone marrow stromal cells in a combined cell-seeding and proliferation perfusion bioreactor. *Journal of Biomedical Materials Research Part A* 79.2: 338-348, **2006.**

[85]   Janssen, Frank W., et al. A perfusion bioreactor system capable of producing clinically relevant volumes of tissue-engineered bone: in vivo bone formation showing proof of concept. *Biomaterials* 27.3: 315-323, **2006.**

[86]   Janssen, F. W., et al. Human tissue-engineered bone produced in clinically relevant amounts using a semi-automated perfusion bioreactor system: a preliminary study. *Journal of Tissue Engineering and Regenerative Medicine* 4.1: 12-24, **2010.**

[87]   Timmins, Nicholas E., et al. Three-dimensional cell culture and tissue engineering in a T-CUP (tissue culture under perfusion). *Tissue engineering* 13.8 2021-2028, **2007.**

[88]   Wendt, D., et al. Oscillating perfusion of cell suspensions through three-dimensional scaffolds enhances cell seeding efficiency and uniformity. *Biotechnology and Bioengineering* 84.2: 205-214, **2003.**

[89]   Braccini, Alessandra, et al. Three-dimensional perfusion culture of human bone marrow cells and generation of osteoinductive grafts. *Stem Cells* 23.8: 1066-1072, **2005**.

[90]   Cartmell, Sarah H., et al. Effects of medium perfusion rate on cell-seeded three-dimensional bone constructs in vitro. *Tissue Engineering* 9.6: 1197-1203, **2003.**

[91]   Porter, Blaise D., et al. Noninvasive image analysis of 3D construct mineralization in a perfusion bioreactor. *Biomaterials* 28.15: 2525-2533, **2007.**

[92]   Seitz, Sebastian, et al. Influence of in vitro cultivation on the integration of cell-matrix constructs after subcutaneous implantation. *Tissue Engineering* 13.5: 1059-1067, **2007.**

[93]   Volkmer, Elias, et al. Hypoxia in static and dynamic 3D culture systems for tissue engineering of bone. *Tissue Engineering Part A* 14.8: 1331-1340, **2008.**

[94]   Yang, Jinfeng, et al. Proliferation and osteogenesis of immortalized bone marrow-derived mesenchymal stem cells in porous polylactic glycolic acid scaffolds under perfusion culture. Journal of Biomedical Materials Research Part A 92.3: 817-829, **2010.**

[95]   Zhao, Feng, and Teng Ma. Perfusion bioreactor system for human mesenchymal stem cell tissue engineering: dynamic cell seeding and construct development. *Biotechnology and Bioengineering* 91.4: 482-493, **2005.**

[96]   Zhao, Feng, et al. Effects of oxygen transport on 3-d human mesenchymal stem cell metabolic activity in perfusion and static cultures: Experiments and mathematical model. *Biotechnology Progress* 21.4: 1269-1280, **2005.**

[97]   Zhao, Feng, Ravindran Chella, and Teng Ma. Effects of shear stress on 3-D human mesenchymal stem cell construct development in a perfusion bioreactor system: Experiments and hydrodynamic modeling. *Biotechnology and Bioengineering* 96.3: 584-595, **2007.**

[98]   Zhao, Feng, et al. Perfusion affects the tissue developmental patterns of human mesenchymal stem cells in 3D scaffolds. *Journal of Cellular Physiology* 219.2: 421-429, **2009.**

[99]   Hosseinkhani, Hossein, et al. Impregnation of plasmid DNA into three-dimensional scaffolds and medium perfusion enhance in vitro DNA expression of mesenchymal stem cells. *Tissue Engineering* 11.9-10: 1459-1475, **2005.**

[100]   Hosseinkhani, Hossein, et al. Enhanced ectopic bone formation using a combination of plasmid DNA impregnation into 3-D scaffold and bioreactor perfusion culture. *Biomaterials* 27.8: 1387-1398, **2006.**

[101]   Hosseinkhani, Hossein, et al. Ectopic bone formation in collagen sponge self-assembled peptide–amphiphile nanofibers hybrid scaffold in a perfusion culture bioreactor. *Biomaterials* 27.29: 5089-5098, **2006.**

[102]   Wang, Yichao, et al. Application of perfusion culture system improves in vitro and in vivo osteogenesis of bone marrow-derived osteoblastic cells in porous ceramic materials. *Tissue Engineering* 9.6: 1205-1214, **2003**.

[103]   COMSOL   Multiphysics,   Users   Guide   2010,   http://chemelab.ucsd.edu/ CAPE/comsol/Comsol_UserGuide.pdf (June 2016).

[104]   Kuzmin, Dmitri. Introduction to computational fluid dynamics. *University of Dortmund*, Dortmund (2014).

[105]   Chapra, Steven C., and Raymond P. Canale. *Numerical Methods for Engineers*. Vol. 2. New York: McGraw-Hill, **1998**.

[106]   FLUENT, http://www.fluent.com (June, **2016**).

[107]   Patrachari, Anirudh R., Jagdeep T. Podichetty, and Sundararajan V. Madihally. Application of computational fluid dynamics in tissue engineering. *Journal of Bioscience and Bioengineering* 114.2: 123-132, **2012.**

[108]   Yan, X., X. B. Chen, and D. J. Bergstrom. Modeling of the flow within scaffolds in perfusion bioreactors. *American Journal of Biomedical Engineering* 1.2: 72-77, **2011.**

[109]   McCoy, Ryan J., C. Jungreuthmayer, and Fergal J. O'Brien. Influence of flow rate and scaffold pore size on cell behavior during mechanical stimulation in a flow perfusion bioreactor. *Biotechnology and Bioengineering* 109.6: 1583-1594, **2012.**

[110]   Lovett, M., Rockwood, D., Baryshyan, A., Kaplan, D.L., Simple modular bioreactors for tissue engineering: a system for characterization of oxygen gradients, human

mesenchymal stem cell differentiation, and prevascularization, *Tissue Engineering Part C*, Methods, 16, 1565-73, **2010**.

[111] Andrade Jr, J. S., et al. Fluid flow through porous media: the role of stagnant zones. *Physical Review Letters* 79.20: 3901, **1997.**

[112] Pollack, S. R., et al. Numerical model and experimental validation of microcarrier motion in a rotating bioreactor. *Tissue Engineering* 6.5: 519-530, **2000.**

[113] Williams, Kenneth A., Sunil Saini, and Timothy M. Wick. Computational Fluid Dynamics Modeling of Steady-State Momentum and Mass Transport in a Bioreactor for Cartilage Tissue Engineering. *Biotechnology Progress* 18.5: 951-963, **2002.**

[114] Lappa, Marcello. A CFD level-set method for soft tissue growth: theory and fundamental equations. *Journal of Biomechanics* 38.1: 185-190, **2005.**

[115] Singh, Harmeet, et al. Flow modelling within a scaffold under the influence of uni-axial and bi-axial bioreactor rotation. *Journal of Biotechnology* 119.2: 181-196, **2005.**

[116] Bueno, Ericka M., Bahar Bilgen, and Gilda A. Barabino. Wavy-walled bioreactor supports increased cell proliferation and matrix deposition in engineered cartilage constructs. *Tissue Engineering* 11.11-12: 1699-1709, **2005.**

[117] Boschetti, Federica, et al. Prediction of the micro-fluid dynamic environment imposed to three-dimensional engineered cell systems in bioreactors. *Journal of Biomechanics* 39.3: 418-425, **2006.**

[118] Ye, Hua, et al. Modelling nutrient transport in hollow fibre membrane bioreactors for growing three-dimensional bone tissue. *Journal of Membrane Science* 272.1: 169-178, **2006.**

[119] Dusting, Jonathan, John Sheridan, and Kerry Hourigan. A fluid dynamics approach to bioreactor design for cell and tissue culture. *Biotechnology and Bioengineering* 94.6: 1196-1208, **2006.**

[120] Cheng, Gang, et al. Cell population dynamics modulate the rates of tissue growth processes. *Biophysical Journal* 90.3 2006: 713-724, **2006.**

[121] Bilgen, B., Barabino, G.A., Location of scaffolds in bioreactors modulates the hydrodynamic environment experienced by engineered tissues, *Biotechnology and Bioengineering*, 98, 282-94, **2007**.

[122] Galbusera, F., et al. Computational modeling of combined cell population dynamics and oxygen transport in engineered tissue subject to interstitial perfusion. *Computer Methods in Biomechanics and Biomedical Engineering* 10.4: 279-287, **2007.**

[123] Lemon, G., and J. R. King. Multiphase modelling of cell ehavior on artificial scaffolds: effects of nutrient depletion and spatially nonuniform porosity. *Mathematical Medicine and Biology* 24.1: 57-83, **2007.**

[124] Maes, Frédéric, et al. Modeling fluid flow through irregular scaffolds for perfusion bioreactors. *Biotechnology and Bioengineering* 103.3: 621-630, **2009.**

[125] Hidalgo-Bastida, L. Araida, et al. Modeling and design of optimal flow perfusion bioreactors for tissue engineering applications. *Biotechnology and Bioengineering* 109.4: 1095-1099, **2012.**

[126] Liovic, Petar, et al. Fluid flow and stresses on microcarriers in spinner flask bioreactors. *Proceedings of the 9th International Conference on CFD in the Minerals and Process Industries*, **2012.**

7. CURRICULUM VITAE

Credentials

Name, Surname	:	Alper Cengiz
Place of Birth	:	Kocaeli
Marital Status	:	Single
E-mail	:	alper.cengiz@hacettepe.edu.tr
Address	:	Hacettepe University, Department of Bioengineering, Ankara

Education

High School	:	Kocaeli Anadolu Lisesi (2009)
BSc.	:	Hacettepe University, Department of Statistics (2014)
MSc.	:	Hacettepe University, Department of Bioengineering (2017)

Foreign Languages
- English : Advanced
- German : Intermediate

Work Experience
- Project Assistant (2015-2017)

Field of Experience
- Bioreactor applications for mesenchymal stem cell cultures.
- Mathematical modeling with computational fluid dynamics software in tissue engineering.
- Statistical analysis and evaluation

Projects and Budgets

- The Development of Perfusion Bioreactor Using Tissue Scaffolds for Bone Patches:: Evaluation of Operational Parameters and CFD Modeling Studies, TUBITAK Project No: 214M100, 2015-Ongoing.

Publications

- Arslan, A., Çakmak, S., Cengiz, A., & Gümüşderelioğlu, M.. Poly (butylene adipate-co-terephthalate) scaffolds: processing, structural characteristics and cellular responses. *Journal of Biomaterials Science, Polymer Edition* 27.18 (2016): 1841-1859.

Oral and Poster Presentations

-

HACETTEPE UNIVERSITY
GRADUATE SCHOOL OF SCIENCE AND ENGINEERING
THESIS/DISSERTATION ORIGINALITY REPORT

HACETTEPE UNIVERSITY
GRADUATE SCHOOL OF SCIENCE AND ENGINEERING
TO THE DEPARTMENT OF BIOENGINEERING

Date: 06/07/2017

Thesis Title / Topic: BONE TISSUE ENGINEERING WITH MESENCHYMAL STEM CELL SEEDED SCAFFOLD ASSISTED

PERFUSION BIOREACTORS

According to the originality report obtained by myself/my thesis advisor by using the *Turnitin* plagiarism detection software and by applying the filtering options stated below on 05/07/2017 for the total of 86 pages including the a) Title Page, b) Introduction, c) Main Chapters, d) Conclusion sections of my thesis entitled as above, the similarity index of my thesis is 9 %.

Filtering options applied:
1. Bibliography/Works Cited excluded
2. Quotes excluded / included
3. Match size up to 5 words excluded

I declare that I have carefully read Hacettepe University Graduate School of Sciene and Engineering Guidelines for Obtaining and Using Thesis Originality Reports; that according to the maximum similarity index values specified in the Guidelines, my thesis does not include any form of plagiarism; that in any future detection of possible infringement of the regulations I accept all legal responsibility; and that all the information I have provided is correct to the best of my knowledge.

I respectfully submit this for approval.

Date and Signature

Name Surname:	ALPER CENGİZ	06.07.2017
Student No:	N14126860	
Department:	BIOENGINEERING DEPARTMENT	
Program:	MASTER OF SCIENCE	
Status:	☒ Masters ☐ Ph.D. ☐ Integrated Ph.D.	

ADVISOR APPROVAL

APPROVED.

Prof. Dr. Menemşe Gümüşderelioğlu

(Title, Name Surname, Signature)